NORTHWESTERN UNIVERSITY

LY6K Promotes Glioblastoma Tumorigenicity via CAV-1-Mediated ERK1/2 Signaling Enhancement

A DISSERTATION

SUBMITTED TO THE GRADUATE SCHOOL
IN PARTIAL FULFILLMENT OF THE REQUIREMENTS

for the degree

DOCTOR OF PHILOSOPHY

Field of Neuroscience

By
Namratha G Sastry

EVANSTON, ILLINOIS

June 2020

ABSTRACT

Background: Glioblastoma (GBM) tumors are the most malignant brain cancers and are characterized as Grade IV astrocytomas by the World Health Organization. GBM tumors can be classified into three molecular subtypes known as proneural, classical, and mesenchymal. In addition, GBM tumors also have a small population of cells known as glioma stem-like cells or GSCs, which can also be classified into subtypes that mirror clinical GBM. Gene expression array data revealed that *Lymphocyte Antigen 6 Complex, Locus K (LY6K)* may be a differentially expressed gene between the PN and MES subtypes within the GSC subpopulation. *LY6K* is a putative oncogene in various cancers, and elevated expression of *LY6K* is correlated with poor patient prognosis in GBM. The aim of our research is to advance our understanding of the mechanism by which LY6K contributes to GBM tumor biology.

Methods: Bioinformatic data mining was used to investigate *LY6K* expression in relation to GBM clinical outcome. To understand the role of LY6K in GBM biology, we utilized patient-derived glioma stem-like cells (GSCs) and U87 glioma cells and conducted cell proliferation assays, tumor sphere forming frequency assays, and utilized orthotopic GBM xenograft models in immunocompromised mice. We also studied the mechanism that promotes LY6K-mediated GBM tumorigenicity by employing *in vitro* signaling assays, immunoblotting assays, and immunofluorescent staining. Finally, we analyzed the importance of methylation on *LY6K* gene expression by using combined bisulfite and restriction analyses and bisulfite sequencing. We also demonstrated the clinical significance of LY6K by using ionizing radiation treatment and evaluating the effect on GSC proliferation.

Results: Increased expression of *LY6K* inversely correlates with survival of patients with GBM. Our results show that LY6K promotes tumorigenicity in GBM cells both *in vitro* and *in vivo*. The mechanism underlying this tumorigenic behavior is enhancement of ERK1/2 signaling. Interestingly, we observed that tumor-promoting LY6K-ERK1/2 signaling is mediated by the interaction of LY6K with caveolin-1, rather than through oncogenic receptor tyrosine kinase (RTK)-mediated signaling. Moreover, association of LY6K with the cell membrane is crucial for its tumorigenic functions. Finally, DNA methylation maintains *LY6K* silencing, and hypomethylation of the *LY6K* promoter increases its expression. In GSCs, ionizing radiation leads to demethylation of the *LY6K* promoter, thereby increasing LY6K expression and GSC resistance to radiation therapy (RT).

Conclusion and Significance: Our study highlights the importance of the contribution of LY6K to GBM tumor biology and suggests LY6K as a potential membrane target for treating GBM. Although LY6K was reported as an oncogenic protein that promotes tumorigenicity in multiple types of cancers, its role in GBM and the underlying mechanism by which LY6K mediates oncogenic signaling are unknown. Here we determined oncogenic functions of LY6K in GBM and describe a novel mechanism by which membrane-anchored LY6K stimulates ERK1/2 signaling through its association with caveolin-1 (CAV-1). Additionally, *LY6K* expression is regulated by gene promoter methylation, and irradiation induces *LY6K* expression by demethylating the *LY6K* promoter. This is the first study to determine the role and mode of action of LY6K in GBM biology. Our study highlights the importance of LY6K in enhancing tumorigenicity in GBM and suggests LY6K as a potential target for reducing GBM resistance to ionizing radiation (IR).

Key points

1. Elevated *LY6K* expression correlates with poor prognosis and tumorigenicity in GSCs and GBM cells.
2. LY6K functions by enhancing ERK1/2 signaling through interactions with CAV-1.
3. DNA methylation regulates *LY6K*. IR promotes *LY6K* promoter demethylation, thereby increasing *LY6K* expression.

Importance of Study

Although LY6K was previously implicated in tumorigenicity of multiple types of cancers including GBM, its role in GBM and the underlying mechanistic basis by which LY6K mediates tumor-promoting signaling are unknown. Here, we illustrate a novel signaling mechanism by which membrane-anchored LY6K enhances ERK1/2 signaling through its association with caveolin-1 to facilitate GBM tumorigenicity. Additionally, DNA methylation contributes to *LY6K* expression, and irradiation induces *LY6K* expression by promoter demethylation, resulting in enhanced radiation resistance in GSCs. This is the first study to investigate the function and underlying mechanism of LY6K in GBM tumor biology. Our study highlights LY6K as a potential targetable protein to promote radiation sensitivity in GBM.

ACKNOWLEDGEMENTS

After five years, my journey through graduate school is coming to an end. There are so many wonderful people who have helped me finish my PhD, and I could not have accomplished this without their support.

First and foremost are the wonderful members of my laboratory. My advisor, Dr. Shi-Yuan Cheng, is an incredible mentor, and I have learned so much from him. He has absolutely made me a better scientist, communicator, and critical thinker. When I first joined the laboratory, I had little to no experience with cell culture or even cancer biology. I struggled quite a bit early on in my PhD research, but Dr. Cheng's guidance and patience were crucial for me to navigate those early obstacles and eventually have a successful PhD career. His didactic mentorship was instrumental for my successful grant applications as well as my final manuscript. Another critical part of overcoming those challenges are the amazing members of my laboratory. Firstly, I have to thank Dr. Bo Hu, our brilliant research associate professor. She has been a constant presence in the laboratory and is always available whenever I have needed assistance with anything. From helping me make sure that I am ordering the correct reagents to guiding me on what to do next when I get bizarre western blot results, I cannot imagine completing my PhD without her guidance and leadership.

In addition, Dr. Angel Alvarez was my first supervisor in the laboratory and as I had joked with him "my lab big brother". Angel taught me most of the techniques that I needed throughout my PhD, including western blotting, animal protocols, and basic cell culture. He has always been a great resource whenever I need assistance with laboratory troubleshooting, and I am incredibly

grateful for his friendship and support. The other members of the laboratory who were also invaluable resources are Drs. Tianzhi Huang and Raj Pangeni. Tianzhi helped me with most of my xenograft experiments for my project, and I really value his time and assistance for all of my animal experiments. Raj taught me nearly everything I know about epigenetics and associated techniques. Raj also became a good friend who was happy to help me with anything I needed in or out of the laboratory.

Furthermore, I had the good fortune of having some great post-doctoral fellows join our laboratory in the middle of my PhD studies. Drs. Xiao (Lisa) Song, Xuechao Wan, and Yongyong (Jack) Yang all joined our laboratory within months of one another and have all given me very useful advice and help with various aspects of my paper. Finally, much more recently, we had a few new post-docs and fellows join our laboratory. Drs. Anshika Goenka, Deanna Tiek, and Bingli Wu all joined the laboratory within the last year. Although my work was wrapping up, they still provided invaluable input into helping me put the final touches on my manuscript and make sure that it was publication-ready. They have also become wonderful friends and I am very happy to have had the opportunity to get to know them so well.

In addition to my laboratory, I would also like to thank my thesis committee members. Firstly, my committee chair, Dr. David James, has been a remarkable mentor. Every time I had a committee meeting, Dr. James gave me incredibly insightful advice and guidance to help me advance my work. This was also evident when he reviewed my manuscript prior to submission. I was amazed at the amount of time he spent going over my manuscript and the incredible attention to detail. His comments were very astute, and my final paper was infinitely improved thanks to his

feedback and assistance. I would also like to thank Drs. Craig Horbinski and Alex Stegh. Craig and Alex both gave me excellent comments during my committee meetings and were always available if I needed assistance with anything related to my PhD research. Moreover, all of my committee members took time to write letters of recommendation for my NIH F31 NRSA application, which was successfully funded. I am so grateful to all of them for their guidance throughout my PhD.

Additionally, I would like to thank the funding sources that supported me throughout my graduate career. In addition to the generous funding sources available to Dr. Cheng, the collaborative environment of our laboratory and the didactic mentorship provided by Dr. Cheng presented me with two individual funding opportunities. Firstly, I received the prestigious Robert H. Lurie Comprehensive Cancer Center Fishel Award for predoctoral trainees. This award was renewed for a second year and provided me with funding and resources for my work. Moreover, this award was a crucial piece during my successful application to the NIH F31 NRSA. For the past two years of my PhD studies, the support from my NRSA provided me with resources to effectively develop my research plan and conduct my research on the pathophysiology of GBM.

Moreover, I would like to thank my graduate program, NUIN, for all of the support I have received during my entire PhD career. The program provided me with structure and a plethora of resources to ensure that I would be successful during my PhD. Specifically, I would like to thank our previous Assistant Director, Dr. Sally McIver. Sally proved to be a blessing during my early years. She helped me navigate my first year and genuinely cared about my success. This was apparent during the time she took to help me find my thesis laboratory, despite my early struggles

with this and was most evident during my second year during my PhD candidacy exam. Unfortunately, I did not pass my qualification exam on my first attempt and was thoroughly depressed after this initial result. There are whole host of people who helped me on my second successful attempt, for whom I am infinitely thankful. Of these, Sally is perhaps the most notable because of her dedication to my success. She spent hours with me, going over my presentation and helping me to organize it cohesively. During this time of intense stress and frustration, she showed me how much she cared about my career, and I know that my success was only possible with her help. She helped me become a much better presenter, critical thinker, and most importantly, a confident young scientist.

Finally, I would like to thank my family. I cannot complete my PhD studies without thanking my beloved parents and sister. They showed me the importance of a quality education from childhood and have been my constant cheerleaders and advocates throughout my life. I could write an entire dissertation just about how much their encouragement has meant to me. My mother has been my champion since the day I was born, and she has been an inspiration to me in more ways than I can count. My father is the reason my family moved to America and he has stood by me during all of my educational pursuits and has always believed in my success. Lastly, my sister is my rock and my best role model. She has believed in me more than anyone else including myself and saw my potential even when it was hazy to me. It was only because of her faith in my potential that I even attempted most of the challenging endeavors of my young career, and there are not enough words in any language to state how grateful I am for her and how much she means to me. She also gave me a wonderful brother-in-law and two beloved nephews who I am thankful for

every day. Finally, last but absolutely not least, I thank my husband. I had the wonderful pleasure of meeting him during my PhD work, and we got married in 2018. I can't begin to say how much I value patience when I need to cancel plans due to lab work or vent about an experiment that isn't working or any other frustrations that come with grad school. He is always supportive and loving and has been without doubt, the best part of my PhD.

Thank you all so much!!!

LIST OF PRIMARY ABBREVIATIONS

Cancer Stem Cells	CSC
Caveolin-1	CAV-1
Classical	CL
Combined Bisulfite and Restriction Analyses	CoBRA
Epidermal Growth Factor	EGF
Epidermal Growth Factor Receptor	EGFR
Extracellular Signal-Regulated Kinase	ERK
Glioblastoma	GBM
Glioma Stem-Like Cell	GSC
Glyceraldehyde 3-Phosphate Dehydrogenase	GAPDH
Glycosylphosphatidylinositol	GPI
Ionizing Radiation	IR
Lymphocyte Antigen 6 Complex, Locus K	LY6K
Mannosamine Hydrochloride	Mann-HCl
Mesenchymal	MES
Mitogen Activated Protein Kinase	MAPK
Phosphatidylinositol-Phospholipase C	PI-PLC
Proneural	PN
Radiation Therapy	RT
Receptor Tyrosine Kinase	RTK
Short Hairpin RNA	shRNA

DEDICATION

This dissertation is dedicated to my mother, who's own struggle with breast cancer was the motivation for my pursuit of cancer research during my PhD. Through her battle with her cancer and enduring the exhaustive effects of surgery and chemotherapy, my mother's resilience and strength inspired me to dedicate my research to understanding and combating cancer. I sincerely hope that my research will someday help a cancer patient fight this terrible disease, just as my mother successfully did. I love you Amma!

TABLE OF CONTENTS:

LIST OF TABLES, ILLUSTRATIONS, FIGURES, OR GRAPHS

CHAPTER 1: INTRODUCTION

The brain is an incredibly complex organ that contains two main types of cells: neurons and glia. Glia in the brain can be further diversified into groups, including radial glia, oligodendrocytes, oligodendrocyte progenitor cells, microglia, and astrocytes.[1] While astrocytes have many important functions in the brain, such as their involvement in the blood-brain barrier, tripartite synapses, and metabolic support for neurons,[2] abnormal proliferation of astrocytes can lead to a class of gliomas called astrocytomas.[3] Astrocytomas can be divided, based on severity of disease into various grades as classified by the World Health Organization with Grade IV astrocytomas, or glioblastomas (GBM)[4] being the most malignant brain cancer.[5]

Characterizing GBM Tumors

GBM tumors can either progress from low-grade gliomas (LGG) as secondary GBMs or can form de novo as primary tumors. Primary GBM tumors have worse survival, and mutations in the gene *isocitrate dehydrogenase 1 (IDH1)* strongly predict GBM patient prognoses.[4] Specifically, the *IDH-R132H* mutation is present in ~10% of primary GBM and is a prognostic indicator of secondary GBM as well as the glioma cytosine-phosphate-guanine (CpG) island methylator phenotype (G-CIMP). The vast majority of gliomas carrying the *IDH-R132H* mutation are also G-CIMP$^+$ and have much better prognosis than those that are *IDH-WT* and G-CIMP$^-$. *IDH1* encodes the IDH1 protein that is involved in the tricarboxylic acid cycle and is responsible for converting isocitrate into α-ketoglutarate.[6] However, in *IDH* mutant tumors, a mutated subunit of IDH1 forms a heterodimer with a WT subunit and gains the ability to convert α-ketoglutarate into the oncometabolite 2-hydroxyglutarate (2-HG). Accumulation of 2-HG can lead to changes

in cellular epigenomics including genome-wide alterations in DNA methylation that lead to cell transformation.[7]

Distinct molecular characteristics and inherited heterogeneity are two features that render GBM tumors resistant to current therapies leading to poor overall survival. Intra-tumoral heterogeneity is considered a key contributor to GBM therapy resistance, which in turn promotes poor survival outcomes. As shown in Figure 1, integrated genomic analysis of primary, *IDH-WT* GBM tumors led to their classification into three molecular subtypes: proneural (PN), classical (CL), and mesenchymal (MES).[8,9]

PN tumors are known to have relatively better survival and are associated with mutations in *tumor protein 53 (TP53)* and *platelet-derived growth factor A (PDGFRA)*. Overexpression of *epidermal growth factor receptor (EGFR)* is primarily seen in CL tumor, as well as the oncogenic mutant *EGFRvIII*. Finally, the MES subtype is known for mutations in the tumor suppressive *neurofibromin 1 (NF1)* gene. Regardless of subtype classification however, each tumor mass can be comprised of multiple cell subpopulations and multiple subtypes as measured by simplicity scores.[8,10] For various human cancers including GBM, tumor heterogeneity can also involve a small population of cells, called cancer stem cells. Specifically in glioma, these are referred to as glioma-initiating or glioma stem-like cells (GSCs).[11]

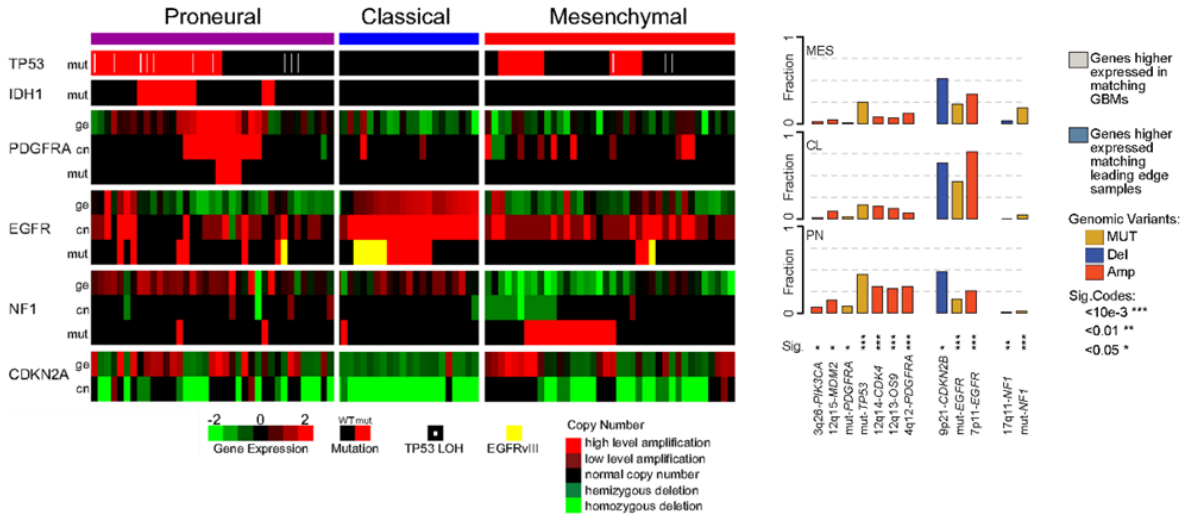

Figure 1: GBM Subtypes

There are three main subtypes in GBM, each with its own gene expression profile. Proneural subtypes are characterized as having mutations in genes such as *TP53* and *PDGFRA*. *IDH1* mutations seen in proneural tumors and have a distinct methylation phenotype called G-CIMP. Classical subtypes are primarily characterized as overexpression of *EGFR*. Mesenchymal tumors have mutations in NF1 and are associated with having the worst overall survival in patients. Adapted from Verhaak et al[9] and Wang et al[8].

Cancer Stem Cells

Stem cells (SCs) are critical during normal human development and are defined based on their ability to self-renew and differentiate. During development, the growing organism requires these malleable cells in order to properly form and organize various organs and tissues.[12] Moreover, SC pools are also essential for tissue repair after injuries. SCs use two different methods of cell division to accomplish these dynamic tasks.[12] Symmetric cell division is the process by which one SC divides to form either two identical daughter stem cells or two identical daughter differentiated cells. Asymmetric cell division allows one SC to achieve both of these results together by producing one daughter stem cell and one daughter differentiated cell.

CSC Self-Renewal and Differentiation

Although critical for normal functions, the unique ability of SCs to self-renew mandates thorough regulation to ensure that SCs are free from harmful mutations that can be passed onto future generations. Cells accomplish this regulation through transcriptional and/or epigenetic means.[13] While cellular microenvironments are generally very adept at this function, lack of proper regulation can result in extreme consequences such as cancer. Cancer cells exhibit certain hallmarks that allow a tumor to develop and grow.[14] More specifically, cancer stem cells (CSCs) are a subpopulation of tumor cells that are cancerous but retain the ability of adult SCs to self-renew and differentiate.[15] This allows SCs to initiate tumor formation and/or promote tumor growth.[11]

The first evidence for CSCs was presented with the discovery that single melanoma cells could give rise to tumors in NOD/SCID mice.[16] Since then, evidence for the ability of CSCs to initiate tumors using proteins and pathways characteristic of normal stem cells has been shown in various types of solid tumors[15], such as breast[17,18], prostate[19], colorectal[20], and brain[11,21] cancers.

Characterizing CSCs

Various methods exist to characterize CSCs and determine the degree to which a cell possesses renewal abilities.[22] CSCs form spheres *in vitro* that are maintained through serial passages, while progenitor or differentiated cells lack this ability.[11] Moreover, unlike differentiated cells, *in vivo* xenografts with CSCs yield sizable tumors in immunocompromised mice, and these can be faithfully recapitulated with serial transplantations. In addition, cell surface markers have

been a useful tool to characterize CSCs, as many of these markers are present on CSCs and normal stem cells but are not expressed on differentiated cells.[23] For instance, CD133 is a marker for hematopoietic stem cells, but has been widely considered as a CSC marker in breast, prostate, colon, glioma, liver, lung, and ovarian cancers. Finally, lineage tracing studies use a marker (e.g. GFP) to monitor the ability of a cell to give rise and maintain clonal progeny containing the parental marker.[15] CSCs that can grow and maintain these colonies thus demonstrate a hierarchical organization structure.

Plasticity in CSCs

There is growing evidence indicating that the tumor mass composed of CSCs, differentiated cancer cells, and the non-malignant stromal cell network work together to allow the tumor to adapt and thrive in the harsh tumor microenvironment (TME).[24] A well-studied example of cellular plasticity in normal cells is the intestinal stem cell population,[25] in which certain differentiated endocrine cells modulate their genetic profiles to resemble intestinal stem cells after tissue injury.[26] In colorectal cancer cells with genetic ablation of leucine-rich repeat-containing G-protein coupled receptor 5 $(LRG5)^+$-CSCs, differentiated keratin 20 $(KRT20)^+$ cancer cells have been shown to become dedifferentiated upon entering a niche previously occupied by $LRG5^+$ CSCs.[27] Such functional plasticity is also seen in GSCs. Upon treatment with receptor tyrosine kinase (RTK) inhibitors, GSCs can adopt a slow cell cycling state that is dependent upon Notch signaling and is associated with chromatin remodeling using H3K27 demethylases.[28] This epigenetic modulation allows GSCs to be persistent when confronted with therapeutic insults, thereby providing an avenue for tumor resistance to therapy. Furthermore in breast cancer,

differentiated basal and luminal cells can revert to stem cell-like states at a low but significant rate.[29] Given sufficient time, subpopulations of stem, basal, or luminal cells cultured individually can eventually recapitulate phenotypic proportions that include the other two cell types, thereby mirroring the original breast cancer line. The ability of cancer cells to endure therapeutic stress is once again evident in this situation.[15,29] Unlike stem cells, basal and luminal breast cancer cells are normally unable to give rise to tumors in mice. However, upon co-inoculation with irradiated cells, all three subpopulations are effectively tumorigenic in animals.

CSCs in Therapeutic Resistance

Perhaps one of the most pressing reasons for targeting CSCs is their resistance to conventional therapies. Conventional anti-proliferative therapies are largely aimed at targeting the non-tumorigenic population of cells. However, such treatments lead to relapse in many types of cancers, and this can be attributed almost entirely to the CSC population and surrounding niche within the tumor.[15] This is primarily due to the ability of CSCs to be plastic and modify their growth patterns to promote favorable outcomes when confronted with therapeutic insults. CSCs can change their proliferation rates to become slow-cycling or quiescent, thereby avoiding chemotherapeutic agents that target highly proliferative cells.[30] In addition to this cell-cycle metabolic plasticity, various other mechanisms exist that allow CSCs to become resistant to therapies. One of the most important mechanism is the ability of CSCs to efficiently repair DNA damage, thereby avoiding apoptosis.[31] Other examples include evading immune surveillance, upregulation of aldehyde dehydrogenase (ALDH) proteins, and autophagy.[31] CSCs tend to be enriched in certain biomarkers, which are useful therapeutic targets. In breast cancer, $CD24^{+}$ cells

proved to be a highly tumorigenic population that efficiently formed tumors in mice, while $CD24^-$ populations failed to do so.[32] Thus, specifically targeting the tumorigenic CSC population is crucial for ensuring tumor elimination. In addition to such stem cell surface markers, treatments have also been aimed at targeting signal transduction pathways that become aberrantly active in cancers. Various drugs and antibody treatments target cytokines, ligands, and cell-surface receptors and aim to curb abnormal signaling.[33] As an example, therapies aimed at the human epidermal growth factor receptor 2 (HER2) have shown substantial improvements in patient survival when combined with traditional therapies. This is likely due to the ability of these therapies to target HER2 in breast CSC populations.[33] Moreover, in prostate cancer, WNT signaling has been studied for its role in prostate CSC therapy resistance.[34] Moreover, ALDH1A1 is overexpressed in prostate cancers and is associated with poor patient survival.[35] In prostate cancer cells, radiation therapy (RT) increased the progenitor cell population and in turn, the progenitor cell populations were resistant to RT. Furthermore, in $ALDH^+$ cells, WNT/β-catenin signaling was upregulated and contributed to radioresistance.[35] In addition to signaling, CSCs are also aided in their therapy resistance by the surrounding niche in the TME. In colorectal cancer, the CSC population is supported by the intestinal crypt which is designed to maintain normal intestinal stem cells.[36] All of these mechanisms combined create a TME that is highly favorable for CSC survival when faced with therapies.

Tumor Immunology

In recent years, the promise of immune-based therapies has provided a novel treatment method, especially for cancers that are unresponsive to other forms of therapy. Immunotherapies

are thought to act on T-cells in the cancer-immunity cycle.[37] This is a model which begins with a dying cancer cell releasing antigens that are taken up by dendritic cells or antigen presenting cells. Upon capture, these cells prime T-cells by presenting the cancer antigens on major histocompatibility complexes I and II to the T-cell receptor. Once activated, cytotoxic T-lymphocyte cells (CTLs) traffic to the tumor site and clonally expand to the specific antigen presented by the dendric cells. Once the CTLs extravasate from the blood vessel and infiltrate the tumor, they are equipped to recognize the cancer cells, based on the antigen to which they are responding. Once a CTL recognizes a cancer cell based on this antigen, the CTL can kill the cell, which releases further antigens and propagates the cycle.[38]

One of the hallmarks of cancer cells is to try to suppress the immune system and evade immune surveillance.[14] Although GBM tumors are often considered "immune-privileged" and are known for being immunosuppressive or "cold" tumors, various avenues exist for targeting GSCs, many of which involve immune-based therapies.[39,40] An immune checkpoint pathway that has come under intense scrutiny for its role in immune suppression is the programmed death 1 (PD1), which is expressed on T-cells after priming, and PD-ligand 1 (PD-L1), which is expressed on tumor cells.[38] When PD-L1 binds PD1, the overall effect is immunosuppressive, thereby halting the function of CTLs. [41] Indeed, immunotherapeutic agents such as nivolumab are focused on inhibiting this effect by creating monoclonal antibodies against PD1. Another checkpoint protein that has received significant attention is CTL antigen 4 (CTLA4), which is present on T-cells. CTLA4 competes with a pro-stimulatory molecule for binding to the CD80 ligand present on dendritic cells. Binding of CTLA4 to CD80 suppresses the function of the T-cells. Similar to PD-

1, antibodies against CTLA4 such as ipilimumab are also being investigated for their utility in cancer therapy.[38] In GBM, clinical trials based on immune checkpoint inhibitors such as nivolumab have failed to generate significant increases in overall patient survival. However, there are some select patients that have benefited from therapy,[42] and the characteristics that allow for prolonged survival in this small subset should be further investigated. In addition, combinations treatments have the potential for inducing longer survival when mono-therapeutics fail to significantly improve patient survival. Indeed, PD1 treatment in conjunction with RT and an inhibitor again indolamine 2,3-dioxygenase 1 (IDO1) significantly improved survival in mice, whereas mono or dual treatment in any combination failed to do so.[43]

Another promising field of GBM immunotherapy is treatment with chimeric antigen receptor (CAR)-modified T cells. CAR-T cell therapy is a method by which T cells are engineered to recognize and respond to tumor-associated antigens. Therefore, they can theoretically infiltrate the tumor and target/kill cancer cells.[44] In GBM, CAR-T cells have been shown to infiltrate the tumor and initiate an immune response, although no major increases in survival have yet been reported.[44] Furthermore, oncolytic viruses have been studied for their potential to selectively infect and kill tumor cells. The modified polio virus PVSRIPO has shown promising results and prolonged GBM patient survival.[45] While oncolytic viruses are known to act by directly targeting and killing cancer cells, other mechanisms of actions may also be at play. PVSRIPO acts by targeting the CD155 receptor on the surface of GBM cells. Following oncolysis, GBM cells can release factor that stimulate antigen presenting cells, which then migrate to the draining lymph node. At this point, resident CTLs can become primed, which initiate their migration to the tumor

site.[46] Therefore, oncolytic viruses may function by directly killing tumor cells and leading to secondary immune responses.

While immunotherapies hold strong promise in treating the tumor mass, there has been little evidence showing their efficacy in CSCs. CSCs, including GSCs, can release various cytokines and immunosuppressive molecules to dampen the immune response and evade surveillance.[47] GBM and the associated tumor microenvironment (TME) are particularly immunosuppressive tumor, and GBM cells have high levels of checkpoint proteins and can release various molecules to suppress the immune response, such as transforming growth factor β (TGFβ) and interleukin (IL)-10.[48] However, immunogenicity can be rescued in GSCs, when they are treated with interferon γ (IFNγ) or a demethylating agent, indicating that tailored immunotherapies can be useful for GBM treatment.[49] Moreover, natural killer (NK) cells of the innate immune system may be a potential avenue to combat GSC immunosuppression. In many cancers including gliomas, activated NK cells have been shown to target CSC populations both *in vitro* and *in vivo*.[50,51] In addition, immune responses can also be elicited with cancer vaccines directed at dendritic cells and prolong rodent survival.[52] Notably, vaccine therapies have been introduced in the clinic with notable immunogenicity in GSCs.[53,54]

Similar to other CSCs, GSCs are also known to be resistant to conventional therapeutics. The first line of treatment for GBM patients include a chemotherapeutic agent called temozolomide (TMZ) and radiation therapy (RT). The seminal discovery of TMZ as an antitumor compound has been perhaps the most influential finding in GBM treatment in the past two decades. Concomitant TMZ treatment with RT extends patient survival by 2.5 months relative to RT

alone.[55] However, such conventional therapies have limited effects on GSCs.[40] As discussed above, immunotherapies are being more commonly studied as a viable new treatment for GBM. While GBM has proven itself to be a difficult target for immunotherapies, clinical trials have shown some increases in immune responses following treatment. Therefore, further research for GBM immunotherapies, and specifically therapies targeting GSCs, is warranted.

LY6K

Our previous studies on gene expression profiling classified patient-derived GSCs into subtypes that phenotypically resemble GBM, with MES-like GSCs being more aggressive relative to PN-like GSCs.[21] Among the 3,000 differentially expressed genes between these GSC subtypes, *Lymphocyte Antigen 6 Complex, Locus K* (*LY6K*) was one of the top differentially expressed genes. Located on chromosome 8q24.3, *LY6K* encodes the protein LY6K, which is a member of the LY6/uPAR family. The protein is initially translated as a 165 amino acid precursor, which is then modified into a 121 amino acid mature protein. *LY6K* contains 3 exons, which make up three unique domains in the protein as shown in Figure 2. The first exon encodes the signal peptide. The second and part of the third exons make up the **L**Y6/**u**PAR (LU) domain. The LU domain consists of a three-finger motif that is made up of disulfide bridges constructed from each of 10 cysteine residues. Finally, the latter part of the third exon encodes the glycosylphosphatidylinositol (GPI) anchor domain, which results in its localization on the plasma membrane.[56]

Figure 2: Structure of the *LY6K* gene

Depiction of the three exons characteristic of LY6 family members. Exon 1 encodes the 5'-UTR and N-terminus signal peptide. Exon 2 and the 5' of exon 3 encode the LU domain. The LU domain consists of 80-90 amino acids containing 10 cysteine residues, which can form three fingered structural motif (3F) via disulfide bonds. Finally, the 3' of exon 3 encodes the GPI-anchor domain, which serves as the attachment site for the GPI anchor after post-translational processing. Adapted from Loughner et al.[56]

Function of LY6K

Ly6k is a cancer/testis antigen that has been examined for its role in sperm migration[57,58] and spermiogenesis.[59] Although primarily expressed in the testis with weak expression in other reproductive tissues, *LY6K* does have low levels of expression in non-reproductive organs including the brain as shown in Figure 3.[60] Ly6k has been established for its expression in testicular germ cells and is known to associate with germ cell marker, testis expressed gene 101 (Tex101),[58,61] thereby localizing to lipid rafts.[62] Male mice lacking Ly6k had substantially decreased rates of pregnancy induction, despite having no difference in copulation. Moreover, sperm from Ly6k-deficient mice significantly failed to bind and fertilize eggs.[58] Ly6k has been speculated to have 2 isoforms in mice, one that is GPI-anchored and another that lacks the GPI anchor and is thus soluble;[57,60] however, this has not been confirmed in primates. At the cell membrane, Ly6k is thought to form a complex with Tex101 that is essential for proper sperm migration. Mice lacking GPI-anchored Tex101 also lacked Ly6k in both water-soluble and triton-soluble fractions. However, Ly6k expression in extracellular fractions decreased but was still

present.[57] Indeed, a missense variant of TEX101 in human males led to substantially decreased levels of both TEX101 and LY6K and has been suggested as a marker of male infertility.[63] Although the precise mechanism for this infertility is yet unclear, rodent studies have indicated that the Tex101/Ly6k complex is essential for proper process and localization of the sperm membrane protein, a disintegrin and metalloprotease 3 (Adam3), which has been established for its role in sperm migration.[58]

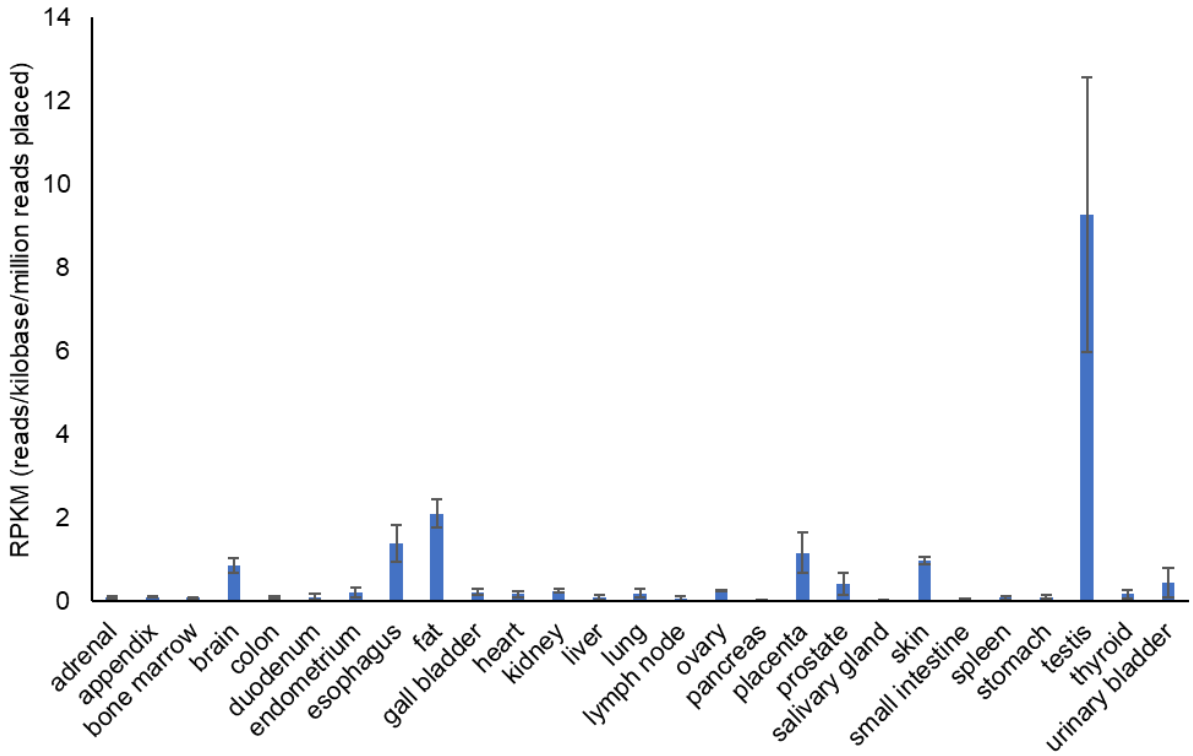

Figure 3: *LY6K* Expression Across Tissues

RNA-Seq data from 95 individuals, representing 27 tissue samples, showing the distribution of *LY6K* based on reads per kilobase per million reads placed (RPKM). Analysis from BioProject: PRJEB4337[64]

LY6K in Cancer

Although its precise role in physiological processes is yet unknown, LY6K is known to be upregulated in several types of human cancers.[65,66] In both lung and esophageal cancers, LY6K was identified as a serologic biomarker and has been associated with poor survival in patients.[67,68] Similarly, genome-wide profiling indicated that LY6K is overexpressed in gingivobuccal cancer,[69] cervical cancer,[70] as well as bladder cancer, in which it may regulate cell growth and metastasis.[71]

Various studies have examined the transcriptional and epigenetic mechanisms promoting *LY6K* expression in cancers. Heat shock factor 1 (HSF1) and its targets produce distinct cancer signatures that have prognostic potential. In breast, colon, and lung cancers, HSF1 strongly binds *LY6K* in both cell lines and patient samples to support oncogenic processes.[72] In addition, activator protein 1 (AP-1) transcription factor binding in the absence of methylation is thought to promote *LY6K* expression in breast cancer, thereby increasing cell invasion and metastasis.[73] Conversely, methylation of the *LY6K* promoter in which a single nucleotide polymorphism has been introduced, leads to suppression of *LY6K*, which is mediated by the paired box gene 3 (PAX3) transcription factor.[74] Tamoxifen is a well-established hormone treatment for patients with estrogen receptor (ER)-positive breast cancer, and tumors that lose ERα expression become less susceptible to tamoxifen treatment. In $ER\alpha^+$ breast cancer cells, ERα has been shown to induce expression of a microRNA that then negatively regulates LY6K and promotes tamoxifen susceptibility. However, in $ER\alpha^-$ cells, LY6K can induce a different miRNA that then inhibits ERα expression, thereby promoting tamoxifen resistance.[75] Similarly, evidence for miRNA regulation of LY6K has also been studied in non-small cell lung cancer (NSCLC).[76]

Despite the growing evidence for upregulation of LY6K in various types of cancers[66,77], relatively few studies have examined the precise mechanisms by which LY6K functions in cancers. In breast cancer, LY6K and a related family member, LY6E, are upregulated and are associated with poor clinical outcomes.[78] Interestingly, LY6K and LY6E mediate tumor progression and are required for phosphorylation of both SMAD2/3 and SMAD1/5, thereby regulating both TGFβ and bone morphogenetic protein (BMP) signaling in cells. In addition, both LY6K and LY6E are important for helping cancer cells escape immune surveillance and may prove to be useful targets in drug-resistant cancers.[78] Notably, LY6K has been shown to induce immune responses and has been proposed as a useful target for immunotherapies in clinical trials. Transgenic mice expressing LY6K show a decrease in the proportion of functional T cells, indicating a propensity to suppress the immune system.[79] A peptide epitope derived from LY6K elicited a strong response in CTL[80], which could be detected among tumor-infiltrating lymphocytes, regional lymph node lymphocytes, and peripheral blood lymphocytes in esophageal cancer.[81] Indeed, clinical trials in esophageal cancer patients aimed at testing the efficacy of a tri-peptide vaccine that included LY6K showed increased T-cell responses[82,83] with slightly improved survival.[84] Such immune responses to peptide vaccines have been seen in multiple other cancers including NSCLC [85,86] and gastric cancer.[87] LY6K is also identified as a putative target[88] in both human papillomavirus $(HPV)^{+}$ and HPV^{-} subtypes of head and neck squamous cell carcinomas (HNSCC).[89] Peptide vaccines containing LY6K induced CTL responses as well as significantly improved overall HNSCC patient survival with one patient exhibiting a complete response.[90] Head and neck tumors have also shown responses in T helper cells in addition to CTLs.[91]

Although various studies have shown the importance of LY6K in other cancers, few studies have examined its utility in GBM and the underlying mechanism of LY6K function has not yet been investigated. Recently, a study aimed at profiling alternative splicing (AS) signatures in GBM using TCGA RNA-Seq data showed that AS events in numerous genes are related to both overall survival and disease-free survival.[92] The authors then detected 1,829 AS events in 1,311 genes related to overall survival and 1,667 AS events in 1,146 genes related to disease-free survival. Of these, genes with a correlation coefficient between gene expression profiles and AS events of > 0.2 or < -0.2 were selected. Among the genes that are related to both overall and disease-free survival, they found a set of five "feature" genes that may be useful prognostic indicators for GBM patient treatment. These include *S100A4*, *ECE2*, *CAST*, *ASPH*, and *LY6K*. Of these five genes, AS events of *LY6K* were negatively correlated with its expression. Together with the other four genes, this allowed for construction of a prognostic predictor that uses AS events to predict patient clinical outcome.[92] In addition, peptide-based vaccines have also been tested in glioma patients. Similar to other cancers, a vaccine cocktail that included an epitope derived from LY6K showed immunoreactivity and CTL responses in all patients tested.[54] While there was some improvement in patient survival, further research is required to establish a more efficient treatment regimen.

Regulation of Gene Expression & Epigenetics

Gene expression in a eukaryotic cell is tightly regulated and controlled by a plethora of factors. At the transcriptional level, transcription factor binding to promoter and enhancer regions as well as repressor regions control which genes are transcribed.[93] Post-transcriptionally, transcripts are subjected to alternative splicing, polyadenylation, and 5'-capping.[94] One class of

key regulators of gene expression is the family of microRNAs (miRNA) within the cell. miRNAs are small (~22 nucleotide long) non-coding RNAs that generally function to diminish messenger RNAs (mRNA) and post-transcriptional gene expression. This is accomplished through the RNA-induced silencing complex (RISC), which primarily works by mRNA degradation or translation inhibition[95]. However, dysregulation of miRNAs, either via genetic or epigenetic mechanisms, can cause the cell to gain oncogenic properties, often due to downregulation of tumor suppressive miRNAs.[96] Previously work from our laboratory showed that miRNAs can be differentially expressed in GSCs.[97] Unpublished data from our laboratory showed that another such differentially expressed miRNA is miR99b as shown in Figure 4. miR99b is downregulated in various cancers, indicating that it might have tumor-suppressive functions in GBM.

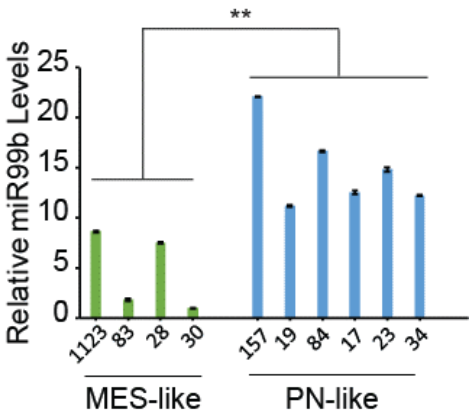

Figure 4: miR99b Expression in MES-like and PN-like GSCs

miRNAs can have differential expression patterns between the MES-like and PN-like subtypes of GSCs. Relative levels of miR99b are shown with high expression in six PN-like GSCs significantly lower expression in four MES-like GSCs.

While the mechanisms listed above list a miniscule portion of all the methods by which cells regulate gene expression, one mechanism that is of particular importance for *LY6K* expression is epigenetic regulation. Epigenetic modifications are present on both histones and nucleic acids. Histones are proteins that around which DNA is wrapped to form chromatin in the nucleus.[98] Histones can be subjected to various epigenetic modifications that determine the accessibility of the DNA prior to gene transcription such as covalent modifications and chromatin remodeling. Covalent modifications are primarily directed at lysine and arginine residues and involve methylation and acetylation.[99] Chromatin remodeling is governed by specialized proteins called readers, writer, and erasers. While the effect of these epigenetic marks is gene-specific, acetylation often promotes gene expression, while methylation often leads to gene silencing.[99]

Modifications to DNA are also well-studied. DNA methylation occurs at CG dinucleotides (i.e. CpG sites), in which a group of writers called DNA methyltransferases (DNMTs) transfer a methyl group from S-adenosyl methionine (SAM) to the cytosine base of the CpG site.[100] Regions with multiple CpG sites, especially near the promoter of a gene, are referred to as CpG islands. When normal cells become transformed into cancer cells, they modify their epigenetic signatures. Subsequently, they become addicted to the changes in their epigenome in order to survive.[101] CSCs in particular have distinct epigenetic signatures that are necessary for them to maintain their stem-like properties.[100] In GSCs, specialized epigenetic signatures can be used to differentiate methylation patterns that specific to GSCs when compared to GBM bulk tumors and can be further divided to be subtype-specific.[102] This is of particular importance to *LY6K*, given that LY6K is differentially expressed between PN and MES GSCs. In addition, *LY6K* has a CpG island near its

promoter and is thought to be regulated with DNA methylation.[74] Similar to other cancer/testis antigens, *LY6K* has high expression in the testis and very low levels in other tissues.[103] This is due to the *LY6K* gene promoter being methylated in normal tissues. However, in cancer, non-reproductive tissues undergo changes in DNA methylation that results in genes such as *LY6K* being unmethylated.[66] This can then lead to unregulated cell growth and can cause tumor growth or propagation. Moreover, cancer cells can use epigenetic remodeling to survive therapeutic interventions. For instance, following IR treatment, cancer cells can undergo global DNA epigenetic reprogramming to provide them with a survival advantage.[104] Therefore, *LY6K* promoter methylation may be an important factor in regulating *LY6K* expression and subsequent tumor growth in GBM.

Aberrant Signaling in GBM

Receptor Tyrosine Kinases

Approximately half of GBM tumors contain abnormal alterations in the epidermal growth factor receptor (EGFR).[105] EGFR is a receptor tyrosine kinase (RTK), which becomes activated upon EGF-binding and subsequent receptor dimerization and autophosphorylation.[106] The phosphorylated residues create docking sites for growth factor receptor bound protein 2 (GRB2), which then transduces the signal via son of sevenless (SOS). Downstream pathways such as RAS/MEK/extracellular response kinase (ERK), phosphoinositide 3-kinase (PI3K)/AKT/mammalian target of rapamycin (mTOR), or janus kinase (JAK)/ signal transducer and activator of transcription 3 (STAT3) can then lead to biological effects in the cell.[107] RTK

signal transduction pathways are altered in 88% of GBM tumors with nearly 10% of tumors having alterations in multiple RTKs.[105]

Aberrations in EGFR are most notable in the classical subtype of GBM. Classical tumors have both EGFR overexpression and a mutant form EGFR known as vIII.[9] This mutant form lacks exons 2-7 of EGFR, which normally encodes the ligand-binding domain.[108] As a result, EGFRvIII becomes constitutively active.[106] In addition to this deletion, various point mutations, genomic rearrangements, and other less known deletions have been discovered in EGFR.[109], with some alterations correlating with survival. For instance, the $EGFR^{A289D/T/V}$ mutation is associated with significantly worse survival and is thought to influence tumor invasion and proliferation.[110]

Despite the importance of EGFR in GBM, treatments aimed at targeting EGFR remain ineffective.[111,112] Targeting EGFR and EGFRvIII has demonstrated some utility in immunotherapy-based approaches.[113] Monoclonal antibody, mAb806, and some vaccine therapies showed improved survival in preclinical and early clinical studies.[54,113] Although various small molecule tyrosine kinase inhibitors (TKIs) targeting EGFR has been developed, few have shown any major survival benefit in GBM patients.[114] The first FDA-approved TKI is gefitinib, which has been shown to have a dramatic effect on survival in a small subset of NSCLC patients.[115] Similarly, erlotinib is TKI that targets the EGFR active kinase conformation and has been shown to elicit responsiveness in NSCLC patients who have high expression of EGFR.[116] However, these TKIs have failed to illustrate any survival benefits in GBM[111,112]. A potential explanation for this is that compensatory pathways get activated in response to these inhibitors and help sustain cell proliferation. Upon EGFR inhibition with erlotinib, resulting increases in tumor necrosis factor

(TNF) levels can induce activation of c-Jun N-terminal kinase (JNK), AXL receptor, and ERK.[117,118] Moreover, erlotinib targets the active conformation of EGFR. While this has responsiveness in NSCLC, studies suggest that TKIs targeting the inactive conformation of EGFR may have better success in GBM[119]. In GBM cells that failed to respond to erlotinib, there was enhanced responsiveness when treated with lapatinib, a TKI that targets the inactive form of EGFR. Lapatinib decreased the levels of p-EGFR in cells that have mutations in the extracellular domain of EGFR and promoted GBM cell death.[119] Furthermore, other signal pathways may be responsible for this resistance. Upon blocking the insulin receptor (InsR) and insulin-like growth factor 1 receptor (IGF1R), GBM cells were more responsive to treatment with gefitinib, potentially through AKT regulation.[120]

RAS

The mitogen activated protein kinase (MAPK; extracellular signal-regulated kinase, ERK1/2) pathway is among the most highly dysregulated pathways observed in GBM tumors.[105] In the canonical MAPK pathway, a ligand such as EGF binds to its respective RTK (e.g. EGFR) and activates EGFR signaling through receptor dimerization and autophosphorylation.[121] The phosphorylated residues create docking sites for adapter proteins such as GRB2, through its Src homology 2 (SH2) domain.[122] Subsequently, SOS is recruited to GRB2 through the SH3 domain, thereby bringing SOS into close proximity to the membrane-bound RAS oncoprotein.[123] Upon translation, RAS undergoes farnesylation by farnesyltransferases. This post-translational modification allows RAS to localize to the membrane and interact with SOS to affect downstream signaling. SOS is a guanine nucleotide exchange factor (GEF) that facilitates the switching of

inactive GDP-bound RAS to active GTP-bound RAS.[122] The activation or inactivation of RAS is tightly regulated in normal cells. Once active, RAS can activate downstream signaling and subsequently should be inactivated through the action of GTPase activating proteins (GAPs) such as NF1.

The RAS family has three members: NRAS, KRAS, and HRAS, with KRAS being the most predominantly activated in human cancers, and all three have a high degree of sequence homology. Mutations in both RAS and GAPs are well studied in human cancers and other human diseases[124], and RAS mutations are the most frequently seen in cancers, comprising about 20-30% of all cancers.[125,126] In KRAS, G12 mutations are the most common in cancers such as pancreatic ductal adenocarcinoma, colorectal cancer, and lung adenocarcinoma, with the guanine being substituted for a plethora of amino acids, the most prevalent of which include aspartate, valine, and cysteine.[127]

Despite the prevalence of these RAS mutations, targeting RAS and its associated proteins with pharmacological agents has had little success. Drug development has focused on various aspects of RAS signaling including RAS itself, the RAS-binding domain, downstream effectors of RAS, upstream activators of RAS, and farnesyltransferase inhibitors.[127] Recently, novel direct inhibitors targeting RAS^{G12C} have shown promise in clinical trials[128] (Clinical Trial Identifier: NCT03600883, www.clinicaltrials.gov). Another level of regulation of RAS involves phosphorylation. SRC has been shown to phosphorylate RAS-GTP and promote its switch to RAS-GDP, thereby attenuating RAF activation and downstream signaling.[129] However, SHP can dephosphorylate RAS and retain its GTP-bound conformation and continue RAF signaling.

Inhibition of SHP prevents this dephosphorylation and therefore suppresses MAPK signaling and oncogenesis.[129] Interestingly, this phosphorylation-mediated has been studied in GBM and may prove to be a novel mechanism by which RAS can be pharmacologically targeted.

RAF

Once bound to GTP, RAS can activate various effectors, the most well-studied of which is RAF. RAF binds RAS through its RAS-binding domain after being relieved of inhibition by 14-3-3.[130] RAF has the ability to dimerize to help promote its downstream signaling. Of the three members of the RAF family, ARAF, BRAF, and CRAF, both BRAF and CRAF can form homodimers or heterodimers, while ARAF is more resistant to dimerization. Moreover, this dimerization is enhanced upon EGF stimulation and with disease-associated RAF mutants.[131] RAF mutants comprise about 7% of all human tumors.[126] Perhaps the most common activating mutation in RAF is the $BRAF^{V600E}$ mutation, which causes RAF to become constitutively active even as a monomer and become resistant to feedback inhibition.[126,132] Moreover, depending on the type of mutation, RAF mutants can function either as monomers or dimers in a RAS-dependent or RAS-independent manner.

RAF inhibitors can target either RAF monomers or dimers. However, the latter inhibitors can have a tendency to bind one protomer only and require clinically unrealistic concentrations to bind both protomers. As a result, the unbound protomer may become activated and induce downstream signaling.[126] The inhibitor PLX8394 can target BRAF homodimers as well as BRAF-CRAF heterodimers and inhibit downstream ERK signaling in both types of RAF dimers. However, with CRAF-homodimers, PLX8394 promotes ERK signaling.[133] Interestingly,

PLX8394 selectively targets RAS-independent RAF signaling, showing the necessity for a wide array of inhibitors to treat specific cancers.

MEK

Once released from inhibition, active RAF can then activate MEK through phosphorylation of serine resides at positions 218 and 222[130]. Mutations in MEK can occur throughout the protein and is not restricted to specific hotspots as is common for upstream members of the MAPK pathway.[134] MEK family members include MEK1 and MEK2, both of which are serine/threonine and tyrosine kinases. While mutations in MEK1 are relatively rare, MEK1 mutants can be further divided into three classes, based on the necessary of activation by RAF.[126] When S218 and S222 are mutated to alanine, the class of MEK mutant determines its ability to phosphorylate ERK. The first class of MEK1 inhibitors is RAF-dependent. S218A or S222A inhibits phosphorylation of ERK. The second class, RAF-regulated mutants, have some activation of ERK with the mutations but less than non-mutated MEK. Finally, the third class is RAF-independent. In this class, regardless of the mutations of the normally phosphorylated serine residues, phosphorylation of ERK is always present and high.[134]

Although MEK mutations occur in ~1% of human cancers, various inhibitors have been developed to target MEK and many are allosteric kinase inhibitors.[126] Many inhibitors are in clinical trials, including trametinib, MEK162, and cobimetinib.[135] While these have shown some clinical benefits, more robust effects may be seen when used in combination with other therapies. When used in combination with the chemotherapeutic agent docetaxel, selumetinib improved survival in NSCLC patients.[136] Moreover, melanoma patients with $BRAF^{V600}$ mutations treated

with trametinib as well as dabrafenib has significantly higher progression-free survival then with monotherapy alone.[137,138] More recently, MEK inhibitors such as MAP855 have been developed that are ATP-competitive and are thought to be more robust as they are likely to be unaffected by the activation state of MEK.[126]

MAPK (ERK1/2)

The primary downstream target of MEK is MAPK/ERK1/2 as shown in Figure 5. Once phosphorylated by MEK, ERK1/2 can either remain in the cytosol or translocate to the nucleus and phosphorylate over 70 substrates[139] with a wide range of functions, including proliferation, differentiation, and cell division.[138] These substrates include JNK[140], MYC[141], and CREB[142]. Mutations in ERK1/2 are quite rare in cancers making up less than 1% of cancer-related mutations.[126] For this reason, development of inhibitors for ERK1 or ERK2 is less advanced relative to RAF or MEK. Moreover, as ERK1/2 is the only known substrate of MEK, inhibitors against MEK were considered to be of greater importance. However, more attention has been given to ERK1/2 in recent years, owing to the challenges of RAF and MEK inhibitors in clinical trials, as well as the robust feedback signaling mechanisms of the MAPK pathway.[121] ERK inhibitors such as SCH772984 or VTX11e are ATP competitive ERK inhibitors and have shown some potential in preclinical studies. However, as with RAF and MEK inhibitors, the use of ERK inhibitors in clinical settings may be limited. This is due to the fact that prolonged exposure to ERK inhibition can cause cancer cells to acquire resistance to the treatment due to the development of ERK mutations that are favorable to cancer cell survival.[143]

Upon activation, ERK1/2 activates various transcription factors, often related to cell proliferation.[139] The sequential activation of RAS, RAF, MEK and ERK greatly enhance signal amplification, causing robust biological effects. Cancer cells are able to hijack these pathways, leading to the aberrant activation of ERK1/2-mediated oncogenic signaling, thereby promoting abnormal proliferation. Nearly every step of this process is governed by regulated feedback inhibition. For instance, once phosphorylated, active ERK1/2 can then use phosphorylation to inhibit the activated RTK, SOS, RAF, and MEK.[144] Moreover, scaffolding proteins have been discovered that are important for proper alignment of the members of the MAPK pathway and proper execution of signal transduction. Perhaps the most well-studied of these is kinase suppressors of RAS (KSR1).[145] Following activation, ERK1/2 can phosphorylate RAF and KSR1, thereby decreasing their association with the membrane and attenuating the growth factor-mediated signal.[146] RSK is another kinase that can also use phosphorylation to inhibit activated members of the MAPK pathway and halt signal transduction.[144,147] This multistep feedback regulation is crucial to ensuring proper cellular function. Due to the importance of feedback inhibition, targeting the MAPK pathway can lead to unforeseen consequences, and may explain why many inhibitors have failed in clinical trials. Both MEK and ERK inhibit RAF through feedback inhibition; however, when they are inhibited, RAF is released from this inhibition and can go on to active non-canonical downstream effectors, promoting anti-apoptotic cascades.[138]

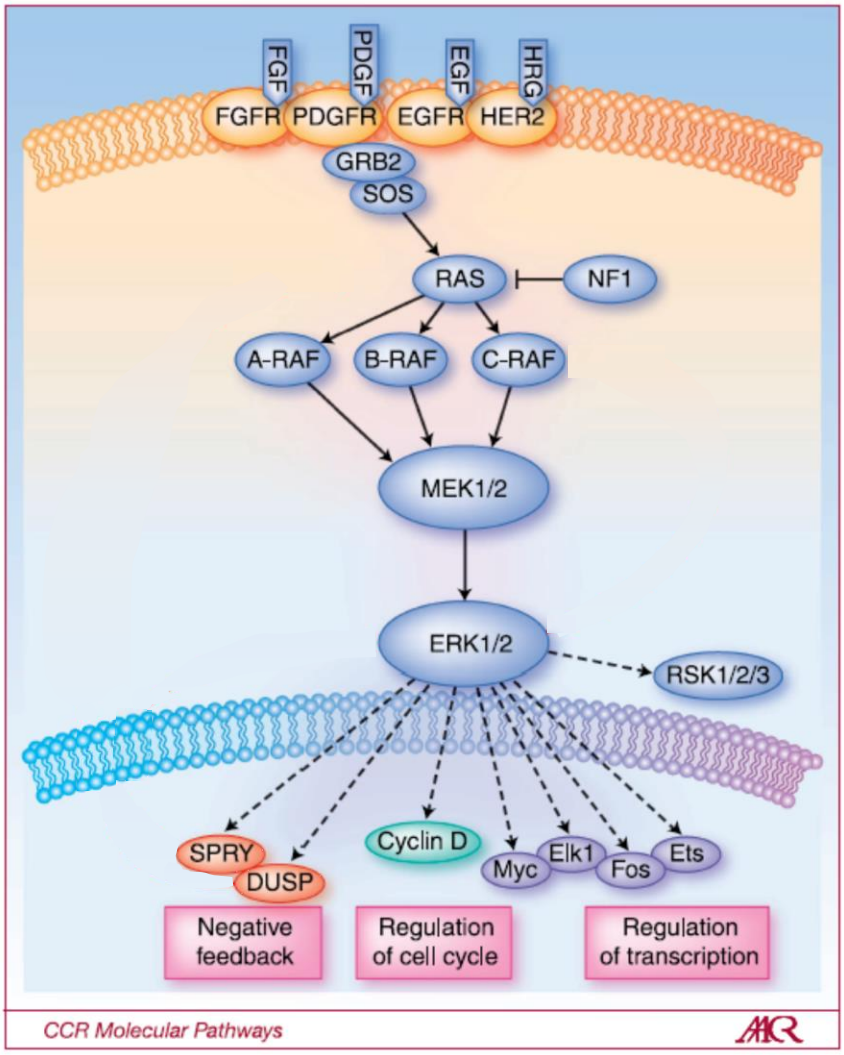

Figure 5: Schematic depiction of the MAPK signaling pathway

Following ligand binding to its respective receptor, downstream adaptor proteins activate RAS-GTP. This activates RAF, which phosphorylates MEK. Active MEK subsequently phosphorylates ERK1/2, which can then activate numerous substrates to affect cellular processes. Adapted from Pratilas & Solit, 2010, *Clin Can Res*.[148]

Caveolin

The MAPK pathway is modulated by various factors within the cell, such as spatiotemporal regulation and negative feedback signaling.[144] Another such modulation is the recruitment of members of the MAPK pathway to caveolae. Caveolae are small membrane invaginations that have been linked to a number of different cellular functions, including endocytosis, protein trafficking, cholesterol transport, and signal transduction.[149] Caveolae are found in the non-planar lipid rafts of the plasma membrane, which also house GPI-anchored proteins. Caveolae are also thought to play a role in maintain membrane organization by acting as a scaffold and sequesters inactive proteins till a signal instructs otherwise.[150] Caveolin proteins are main components of caveolae and come in three isoforms: CAV-1, CAV-2, and CAV-3. CAV-1 and CAV-2 are found in non-skeletal tissues and are capable of heterodimerization. CAV-3 is primarily found in muscle, but some evidence has also been shown for its presence in glia.[150,151] Another important component of caveolae is the cavin family. Cavins are cytosolic proteins that can be recruited to the caveolar domains and have four known isoforms: cavin 1, cavin 2, cavin 3, and cavin 4. Each isoform has a coiled-coil α-helical domain and a membrane association domain and form oligomeric complexes.[149] In cavin-expressing cells, cavin proteins are required for proper formation of caveolae and mice lacking cavin have decreased levels of caveolins. Although the precise function of cavins is still being investigated, they are accepted as crucial members of caveola formation.[150]

The primary structural component of caveolae in tissues is caveolin-1 (CAV-1). Early in tumor progression, CAV-1 suppresses tumor-promoting signaling pathways.[151] However, CAV-1 has a stage-dependent role, whereby it becomes oncogenic in more advanced cancers, including

GBM.[152] Interestingly, this pattern is different for stroma. Stromal cells normally have relatively high levels of CAV-1; however, loss of stromal CAV-1 is directly associated with cancer progression.[153] CAV-1 has been associated with therapy resistance in multiple cancers and may be a useful target for therapies in the future. Functionally, CAV-1 has been shown to be involved in modulating the MAPK signaling pathway, with various members of the MAPK cascade (including RAF) accumulating in caveolae following EGF stimulation[154] Some evidence also indicates that CAV-1 and KSR1 interact and facilitate ERK1/2 activation.[155] EGF stimulation recruits CAV-1 to early endocytic compartments to promote MAPK signaling.[156] While expression of CAV-1 can be variable in different cell types, CAV-1 is highly expressed in glia. In astrocytes specifically, CAV-1 has been shown to facilitate MAPK activation. ERK1/2 activation increases after astrocytes and glioma cells are exposed to reactive oxygen species (ROS) in the form of H_2O_2. In the presence of *CAV-1* siRNA however, both basal levels and ROS-induced p-ERK1/2 is diminished.[157]

In this study, we determined the function and molecular mechanisms of LY6K in GBM. We show that *LY6K* is oncogenic in GBM patients and promotes a more tumorigenic phenotype in GBM cells. Moreover, this phenotype is a result of LY6K-induced ERK1/2 signaling and this enhancement can be further modulated by EGF stimulation. Specifically, LY6K-induced ERK1/2 signaling results from the association of GPI-anchored LY6K with CAV-1. Finally, DNA methylation maintains *LY6K* silencing and irradiation induces the expression of *LY6K* via hypomethylation of *LY6K* gene promoter, thereby promoting GBM tumorigenicity and resistance to radiation therapy.

CHAPTER 2: MATERIALS AND METHODS

Cell Culture

HEK293T cells and U87 glioma cells (ATCC) were cultured in Dulbecco's Modified Eagle's Medium (DMEM, Invitrogen) supplemented with 10% fetal bovine serum (FBS) or 10% cos-FBS and 1% penicillin and 1% streptomycin. Patient-derived glioma stem-like cells (GSCs) that were previously characterized[21] were cultured in stem cell media containing DMEM/F12 (Invitrogen), supplemented with B27 (2%, Invitrogen), 1% penicillin, 1% streptomycin, heparin (5 μg/ml, Sigma-Aldrich), EGF (20 ng/ml), and basic fibroblast growth factor (FGF) (20 ng/ml, PetroTech).

Xenografts, Tumorigenicity Assays, Bioluminescent Imaging, and Immunohistochemistry Studies

All experiments using animals were conducted under an Institutional Animal Care and Use Committee (IACUC)-approved protocol at Northwestern University in accordance with NIH and institutional guidelines. Athymic (Ncr nu/nu) mice at six weeks of age (Taconic Farms) were employed for all animal experiments as described previously.[158,159] Patient-derived GSCs (1×10^4 or 5×10^4 cells) in 2-5 μl culture media were stereotactically implanted into the left striatum of nude mice, with three to five mice per group. All mice were monitored regularly for the development of neurological symptoms due to tumor burden. Mice were maintained until the development of neurological symptoms, including hunched back, loss of body weight, reduced

food consumption, and inactivity. After development of aforementioned symptoms, mice were humanely sacrificed.

For in vivo bioluminescent imaging (BLI) of mice, tumor-bearing mice were injected 200 mg/kg of D-luciferin (potassium salt, Gold Biotechnology) before isoflurane anesthesia. Radiance (photons/s/cm2/steradian) was measured 10 min after substrate injection using Living Image 4.3.1 software (Caliper Life Sciences) or Aura software (Spectral Imaging).

For hematoxylin and eosin (H&E) staining of brain sections, mice were humanely euthanized two to four weeks after implantation, and brains were harvested as previously described.[97,158] Each mouse brain was removed and embedded in O.C.T compound (Thermo Fisher) and stored at -80°C. Brains bearing xenografted tumors were sectioned on a cryostat (Leica) at 8-10 μm thickness. The whole brain was sectioned from most anterior to posterior. Every fifth tumor-bearing brain section of each brain was subjected to H&E staining to determine the locations from beginning to the end of each tumor. After careful comparison, the section with the largest tumor area in each tumor-bearing brain was used for the measurement. Tumor volume was estimated by using the formula $V = \frac{ab^2}{2}$, where a and b are the length and width of the tumor, respectively.

Bioinformatic Analyses

RNA-seq data of expression levels of LY6K and CAV-1 gene expression levels in GBM and low-grade glioma (LGG) of TCGA datasets were downloaded from FireBrowse (http://firebrowse.org/). This includes 530 LGG and 166 GBM samples. A total of 47 classical, 63

mesenchymal, and 39 proneural subtype tumors were included in GBM samples. The Mann-Whitney U-test was performed to determine whether LY6K and/or CAV-1 were differentially expressed in GBM and LGG. One-way ANOVA with the Student-Newman-Keuls post-hoc test was used for the comparison of means among groups. Kaplan-Meier survival analyses were used to assess the correlation between LY6K and/or CAV-1 and overall survival time in patients with gliomas. In the analyses of the TCGA dataset, the median or quartile expression of LY6K and/or CAV-1 in all glioma samples were selected as a cutoff to divide samples as high-and low-expression groups. In addition, a second dataset from GSE4271 was used to confirm the results of TCGA analyses.[160] The numerical data were presented as mean ± standard deviation (SD) of at least three determinations.

For amplification/copy number gain and expression data for *LY6K* (see Figure 7), data were analyzed and downloaded from cBioPortal.[161,162] Amplification, as defined by cBioPortal, indicates high-level amplification/copy number gain. Values are generated from the GISTIC or RAE algorithms. The threshold for amplification/copy number gain for individual cancers is defined by the specific study from which the alteration frequency was generated and details can be viewed in the respective studies.[161,162]

Lentiviral Plasmids & Infection

TRC lentiviral control and target-specific shRNA vectors were purchased from Dharmacon (LY6K: TRCN0000117952 and TRCN0000117956; CAV-1: TRCN0000007999 and TRCN0000011218). TRCN0000117952 (referred to as shL1 in the figures) targets the 5'-UTR of *LY6K* and TRCN0000117956 (referred to as shL2 in the figures) targets the body of the gene. For

LY6K overexpression, the LY6K open reading frame (ORF) was inserted into the pCMV6-Entry vector to generate a construct containing LY6K including Myc and DDK tags. The resulting cDNA fragment was then subcloned into the pCDH-EF1-MCS-IRES-RFP vector to generate pCDH-LY6K lentiviral construct.

For rescue experiments, GSC83 or GSC30 cells stably expressing a lentiviral shRNA vector that targets the 3'-UTR of *LY6K* (TRCN0000117952; shL1) were infected with the *pCDH-LY6K*. For GSC83 or GSC30 cells expressing a lentiviral shRNA vector that targets the body of *LY6K* (TRCN0000117956; shL2), a mutated version of the *LY6K* gene was used. Specifically, the 3rd base of three codons were mutated in the shRNA target gene sequence. This ensured that all mutations were silent, thereby resulting in no change in the amino acid sequence, but rendering the construct resistant to the shRNA based on the sequence. Site-directed mutagenesis was performed with a QuikChange Site-Directed Mutagenesis Kit (Agilent), according to the manufacturer's instructions.

For the LY6K-ΔGPI domain deletion mutant, cloning was performed as described for LY6K-WT above. The open reading frame (ORF) for LY6K-ΔGPI excluded the region of the LY6K gene starting at the most likely ω site (GPI-attachment site),[163] as predicted by UnitProt (www.uniprot.org/uniprot/Q17RY6).

For lentiviral infection, HEK293T cells were seeded at a density of 40 to 50% in 10cm dishes on the evening prior to the transfection. During the morning of the transfection, 6 μg of *psPAX2*, 6 μg of *VSV-G*, and 12 μg of the target vector (shRNA against *LY6K* or *CAV-1*, or full-length *LY6K* or *LY6KΔGPI*) were transfected into cells using polyethylenimine (PEI) as the

lipophilic agent. Serum-containing media was changed 4-6 hours after transfection and cells were incubated for 48 hours at 37^0C. To establish stable cell lines, the HEK293T supernatants containing lentivirus were harvested with polybrene (10 mg/ml, Sigma) and used to infect target cells. 72 hours after transduction, infected cells were selected with fluorescence-activated cell sorting (FACS).

Cell Proliferation Assays

In vitro cell proliferation assays were performed as previously described[97]. Briefly, GSC spheres or U87 glioma cells were dissociated into single cells, and cell density was quantified by counting viable (Trypan Blue-negative) cells using a hematocytometer. Cells were seeded into 24-well or 48-well plates (three wells averaged per time point and three or four time points). Each well contained a density of 6,000 (GSC83 & GSC30), 9,000 (GSC528), or 15,000 (U87) cells per well. Cells were counted at two, four, six, and/or eight days using a hemocytometer. All proliferation assays were repeated three times.

Limiting Dilution Assays

Extreme limiting dilution assays (ELDA)/sphere forming frequency assays were conducted as described previously[158]. Briefly, dissociated cells from glioma spheres were seeded in 96-well plates at densities of 1, 10, 50, and 100 for all assays. For MES-like and PN-like GSCs, 7 and 14 days after seeding respectively, each well was examined for formation of tumor spheres. Subsequently, sphere forming frequencies were calculated using the ELDS software (http://bioinf.wehi.edu.au/software/elda/).[164]

In Vitro Signaling Assays

All signaling assays were conducted with starvation media, lacking either serum and/or growth factors. For all assays with U87 cells, cells were trypsinized and counted using a hemocytometer and seeded in fresh media with 10% FBS. Six hours after seeding, media was removed and replaced with fresh serum-free media overnight. For all assays with GSCs, cells were counted using a hemocytometer and seeded in fresh stem cell media. Six hours after seeding, media was removed and replaced with fresh growth factor-free stem cell media overnight. All treatments below were conducted at 37°C.

For EGF stimulation, EGF (20 ng/ml) was added to cells and incubated for 10 min. For SB590885 (BRAF inhibitor) experiments, 0.1 nM SB590885 was added to cells for 1 hour. For PD98059 (MEK inhibitor) experiments, 50 μM PD98059 was added to cells for 1 hour. For latrunculin A experiments, 10 μM latrunculin A was added to cells for 20 min. For mannosamine hydrochloride experiments, 5 mg/ml D-mannosamine hydrochloride was added to cells for 1 h at 37°C. For MG132 experiments, 10 μM MG132 was added to cells and allowed to incubate overnight at 37°C. For PI-PLC experiments, cells were counted using a hemocytometer and suspended in Opti-MEM with 2 U/ml PI-PLC for 2 hours.

Kyte-Doolittle Hydropathy plot

Kyte-Doolittle Hydropathy plot for LY6K was generated with the ProtScale tool from ExPASy (https://web.expasy.org/protscale/). The full nascent amino acid sequence for LY6K was

used as the input and the resulting plot was analyzed for hydrophobicity patterns typical of GPI-anchored proteins.

Co-Immunoprecipitation

Cells were lysed in radioimmunoprecipitation (RIPA) lysis buffer (ProteinTech) supplemented with protease and phosphatase inhibitor cocktails (Sigma-Aldrich). Lysates were pre-cleared by with 50 µl Protein A agarose bead slurry per 1 mg lysate for 1 hour at 4˚C on a rotator. They were subsequently centrifuged at 1,000 rpm for 3 min at 4˚C. After preclearing, lysates were subjected to immunoprecipitation with either 4 µg LY6K for 12 hours (ProteinTech, Cat 12026-1-AP) or 5 µg CAV-1 overnight (Thermo Fisher, Cat PA1-064) at 4˚C.

Following antibody incubation, the immunocomplex was captured with 50 µl Protein A agarose bead slurry and incubated at 4˚C (LY6K 12 hours; CAV-1 5 hours). The pull-down complex was then washed and eluted twice with a glycine elution buffer. Eluents were pooled, neutralized, and subjected to immunoblotting (IB) analysis with 4X sodium dodecyl sulfate (SDS) sample buffer. Lysates were heated for 10 min, run on a 12% SDS gel, subjected to electrotransfer, and subsequently probed using appropriate antibodies.

Immunoblotting (IB) Analyses

Cells were lysed directly with 2X sodium dodecyl sulfate (SDS) buffer supplemented with protease and phosphatase inhibitor cocktails (Sigma-Aldrich). Protein samples were subjected to SDS- 12% polyacrylamide gel electrophoresis (PAGE) and transferred to polyvinylidene fluoride (PVDF) membranes. Blocked membranes were incubated with indicated antibodies overnight at

4°C (1:500 or 1:1000). For all IB analyses, glyceraldehyde 3-phosphate dehydrogenase (GAPDH) was used as the loading control. Antibodies used include anti-LY6K (ProteinTech, Cat 12026-1-AP), anti-GAPDH (Santa Cruz, Cat sc-47724), anti-p-ERK1/2 (Cell Signaling, Cat 9101S), anti-ERK1/2 (Cell Signaling, Cat 9102S), anti-p-AKT (Cell Signaling, Cat 4060S), anti-AKT (Cell Signaling, Cat 9272S), anti-p-EGFR (Cell Signaling, Cat 3777S), anti-EGFR (BD, Cat 610016), anti-CAV-1 (Thermo Fisher, Cat PA1-064), anti-p-GSK3β (Cell Signaling, Cat 9331S), anti-GSK3β (Cell Signaling, Cat 5676S), anti-p-SMAD2 (Cell Signaling, Cat 8828S), anti-SMAD2 (Cell Signaling, Cat 3102S), anti-p-SRC (Cell Signaling, Cat 2101S), anti-SRC (Santa Cruz, Cat sc-19), anti-p-STAT3 (Cell Signaling, Cat 9131S), anti-STAT3 (Cell Signaling, Cat 9132S), anti-p-PDGFRα (Santa Cruz, Cat sc-12910-R), anti-PDGFRα (Cell Signaling, Cat 3164), anti-p-AXL (R&D Systems, Cat AF2228), anti-AXL (R&D Systems, Cat AF154), anti-p-MET (Upstate Cell Signaling Solutions, Cat 07-211), and anti-MET (Santa Cruz, Cat sc-10) antibodies. Following washing with 0.1% TBS-T, membranes were incubated with corresponding peroxidase-labeled secondary antibodies (1:1000). Blots were developed with enhanced chemiluminescence (ECL, Amersham Bioscience) reaction according to manufacturer's instructions.

Immunofluorescent (IF) Staining

Cells were cultured in chamber slides and fixed with 4% formaldehyde (Fisher) for 30 min. Cells requiring permeabilization were subsequently treated with 0.2% Triton X-100 for two min. Cells were blocked with AquaBlock (East Coast Bio, North Berwick, ME) for 60 min and probed with an anti-LY6K antibody (Abnova Cat PAB21148, 1:100) overnight at 4°C. For co-localization experiments, cells were also probed with an anti-CAV-1 antibody (BD Cat 610493, 1:100)

overnight at 4°C. After being washed three times with PBS, cells were incubated with Alexa 488 labelled secondary antibodies (1:200) and DAPI-containing mounting solution Vectashield (Vector Laboratories), and then visualized by using a Nikon A1R (A) Spectral laser scanning confocal microscope.

Methylation Analyses

Genomic DNA (gDNA) extraction was performed using QIAamp DNA Mini Kit (Qiagen) and used for Illumina 450K array profiling that interrogates 485,577 CpG loci at the NUSeq Core at Northwestern University. Chip processing was carried out according to manufacturer's instructions. The signal intensities obtained from the Illumina GenomeStudio was converted to β-values and normalization was carried out to remove biases between the Infinium I and II probes using established normalization protocols.[165,166] Probes on X and Y-chromosomes were also removed. In order to preserve the biological variations on methylation profiles among different subtypes, no further normalization was performed.[166] In addition to removal of X and Y chromosomes (~12,000 probes), we carefully examined any technical biases. Probes that had unusual distribution of β-values (high variance) on the same sample subtypes were removed. After refining the data, we had a total of 386K probes. Thus, we analyzed approximately 85% of probes to identify differential methylation patterns. Therefore, the probes eliminated due to high variance or positioning on the X and Y chromosomes is about 15%. Data were deposited to GEO with a deposit number of GSE90498.

Methylation analyses of *LY6K* CpG island promoter region was carried out using combined bisulfite and restriction analyses (CoBRA) and direct bisulfite sequencing and confirmed with

clone sequencing as previously described.[102,158] Bisulfite conversion of gDNA was carried out prior to CoBRA analyses using Epitect Bisulfite kit (Qiagen), according to manufacturer's instructions. Methylated positive controls were also generated by incubating unconverted samples with S-Adenosyl methionine (SAM) and DNA methyltransferase (New England Biolabs) at 37°C for 2 hours. Nested CoBRA primers were designed using previously published standard primers designing criteria for bisulfite converted gDNA.[102] 10 µl PCR product was treated for 1 hour with Bsh1236I (Thermo Scientific) at 37°C. After digestion, samples were resolved by agarose gels. Digested (methylated) samples showed multiple bands on the gel, while undigested (unmethylated) samples showed one band matching the uncut samples.

Direct bisulfite sequencing was carried out using agarose gel-purified bisulfite PCR products with the QIAquick Gel Extraction Kit (Qiagen). Samples were then directly submitted to the NUSeq Core. The sequencing chromatograms were compared to the genomic *LY6K* sequence to determine which CpG sites had been subjected to bisulfite conversion and thus were methylated. For each sample, 10 ng of DNA and 10 picomoles/µl primer was used for sequencing. To confirm the results, gel-purified bisulfite PCR products were then subcloned into pGEM-T (Promega, Cat#: A3600). Successful clones were extracted and sequenced by using T7 promoter sequencing primer at the NUSeq Core and subjected to the chromatogram analysis described above. Each sequencing reaction was carried out with samples in triplicates.

Ionizing Radiation (IR) Treatment

GSCs were dissociated into single cells and placed in 6-well plates. Cells were then subjected to 2 Gy IR using an X-Ray Irradiator (RS-2000 Series by Rad Source Technologies,

Inc), followed by incubation at 37°C. Cells were collected at 24, 72, and 120 hours, and 10 days after IR and subjected to bisulfite sequencing analyses. For cell proliferation assays following IR, cells were seeded into 48-well plates and subjected to 2 Gray IR. They were then monitored for proliferation over the next eight days.

Statistics

Statistical analysis was carried out using Microsoft Excel and GraphPad Prism version 5.0 for Windows. Analysis included one-way analysis of variance (ANOVA) with Newman-Keuls post-hoc test and paired two-way Student t-test. Log-rank tests were used to determine significance of Kaplan-Meier curves.

CHAPTER 3: RESULTS

Elevated Expression of LY6K is Inversely Correlated with GBM Patient Survival

(Figures 6 & 7)

Analysis of our previously published gene expression profiling data between PN- and MES-like GSCs[21] showed *LY6K* being among the most highly differentially expressed genes (Fig. 6A). Interestingly, *LY6K* was one of many cancer testis antigens that was differentially expressed between these subtypes. Similar to other types of human cancers, the primary aberration in *LY6K* seen in gliomas was amplification/copy number gain based on the Cancer Genome Atlas (TCGA) data and various publicly available datasets (Fig. 7A), with no known mutations in gliomas (Fig. 7B). Multiple datasets showed that GBM patients with elevated *LY6K* expression had shorter survival compared to patients with lower levels of *LY6K*, illustrating its clinical importance (Fig. 6B, Fig. 7C).[65,160] Moreover, GBM patients under 60 years of age with lower levels of *LY6K* experienced relatively longer survival (Fig. 6C). *LY6K* expression was not prognostically significant when considering tumor *IDH1* status, *TP53* status, or gender (data not shown). Furthermore, MES GBM had relatively higher levels of *LY6K* when compared to PN GBM, and Grade IV gliomas have higher levels of *LY6K* than Grade III, indicating that *LY6K* expression is correlated with the glioma tumor progression (Fig. 6D, Fig. 7D). Consistent with our gene expression profiling data, LY6K protein expression was higher in MES-like GSCs relative to PN-like GSCs, which had undetectable levels (Fig. 6E). Furthermore, its expression in established glioma cell lines was nearly undetectable when compared with HeLa cells, which express LY6K at very high levels (Fig. 6F).

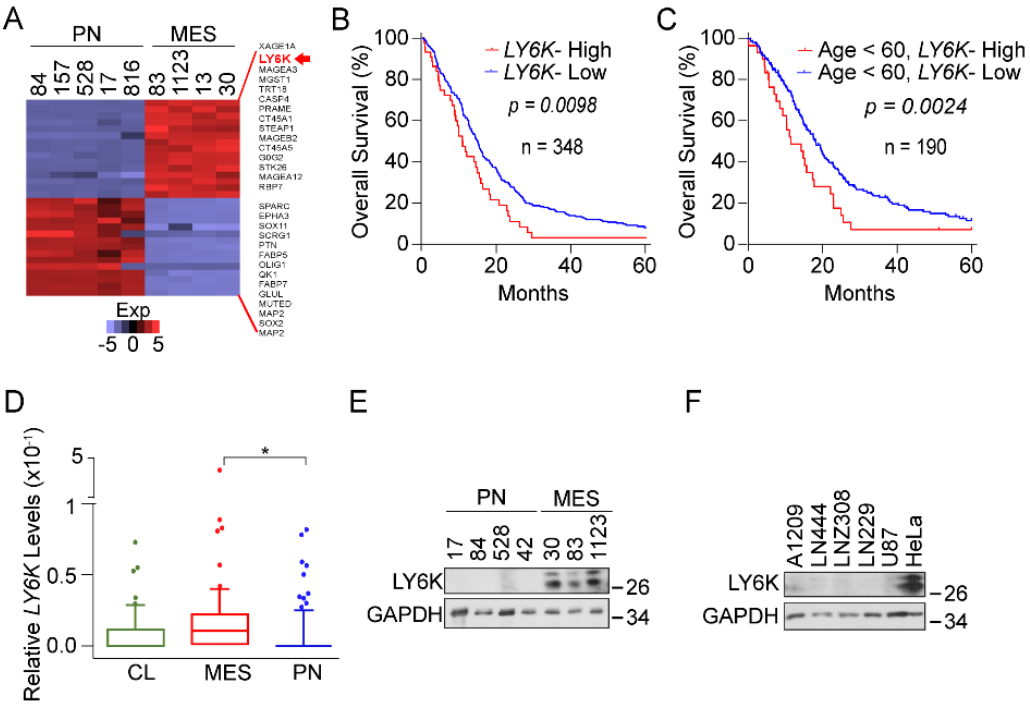

Figure 6.

Elevated expression of LY6K is inversely correlated with GBM patient survival. (**A**) *LY6K* was among the top differentially expressed genes in MES-like GSCs, relative to PN-like GSCs. (**B**) *LY6K* expression correlated with poor patient survival in GBM samples in a five-year analysis of TCGA datasets. (**C**) Among all tested variables, only age (below 60 years) correlated with poor survival in GBM patients in multivariate analyses with *LY6K* in TCGA datasets. (**D**) Expression of *LY6K* was higher in MES GBM samples, relative to CL or PN in TCGA datasets. (**E** and **F**) Immunoblot (IB) for LY6K expression in PN-like and MES-like GSCs (E) and established GBM cell lines as well as HeLa cells (**F**). Data are representative of three independent experiments with similar results. *p < 0.05.

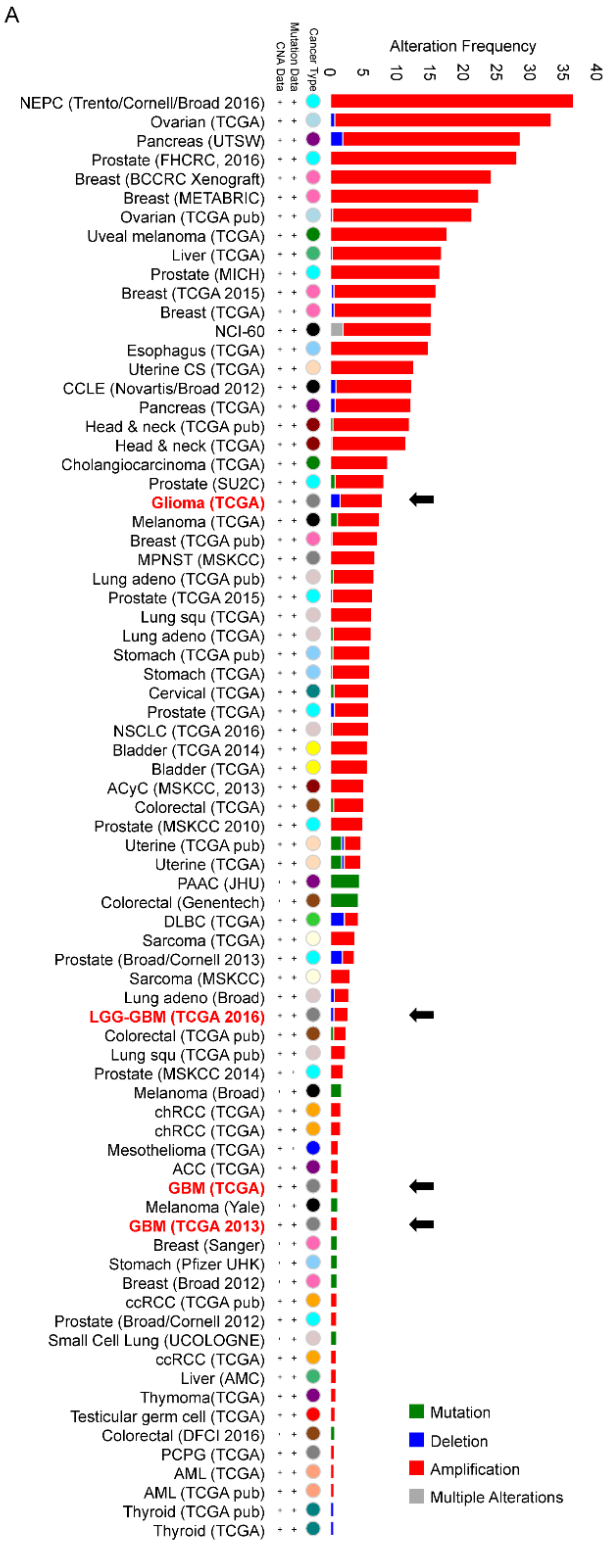

Figure 7.

LY6K is frequently amplified or has copy number gain in clinical cancers. (**A** and **B**) RNA Seq analysis of TCGA data. *LY6K* is amplified or has copy number gain across various cancer types. Only cancers with alteration frequencies above greater than 0% are shown (A). Few mutations and splice variants of *LY6K* have been discovered, but none have been observed in gliomas (B). For A & B: Arrows and corresponding text in red indicate data from glioma or GBM. (C-D) Analyses of dataset GSE4271. Expression of *LY6K* is associated with GBM prognosis (C) and tumor progression (D). *p < 0.05.

Continued on next page

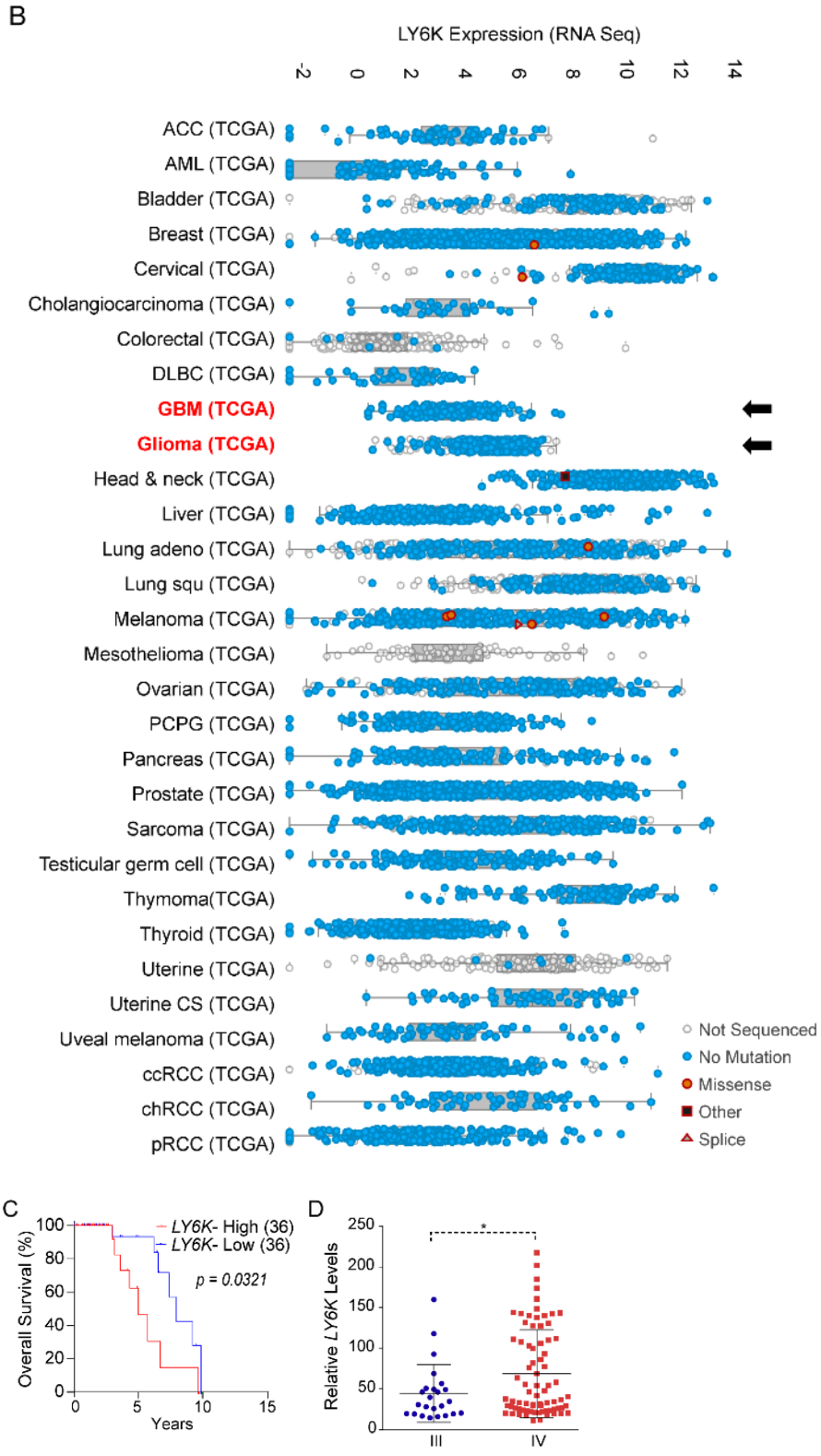
B
LY6K Expression (RNA Seq)
-2
0
2
4
6
8
10
12
14
ACC (TCGA)
AML (TCGA)
Bladder (TCGA)
Breast (TCGA)
Cervical (TCGA)
Cholangiocarcinoma (TCGA)
Colorectal (TCGA)
DLBC (TCGA)
GBM (TCGA)
Glioma (TCGA)
Head & neck (TCGA)
Liver (TCGA)
Lung adeno (TCGA)
Lung squ (TCGA)
Melanoma (TCGA)
Mesothelioma (TCGA)
Ovarian (TCGA)
PCPG (TCGA)
Pancreas (TCGA)
Prostate (TCGA)
Sarcoma (TCGA)
Testicular germ cell (TCGA)
Thymoma(TCGA)
Thyroid (TCGA)
Uterine (TCGA)
Uterine CS (TCGA)
Uveal melanoma (TCGA)
ccRCC (TCGA)
chRCC (TCGA)
pRCC (TCGA)
Not Sequenced
No Mutation
Missense
Other
Splice
C
Overall Survival (%)
100
80
60
40
20
0
0
5
10
15
Years
LY6K- High (36)
LY6K- Low (36)
p = 0.0321
D
Relative LY6K Levels
250
200
150
100
50
0
III
IV
*

LY6K Promotes GSC Proliferation, Sphere Forming Frequencies, and Tumorigenicity

(Figures 8 & 9)

To analyze the tumor-promoting potential of *LY6K* in GSCs, we utilized short hairpin RNAs (shRNAs) to suppress *LY6K* expression in two MES-like GSC lines, GSC83 and GSC30, both of which have high endogenous expression of *LY6K* (Fig. 6E). To ensure shRNA specificity, we used two different shRNAs each targeting separate regions of the *LY6K* gene. shL1 targets the 3'-untranslated region (UTR) of the *LY6K* mRNA, while shL2 targets the body of the *LY6K* mRNA. In both cell lines, knockdown (KD) of *LY6K* significantly inhibited GSC proliferation (Fig. 8A), indicating that LY6K may be important for cell growth. KD also significantly decreased glioma sphere-forming frequencies (Fig. 8B). The ability of cells to form spheres is an indication of their stemness; therefore, enhanced glioma sphere forming abilities indicates that GSCs are relatively more tumorigenic. Finally, we implanted *in vivo* tumor xenografts using these GSCs and measured tumor growth using bioluminescent imaging (BLI) in xenograft-bearing immunocompromised nude mice and hematoxylin/eosin staining on brain sections with xenografts (Fig. 8C, Fig. 9A). Mice bearing xenografts with GSCs that have KD of *LY6K* developed significantly smaller tumors, relative to those with high endogenous *LY6K* levels, as quantified in Figure 9A.

We then tested the specificity of the tumor-promoting roles of *LY6K* in MES-like GSCs by conducting rescue experiments. After knocking down *LY6K*, we subsequently re-expressed *LY6K* by exogenously expressing shRNA-resistant *LY6K* in these GSCs. Rescuing *LY6K* restored cell proliferation (Fig. 8D) and sphere-forming frequencies (Fig. 8E) *in vitro*. We also measured *in*

vivo tumor growth and monitored animal survival using rescue constructs and observed that re-expression of *LY6K* decreases animal survival and increases tumor volumes to levels comparable to controls (Fig. 8F, Fig. 9B). To further demonstrate the specificity of *LY6K*-induced tumorigenicity, we overexpressed *LY6K* in GSC528 and U87 cells. GSC528 is a PN-like GSC line and U87 is an established glioma cell line. Both cell lines have undetectable levels of endogenous LY6K (Figs. 6E, 6F) As expected, exogenous expression of *LY6K* in these cells promoted cell growth and sphere-forming frequencies (Fig. 8G, 8H, 8I). Taken together, these results indicate that elevated expression of *LY6K* enhances tumorigenicity both *in vitro* and *in vivo*.

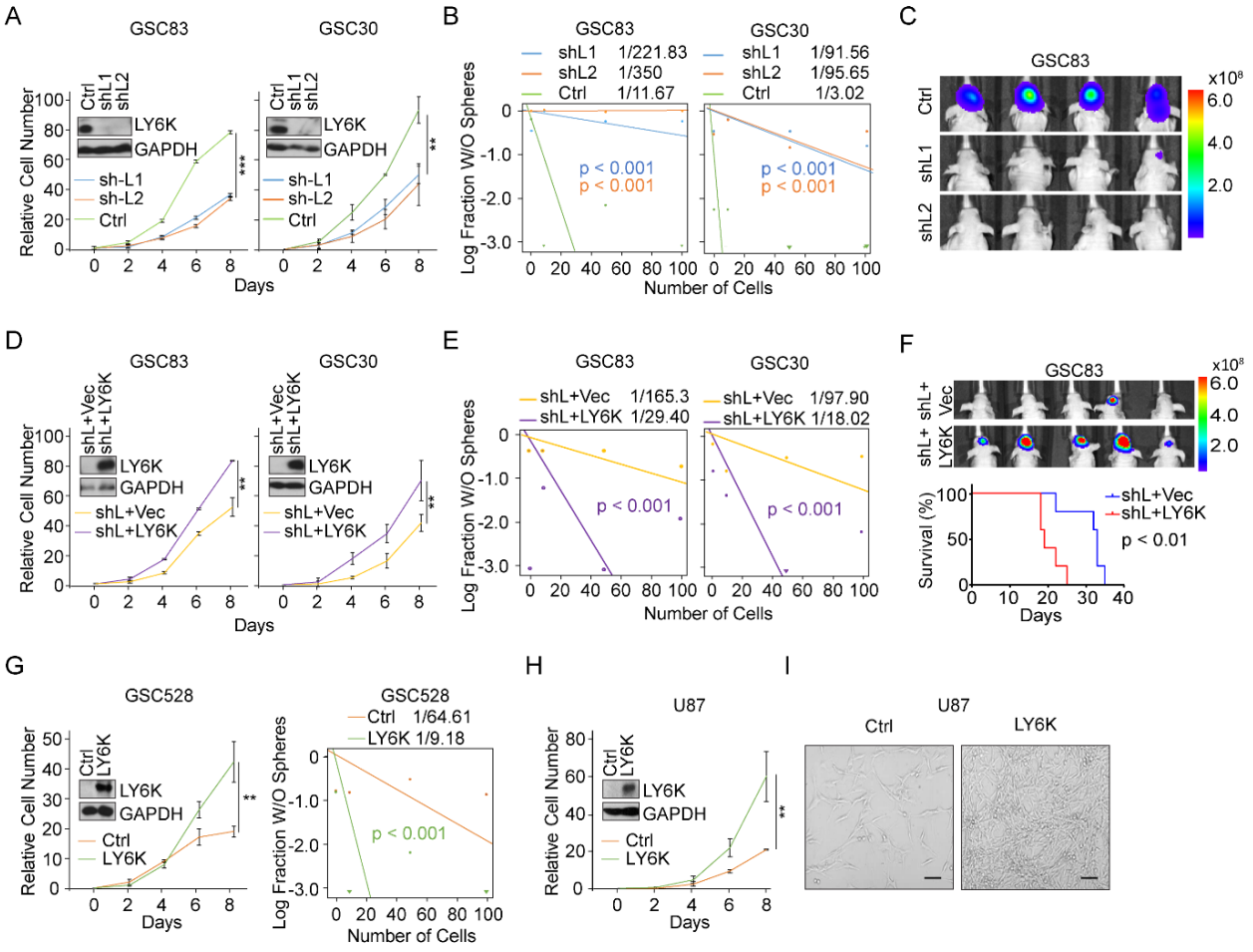

Figure 8.

LY6K enhances GBM cell proliferation, sphere-forming frequencies, and tumorigenicity. (**A** to **C**) In MES-like GSC83 and GSC30, knockdown of *LY6K* suppressed cell proliferation (**A**), sphere-forming frequencies (**B**), and *in vivo* tumor growth (**C**). (**D** to **F**) Rescuing *LY6K* in GSC83 and GSC30 with knockdown of endogenous *LY6K* restored cell proliferation (**D**), sphere-forming frequencies (**E**), and *in vivo* tumor growth and survival (**F**). For (**F**) Top, BLI. Bottom, Kaplan-Meier survival analysis. (**G**) Overexpression of exogenous *LY6K* in GSC528 increased cell proliferation (left) and sphere-forming frequencies (right). (**H**) Overexpression of *LY6K* in U87 cells increased cell proliferation. (**I**) Bright-field phase contrast representative images showing cell growth at Day 8 of proliferation assay from (**H**). Scale bar in (**I**) is 100 μm. Insets in (**A**), (**D**), (**G**), (**H**): IB for LY6K and GAPDH (loading control) in indicated GSCs or GBM cells. Data are representative of two to three independent experiments with similar results. **p < 0.03, ***p < 0.01.

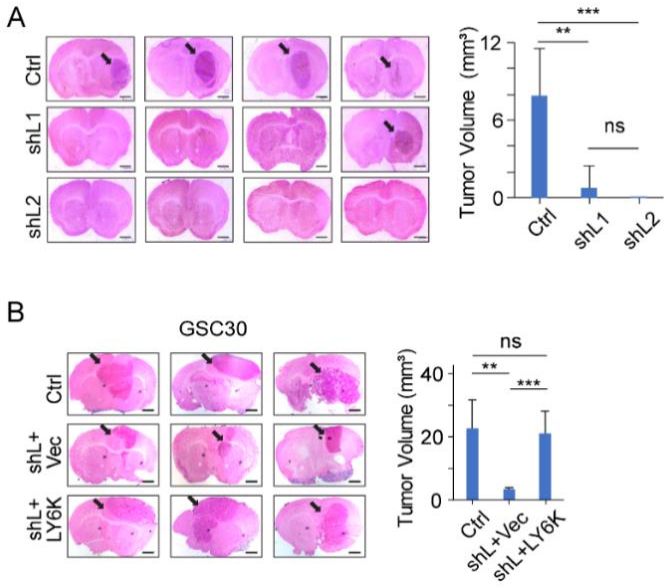

Figure 9

LY6K promotes GBM tumorigenicity *in vivo*. (**A**) H&E staining analysis of mouse brain sections with GSC83 tumor xenografts with indicated modifications. Graph on right shows quantification of tumor volume in indicated GSC83 xenograft tumors. (**B**) H&E staining analysis of mouse brain sections with GSC30 tumor xenografts with indicated modifications. Graph on right shows quantification of tumor volume in indicated GSC30 xenograft tumors. Scale bar in (**A**) and (**B**) is 200 μm. Data are representative from two to three independent experiments with similar results. **p < 0.03, ***p < 0.01.

LY6K Enhances ERK1/2 Activation in GSCs and U87 Cells

(Figures 10, 11 & 12)

To determine the mechanisms underlying the tumorigenic effects of *LY6K* expression, we examined downstream signaling mediators of signaling pathways known to be aberrantly activated in GBM.[8,109] These mediators include phosphorylated (p)-AKT (PI3K/AKT/mTOR pathway), p-ERK1/2 (RAS/RAF/MEK/ERK pathway), p-GSK3β (WNT/Frizzled/GSK3β/β-catenin pathway), p-SMAD2 (TGFβ/SMAD2 pathway), p-SRC (SRC/FAK pathway), and p-STAT3 (JAK/STAT3 pathway) (Fig. 11A). Of these, only p-ERK1/2 levels consistently displayed marked decreases when endogenous *LY6K* was knocked down in GSC83 in GSC30 cells (Fig. 10A). ERK/MAPK signaling is an established cell proliferation pathway and the changes seen in p-ERK1/2 signaling are consistent with the proliferative phenotypes seen in Figure 8. Subsequent re-expression of LY6K in these cells rescued p-ERK1/2 levels. Consistent with these findings, in GSC528 and U87 cells which have undetectable endogenous expression of *LY6K*, exogenous expression of *LY6K* markedly increased p-ERK1/2 levels (Fig. 10B). For both aforementioned experiments, no appreciable alteration in levels of p-AKT was observed (Figs. 10A, 10B), indicating that LY6K selectively induces ERK1/2 signaling in GSCs.

Interestingly, we also observed the effect of LY6K overexpression in JK42, a GSC line that has undetectable levels of endogenous LY6K but has very high levels of p-ERK1/2 (data not shown). We found that in JK42 cells, overexpression of LY6K has no change in p-ERK1/2, as the p-ERK1/2 levels are endogenous saturated. Moreover, we found no change in cell growth in JK42

cells, regardless of LY6K expression, indicating that LY6K may only act on ERK1/2 signaling when there is space to modulate the levels of activated ERK1/2.

Given that ERK1/2 activation is known to be a downstream effect of EGFR signaling in GBM,[105] we examined EGFR as a potential upstream initiator of LY6K-induced ERK1/2 activation. We chose to conduct these experiments in GSC528 and U87 cells because they have undetectable or low levels of endogenous EGFR expression respectively. In both cell lines, p-ERK1/2 levels increased in response to LY6K overexpression. Upon EGF stimulation, cells overexpressing LY6K showed further enhancement of p-ERK1/2 levels; however, no accompanying changes in p-EGFR levels were observed. This suggests that EGFR may not be responsible for LY6K-induced ERK1/2 activation and that EGF may have a function unrelated to EGFR (Fig. 10C, Fig. 11B). To further understand the mechanistic basis of LY6K action, we treated cells with RAF and MEK inhibitors (Fig. 10D). RAF and MEK are kinases that are directly upstream of ERK in the MAPK pathway and are necessary for proper ERK activation. For RAF inhibition, we used the triarylimidazole inhibitor SB590885, which binds the ATP-binding pocket of active BRAF. This inhibitor specifically inhibits BRAF and has minimal effects on ARAF or CRAF.[167] Treatment with SB590885 yielded undetectable p-ERK1/2 levels, regardless of LY6K expression. Moreover, RAF inhibition decreased p-AKT levels, but AKT activation was still detectable. For MEK inhibition, we used the selective allosteric non-ATP-competitive inhibitor, PD98059, which binds an allosteric site and potently inhibits MEK1. Moreover, PD98059 is specific to MEK1 and does not target ERK1/2.[168] While RAF inhibition yielded no detectable levels of pERK1/2, MEK inhibition with PD98059 showed a more nuanced effect. PD98059

blocked LY6K-induced p-ERK1/2 only; thus, MEK inhibition may cause cells to retain basal p-ERK1/2 levels. To further investigate this finding, we tested the effect of SB590885 and PD98059 treatment in GSC528 cells (Fig. 11C). In this cell line, p-ERK1/2 levels were nearly undetectable when treated with either SB590885 or PD98059, potentially due to the presence of different classes of MEK proteins in these various cell lines.[126,134]

Taken together, these data indicate that the observed modulation of ERK1/2 signaling is likely due to other dynamic changes occurring at the membrane, without involvement of EGFR. Therefore, we examined other RTKs that are frequently activated in GBM, including PDGFRα, c-MET, and AXL.[109,117] Modulation of *LY6K* expression did not affect activation of these RTKs (Fig. 11D), thus indicating that LY6K activation of p-ERK1/2 is unlikely to be related to RTK signaling in GBM cells. Since these cells did have a strong reaction to EGF, regardless of EGFR expression, we next examined whether erlotinib would have any effect. Erlotinib is an EGFR inhibitor that targets the active kinase form of EGFR.[169] We found that erlotinib does effectively curtail p-ERK1/2 levels in U87 cells, even in the presence of LY6K (Fig. 12A). However, given that EGFR does not appear to cause the changes we observed in ERK1/2 signaling, we examined other pathways that may be influenced by erlotinib. While erlotinib is best known as an EGFR inhibitor, it is also thought to be involved in the JAK/STAT signaling pathway.[170] Thus, we used another inhibitor known to inhibit JAK1 and JAK2, ruxolitinib.[171] Treatment of U87 cells with ruxolitinib did not alter p-ERK1/2 signaling, thus indicating that the JAK/STAT pathway is not responsible for LY6K-induced ERK1/2 signal enhancement (Fig. 12B).

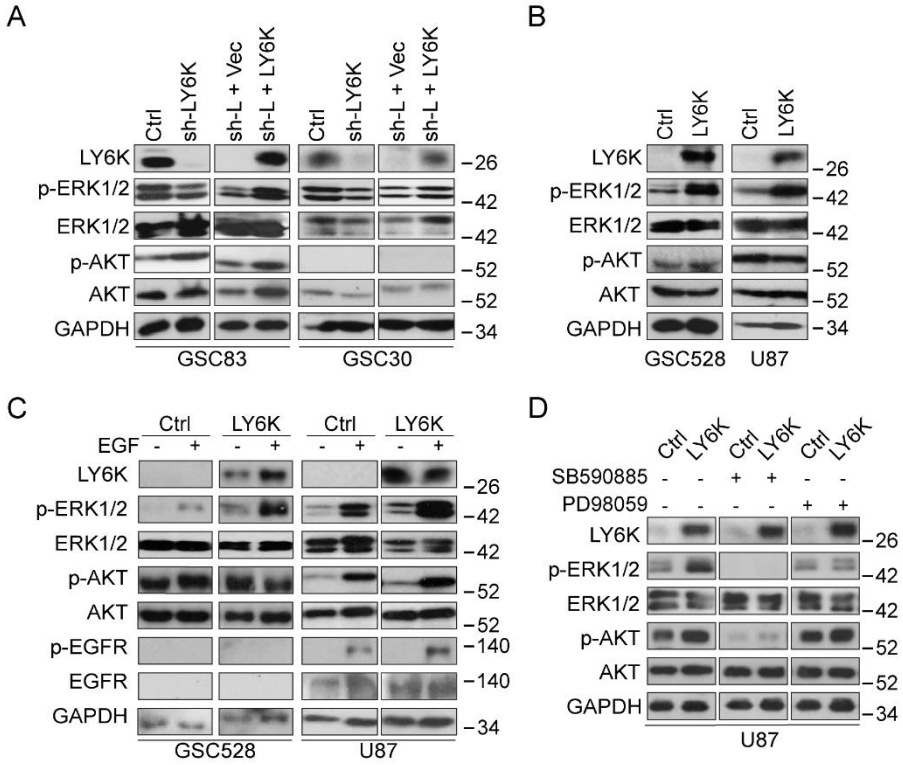

Figure 10.

LY6K promotes ERK1/2 activation in GBM cells. (**A**) IB. *LY6K* knockdown decreased pERK1/2 levels in GSC83 (left) and GSC30 (right) cells, while subsequent expression of exogenous *LY6K* restored p-ERK1/2 levels. (**B**) IB. Exogenous expression of LY6K enhanced p-ERK1/2 in GSC528 (left) and U87 cells (right) with otherwise undetectable levels of LY6K. (**C**) IB. EGF further increased LY6K-induced p-ERK1/2 levels in GSC528 and U87 cells with exogenous LY6K expression. No notable changes in p-EGFR/EGFR were observed. (**D**) IB. RAF inhibition by SB590885 strongly suppressed p-ERK1/2 expression, while MEK inhibition by PD98059 blocked LY6K-induced ERK1/2 signaling. For all IB, p-AKT/AKT were used as non-specific proteins and GAPDH was a loading control. Data are representative of three independent experiments with similar results.

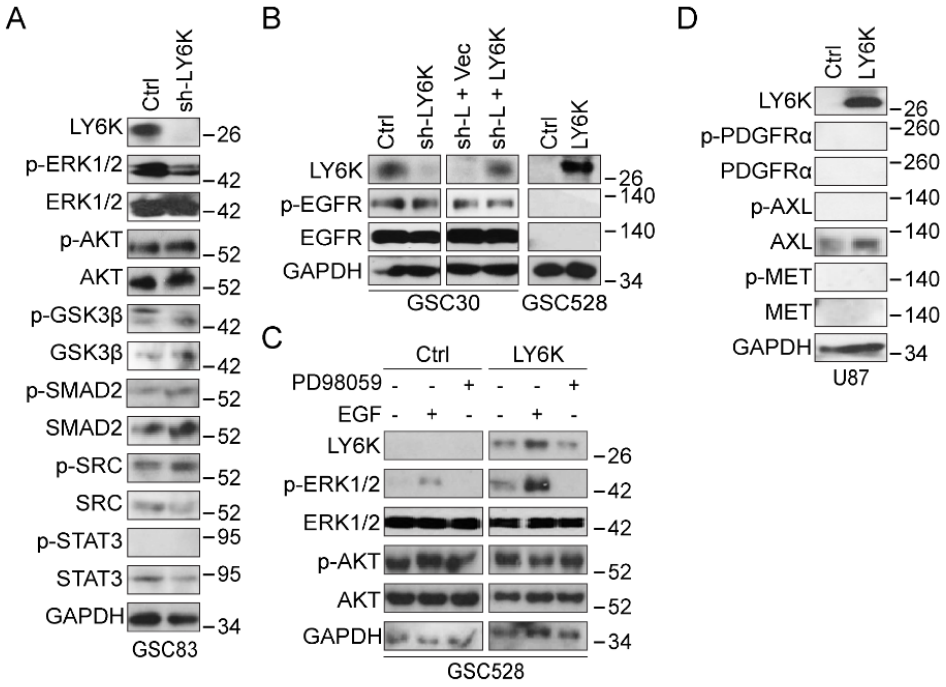

Figure 11.

LY6K selectively activates p-ERK1/2 but not other signaling pathways, and functions independent of EGFR signaling. (**A** to **D**) IB. (**A**) Of all signaling mediators tested, LY6K expression enhanced only p-ERK1/2 expression faithfully and reproducibly. (**B**) No changes in p-EGFR or EGFR were detected commiserate to the changes seen in p-ERK1/2 in GSC30 (left) cells. No p-EGFR or EGFR was detectable in GSC528. (**C**) MEK inhibitor PD98059 inhibited LY6K-induced p-ERK1/2 in GSC528. EGF induced p-ERK1/2 in GSC528 cells, despite these cells lacking EGFR expression as observed in (**B**). (**D**) Activation of PDGFRα, AXL, or c-MET was not affected by the presence of LY6K. For all IB, p-AKT/AKT were used as non-specific proteins and GAPDH was the loading control. Data are representative of three independent experiments with similar results.

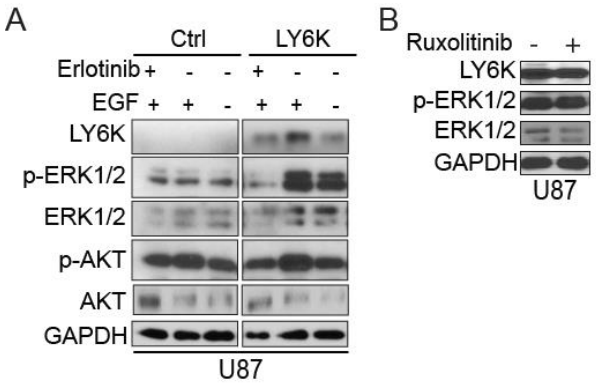

Figure 12.

LY6K responds to erlotinib, but not ruxolitinib. (**A**) In U87 cells, erlotinib causes a decrease in p-ERK1/2 levels regardless of LY6K expression. (**B**) Ruxolotinib does not alter p-ERK1/2 levels in the presence of LY6K. For IB, p-AKT/AKT were used as non-specific proteins and GAPDH was the loading control. Data are representative of two to three independent experiments with similar results.

CAV-1 Mediates LY6K Activation of p-ERK1/2 in GBM Cells

(Figure 13)

Given that the enhancement of ERK1/2 signaling resulting from LY6K is unlikely to be caused by RTK signaling, we focused on other potential activators of MAPK signaling. Since LY6K is a GPI-anchored membrane protein, we analyzed additional proteins, particular those pertaining to the membrane, that may be involved in LY6K-enhanced p-ERK1/2 activation. Reverse phase protein array (RPPA) analysis[172] identified caveolin-1 (CAV-1) as a potential interacting protein based on the correlation between *LY6K* median mRNA levels and CAV-1 protein expression (Fig. 13A). Low levels of *LY6K* mRNA correlate with lower CAV-1 RPPA scores and high levels of *LY6K* mRNA levels correlate with higher CAV-1 RPPA scores. Moreover, CAV-1 was the only protein in the RPPA analysis whose adjusted p-values was significant at 0.00256 and was specific to GBM datasets. No other protein had a significant adjusted p-value.

CAV-1 is a major component of caveolae, which are small, 50-100 nm membrane invaginations that are important for plethora of cellular functions including signal transduction.[149] Caveolae are found in the ordered, dynamic lipid rafts of the plasma membrane, which also house GPI-anchored proteins.[163] LY6 family members are known to utilize CAV-1-mediated endocytosis to influence cell signaling.[173] As CAV-1 is upregulated in GBM and has tumor-promoting roles in advanced cancers,[151,152] we hypothesized that CAV-1 is involved in LY6K-enhanced ERK1/2 signaling. Reciprocal IP-IB analysis showed that LY6K can associate with CAV-1 (Fig. 13B), while no signal was detected in the beads or IgG negative controls. Additionally, high expression of *CAV-1* inversely correlated with poor survival in glioma patients (Fig. 13C). Importantly, high expression of both *CAV-1* with *LY6K* (Fig. 13D) yielded the worst overall survival and low levels of both proteins showed relatively better survival in GBM patients. Together, these data indicate that the interaction between LY6K and CAV-1 may be a cause of the poor prognosis seen in GBM patients with high levels of *LY6K*.

To further assess membrane dynamics, we treated U87 cells with latrunculin A, a toxin isolated from the red sea sponge, *Latrunculia magnifica*. Latrunculin A disrupts proper membrane formation by inhibiting actin polymerization, thereby interfering with CAV-1 distribution[174]. Specifically, latrunculin A sequesters actin monomers and promotes depolymerization of actin filaments.[175] This causes improper caveolae formation and can interfere with downstream signaling pathways. As expected, treatment with latrunculin A caused a marked decreased in the levels of p-ERK1/2 (Fig. 13E). Notably, we also observed a decrease in the levels of p-AKT, implying that disruption of proper membrane formation suppresses multiple signaling cascades.

Significantly, the decrease in p-ERK1/2 was true even in the presence of LY6K (Fig. 13E), indicating that membrane polymerization and proper CAV-1 distribution are necessary for LY6K function.

To further investigate the role of CAV-1 in LY6K-enhanced ERK1/2 signaling, we suppressed *CAV-1* expression through shRNA-mediated KD. *CAV-1* KD had negligible effects on p-ERK1/2 levels in control U87 cells but caused an appreciable decrease in p-ERK1/2 levels in cells overexpressing LY6K (Fig. 13F). In the presence of LY6K, *CAV-1* expressing cells showed strong enhancement of p-ERK1/2 in response to EGF stimulation. However, in cells with *CAV-1* knocked down, EGF stimulation only partially increased LY6K-enhanced p-ERK1/2 levels (Fig. 13F). Finally, we manipulated both CAV-1 and LY6K levels and treated cells with either the RAF inhibitor, SB590885, or the MEK inhibitor, PD98059, as described above (Fig. 13G). Consistent with Figure 10D, *CAV-1* KD suppressed LY6K-enhanced p-ERK1/2 upon inhibition of RAF or MEK. Treatment with SB590885 led to undetectable levels of p-ERK1/2 in all conditions. As seen previously, treatment with PD98059 was more subtle. In the absence of LY6K, PD98059 led to undetectable levels of p-ERK1/2. In the presence of LY6K however, PD98059 led to undetectable levels of p-ERK1/2 only when *CAV-1* was also knocked down. In the presence of *CAV-1*, there was slight activation of p-ERK1/2 (Fig. 13G).

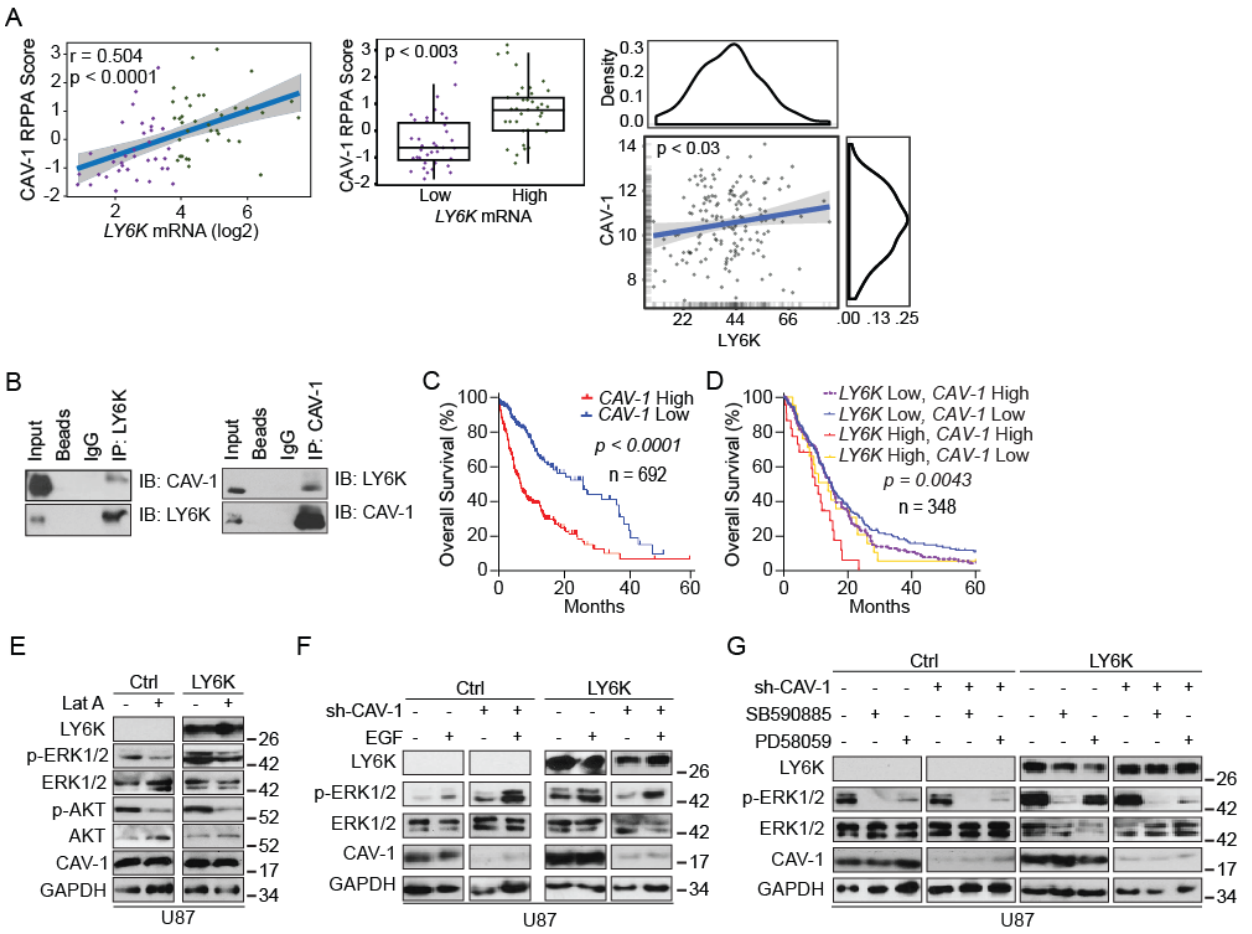

Figure 13.

CAV-1 mediates LY6K-enhanced p-ERK1/2 in GBM cells. (**A**) RPPA analysis. CAV-1 is the only protein whose expression significantly correlated with *LY6K*. (**B**) Reciprocal co-immunoprecipitation analysis. Exogenous LY6K associated with CAV-1. (**C** and **D**) Kaplan-Meier survival analysis of TCGA datasets. High levels of *CAV-1* correlated with poor survival in the TCGA GBM+LGG dataset (**C**). Co-expression of *LY6K* and *CAV-1* correlated with poor survival in the TCGA GBM dataset (**D**). (**E**) IB. Latrunculin A treatment decreased LY6K-enhanced p-ERK1/2 levels. (**F**) IB. *CAV-1* knockdown decreased LY6K-enhanced p-ERK1/2, even in the presence of EGF. (**G**) RAF inhibition by SB590885 strongly suppressed p-ERK1/2 levels, while MEK inhibition by PD98059 blocked LY6K-enhanced p-ERK1/2 only but retained basal p-ERK1/2 levels. Knockdown of *CAV-1* suppressed even basal levels of LY6K-enhanced pERK1/2. For all IB, U87 cells with indicated modifications were used. p-AKT/AKT were used as non-specific proteins and GAPDH was a loading control. Data in **B** and **E** to **G** are representative of three independent experiments with similar results.

GPI-Anchor Domain of LY6K is Necessary for LY6K-Enhanced ERK1/2 Signaling and Tumorigenicity.

(Figures 14 & 15)

Similar to other members of the LY6 family, LY6K is predicted to have a glycosylphosphatidylinositol (GPI) anchor that anchors it to the extracellular surface of the plasma membrane.[176] We confirmed this prediction by analyzing a Kyte-Doolittle hydropathy plot (Fig 14A), which indicated that the LY6K amino acid sequence is consistent with GPI-anchored proteins. Specifically, we observed high hydrophobic regions at the N and C termini, which is indicative of the presence of a GPI anchor. Furthermore, we experimentally corroborated this finding by treating cells with phosphatidylinositol-phospholipase C (PI-PLC). PI-PLC is an enzyme that specifically cleaves GPI-anchors, thus releasing GPI-anchored proteins from the membrane.[176] When U87 cells overexpressing LY6K were treated with PI-PLC, we observed decreased levels of LY6K as well as p-ERK1/2 (Fig. 14B). To further demonstrate the necessity of membrane association of LY6K in ERK1/2 activation, we treated cells with mannosamine hydrochloride (Mann-HCl). Mann-HCl inhibits incorporation of GPI anchors into their respective proteins, thereby causing these proteins to accumulate along the secretory pathway instead of localizing to the membrane.[177] Treatment with Mann-HCl resulted in a notable shift in molecular weight of LY6K, due to the loss of the GPI anchor. Importantly, Mann-HCl treatment also decreased p-ERK1/2 levels in cells expressing LY6K (Fig. 15A). Thus, inhibition of LY6K membrane-association abrogates the role of LY6K in ERK1/2 activation.

To complement these pharmacological manipulations, we generated U87 cells that stably express a mutant LY6K, LY6K-ΔGPI, which lacks the GPI anchor domain (Fig. 14C). We determined proper subcellular localization of LY6K based on the presence of the GPI anchor by using immunofluorescent staining. In the absence of triton-mediated membrane permeabilization, LY6K was undetectable in both control and LY6K-ΔGPI-expressing cells, whereas strong LY6K expression was seen in LY6K-WT-expressing cells (Fig. 14D). Moreover, LY6K-WT-expressing cells also showed clear co-localization between LY6K and CAV-1, while control and LY6K-ΔGPI-expressing cells showed no co-localization between LY6K and CAV-1 (Fig. 15B). This shows that LY6K-WT and CAV-1 can localize to the membrane, further providing evidence for their potential to interact directly. However, in the presence of triton-mediated membrane permeabilization, LY6K expression was detected in both LY6K-ΔGPI- or LY6K-WT-expressing cells. These data indicate that deletion of the GPI anchor domain prevents LY6K from localizing to the membrane and associating with CAV-1, thus retaining it in the cytosol. We then examined p-ERK1/2 signaling in these cells. Compared to LY6K-WT, U87 cells expressing the LY6K-ΔGPI mutant failed to enhance p-ERK1/2 relative to control, even in the presence of EGF stimulation (Fig. 14E). Together, these data suggest that the GPI anchor and proper membrane localization are crucial for LY6K-enhanced ERK1/2 signaling.

Additionally, proteasome inhibition attenuates ERK1/2 signaling and reduces cell proliferation[178] by suppressing degradation of dual specificity phosphatases (e.g. MAPK-phosphatase-1). Moreover, we observed that total levels of LY6K increase when GSC528 cells were subjected to EGF stimulation (see Fig. 11C). We also observed that the total levels of LY6K

decreased when U87 cells are cultured in serum-free media, relative to serum-containing media (Fig. 15C). Both of these effects indicate that LY6K protein stability may vary based on the specific culture conditions. To determine whether proteasome inhibition modulates LY6K-enhanced ERK1/2 activation, we treated U87 cells expressing a control vector, LY6K-ΔGPI, or LY6K-WT with a proteasome inhibitor, MG132 (Fig. 14F). While treatment with MG132 markedly reduced p-ERK1/2 levels in all conditions (Fig. 14F), cells expressing a control vector or LY6K-ΔGPI showed more pronounced reduction of p-ERK1/2 relative to cells expressing LY6K-WT (Fig. 14F, right). Of note, MG132 treatment resulted in the appearance of different sizes of LY6K, suggesting that LY6K requires processing prior to its maturation as a functional protein.

Finally, to assess the importance of the GPI anchor of LY6K on GBM tumorigenicity, we conducted *in vivo* xenograft experiments using GSC83 cells with knockdown of endogenous *LY6K* and subsequent exogenous expression of either LY6K-ΔGPI or a control vector (Fig. 14G). Unlike LY6K-WT (Fig. 8F), exogenous expression of LY6K-ΔGPI failed to rescue LY6K-enhanced GSC intracranial tumor growth and overall survival of tumor-bearing animals relative to controls. This highlights the importance of the GPI anchor for LY6K-mediated GBM tumorigenicity.

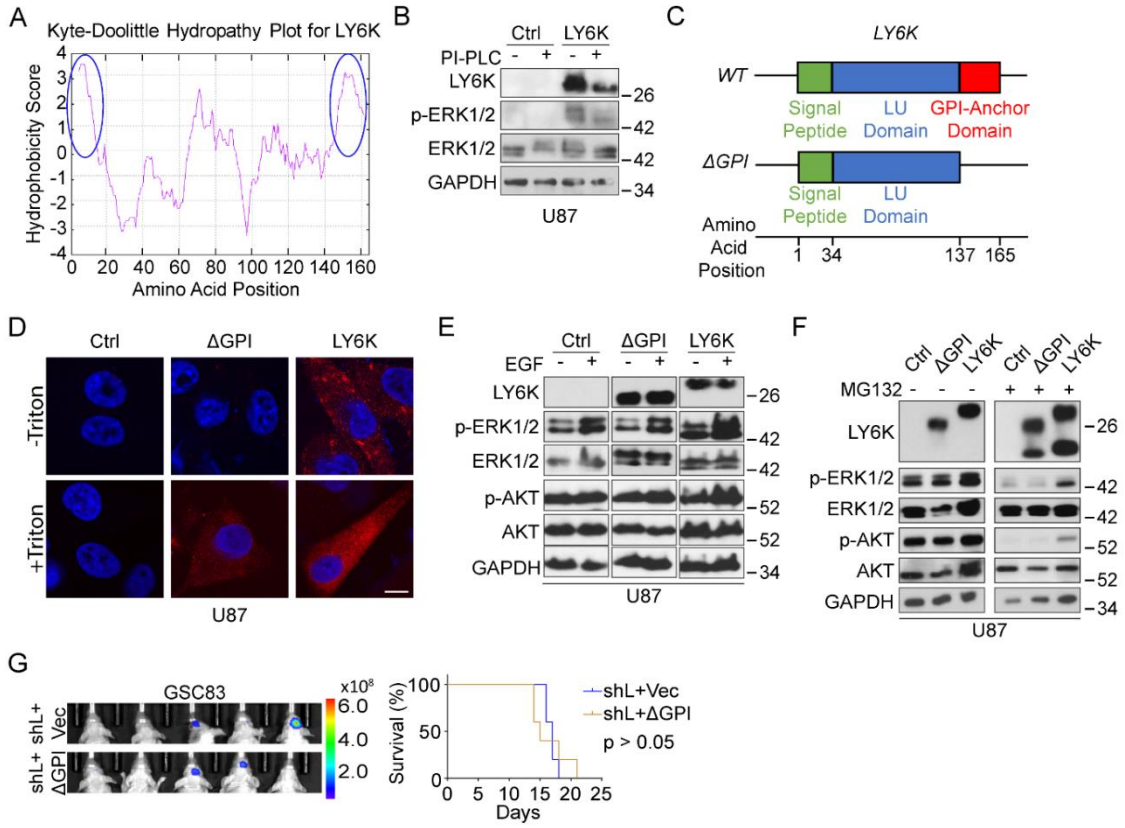

Figure 14.

The GPI-anchor domain of LY6K is necessary for LY6K-enhanced ERK1/2 signaling and tumorigenicity. (**A**) Kyte-Doolittle Hydropathy Plot analysis. LY6K fits the typical hydrophobicity profile for GPI-anchored proteins (see blue circles marking highly hydrophobic regions at N- and C-termini). (**B**) IB. Treatment with PI-PLC decreased molecular weight of decreased levels LY6K and showed accompanying suppression of p-ERK1/2 levels. (**C**) Schematic of the three domains of the transcribed sequence for LY6K-WT (signal peptide, LU domain, and GPI-anchor domain) and the constructed mutant LY6K-ΔGPI, which lacks the GPI-anchor domain. The predicted amino acid position corresponding to each domain is depicted below. (**D**) Immunofluorescent staining. Unlike the LY6K-ΔGPI mutant, LY6K-WT is present on the cell membrane. LY6K-ΔGPI could not be visualized in the absence of membrane permeabilization (-Triton). (**E**) IB. Expression of LY6K-WT enhanced p-ERK1/2 levels, whereas LY6K-ΔGPI failed to do so, even in the presence of EGF. (**F**) IB. Proteasomal inhibitor MG132 reduced LY6K-enhanced p-ERK1/2. (**G**) GBM xenograft experiments. In GSC83 cells with knockdown of endogenous LY6K, subsequent expression of LY6K-ΔGPI mutant failed to restore tumorigenicity. Left, BLI images. Right, Kaplan-Meier survival analysis. For all IB, U87 cells with indicated modifications were used. p-AKT/AKT were used as non-specific proteins and GAPDH was a loading control. Scale bar in **D** is 10 μm. Data in **B** and **D** to **G** are representative from two to three independent experiments with similar results.

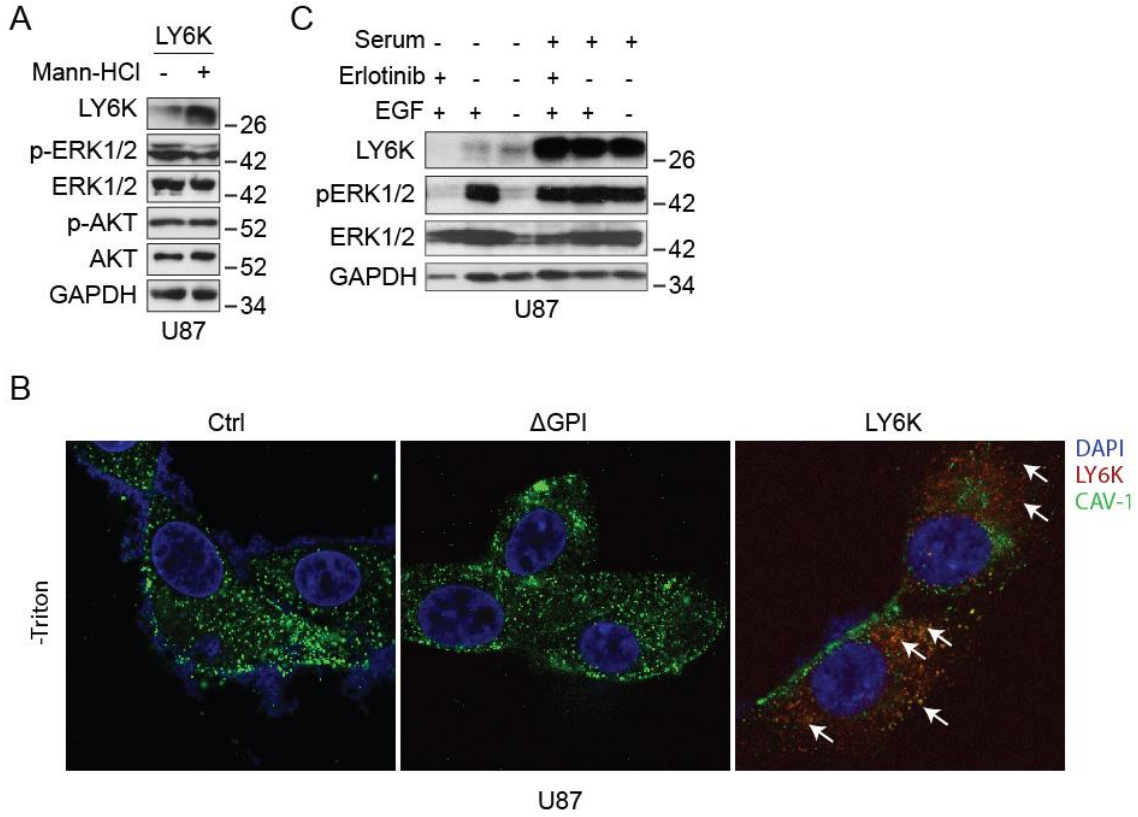

Figure 15.

The GPI-anchor domain of LY6K is required for its activity. (**A**) IB. Treatment with mannosamine hydrochloride (a compound that inhibits GPI anchor incorporation) reduced LY6K-enhanced p-ERK1/2 levels. (**B**) Immunofluorescent staining. Unlike control cells and the LY6K-ΔGPI mutant, LY6K-WT can co-localize with CAV-1 on the cell membrane. White arrows indicate the co-localization between LY6K and CAV-1. Scale bar in **B** is 10 μm. (**C**) IB. Serum-rich media stabilizes overall levels of LY6K expression. Serum-free media promoted decreased expression of LY6K and treatment with erlotinib further decreases LY6K levels.

Promoter Methylation Contributes to *LY6K* Gene Expression and GBM Response to Radiation

(Figures 16 & 17)

Cancer/testis antigens are epigenetically silenced in non-reproductive tissues, but can become aberrantly activated during cancer.[103] Since LY6K is a cancer/testis antigen, we investigated whether *LY6K* expression is silenced by DNA methylation in GBM. Characterization of the gene locus of *LY6K* revealed a CpG island along its promoter region (Fig. 17A, green bar). Analysis of these CpG sites using our published 450K Methylation Array dataset[102] revealed that PN-like GSCs have significantly higher levels of methylation relative to MES-like GSCs, which is consistent with PN-like GSCs having lower levels of *LY6K* expression relative to MES-like GSCs (Fig. 17B, left & Fig 6E). Interestingly, this differential methylation appears to be limited to GSCs, as methylation analysis of TCGA GBM samples showed high levels of methylation for all probes examined, regardless of GBM subtype (Fig. 17B, right). We validated these results by using combined bisulfite and restriction analysis (CoBRA), which revealed that *LY6K* is hypermethylated (cut) in PN-like GSCs and hypomethylated (uncut) in MES-like GSCs (Fig. 16A). These methylation profiles were further confirmed at single-base resolution with bisulfite sequencing analysis. Over 90% of CpG sites in PN-like GSCs were methylated while less than 10% of CpG sites in MES-like GSCs were methylated (Figs. 16B, 17C). We also saw that individual CpG sites have high β-values (high methylation levels) in PN-like GSCs but have very low β-values in MES-like GSCs (Fig. 17D). Using a β-value threshold of 0.4, we were able to effectively distinguish between PN-like and MES-like GSCs with individual CpG sites within the

CpG island. The primers used for PCR for both CoBRA and bisulfite sequencing are illustrated in Figure 17E and the abbreviations used in Figures 17A, 17B, and 17D are shown in Figure 17F.

Radiation therapy (RT) is the first line of treatment for GBM patients,[158] and RT is known to alter cancer cell epigenomes.[99,101,179] Therefore, we tested whether ionizing radiation (IR) alters *LY6K* promoter methylation with corresponding alterations in *LY6K* expression. IR markedly increased *LY6K* expression in PN-like GSCs[180], whereas minimal changes were found in IR-treated MES-like GSCs (Fig. 16C). Moreover, the increase in *LY6K* expression we observed in PN-like GSCs could be seen in as little as 24 hours and lasts up to120 hours (Fig. 17G). We then subjected PN-like GSC17 and GSC19, and MES-like GSC83 to 2 Gy IR and subsequently isolated genomic DNA at 24h, 72h, and 120h after IR. IR-treated PN-like GSCs showed markedly decreased CpG island methylation (Fig. 16B) and induction of LY6K protein expression (Fig. 16D). For GSC17 cells, the change in methylation and induction of protein expression were only apparent 72h after IR, while GSC19 showed changes within 24h (Figs. 16B, 16D). We also observed changes in cellular morphology in response of IR in PN-like GSCs. (Fig. 17H). In contrast, MES-like GSC83 showed no changes in promoter methylation (Fig. 16B), LY6K expression (Fig. 16D), or cell morphology (Fig. 17H). Notably, 10 days after IR, expression of LY6K was comparable between PN-like and MES-like GSCs (Fig. 16D).

Finally, using MES-like GSC83 cells, we determined the effect of modifying *LY6K* expression on response to IR. Knockdown of endogenous *LY6K* and subsequent expression of LY6K-WT rendered GSC83 cells resistant to 2 Gy IR. However, cells with *LY6K* KD and subsequent expression of LY6K-ΔGPI or a control vector showed sensitivity to the same treatment

(Fig. 16E). These data are consistent with our previous finding that MES-like GSCs are resistant to IR *in vitro*,[21] and suggest that up-regulation of *LY6K* in MES-like GSCs contributes to GBM RT resistance. Taken together, these results indicate that *LY6K* promoter methylation is especially important for GSC subpopulations, particularly with respect to modulating GSC response to RT.

Finally, we determined how MES-like GSC83 cells respond to IR when *LY6K* expression is modulated. Without IR treatment, cells with knockdown of endogenous LY6K, re-expression of exogenous LY6K-WT maintained the potential of cell proliferation whereas re-expression of a LY6K-ΔGPI mutant (Fig. 14) had similar inhibitory effects to that with a vector control (Fig. 16E, left). Moreover, when cells were exposed to 2 Gy IR, re-expression of LY6K-WT rendered GSC83 cells resistant to IR, while LY6K-ΔGPI- or vector-expressing cells responded to IR treatments (Fig. 16E, right). These data are consistent with our previous finding that MES-like GSCs are resistant to IR *in vitro*,[21] and strongly suggest that up-regulation of *LY6K* in MES-like GSCs contributes to GBM resistance to RT.

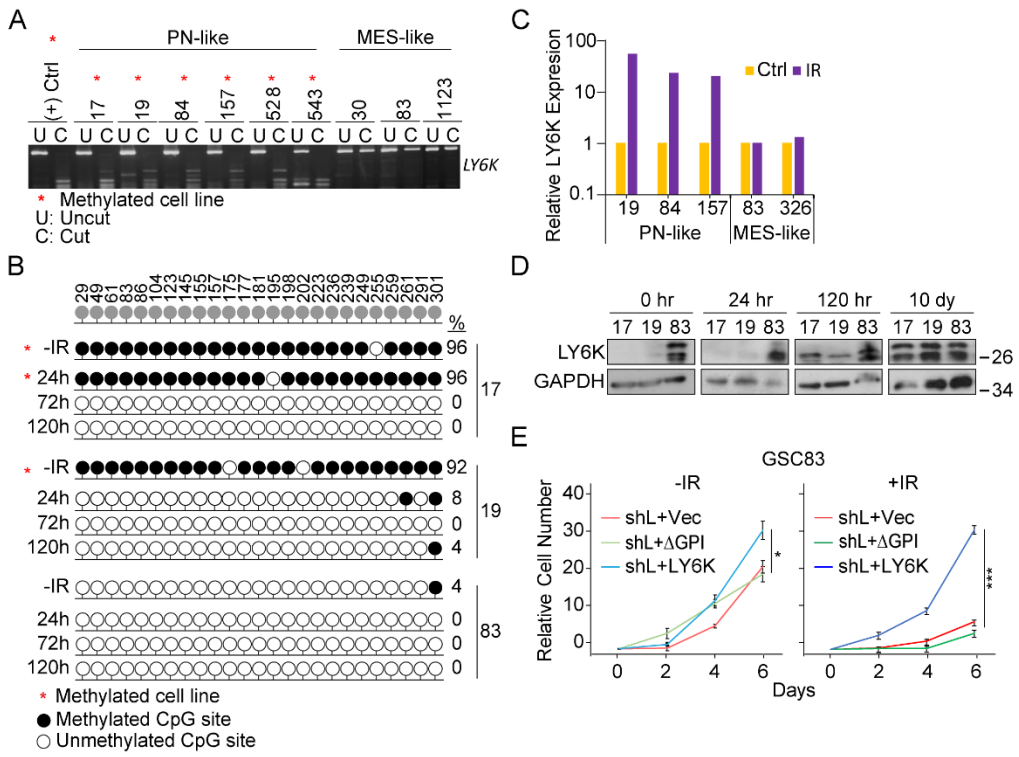

Figure 16.

Promoter methylation contributes to LY6K gene expression and modulates GBM cell response to radiation. (**A**) CoBRA. *LY6K* was methylated in PN-like GSCs and was unmethylated in MES-like GSCs. DNA incubated with S-adenosyl methionine was used as a positive control. (**B**). Bisulfite sequencing analysis. In the absence of IR, PN-like GSC17 and GSC19 had high levels of methylation of the *LY6K* gene promoter, while GSC83 had relatively low DNA methylation. Within 72h or 24h after 2 Gy IR, the methylation profile switched to be much more MES-like in both GSC17 and GSC19, respectively. The methylation profile for GSC83 remained stable, regardless of IR. Filled circles indicate methylated CG sites. Clear circles indicate unmethylated CG sites. Percentage of CG sites methylated is shown on the right. Base pair location is listed on top. (**C**) Analysis of DNA expression array data of GSCs treated with 2 Gy IR.[180] IR induced 20 and 50-fold higher *LY6K* expression in PN-like GSCs, whereas *LY6K* expression remained stable in IR-treated MES-like GSCs. (**D**) IB. IR-induced LY6K protein expression levels in PN-like GSC17 and GSC19 increases with time, whereas LY6K expression in IR-treated MES-like GSC83 remained stable. GAPDH was a loading control. (**E**) Cell proliferation assay. In GSC83 cells with knockdown of endogenous *LY6K*, expression of LY6K-WT increased cell proliferation and resistance to IR, unlike LY6K-ΔGPI or a control vector. Red asterisks (*) in **A** and **B** indicate methylated cell lines. Data in **A**, **B**, **D**, and **E** are representative from two to three independent experiments with similar results. *$p < 0.05$, ***$p < 0.001$.

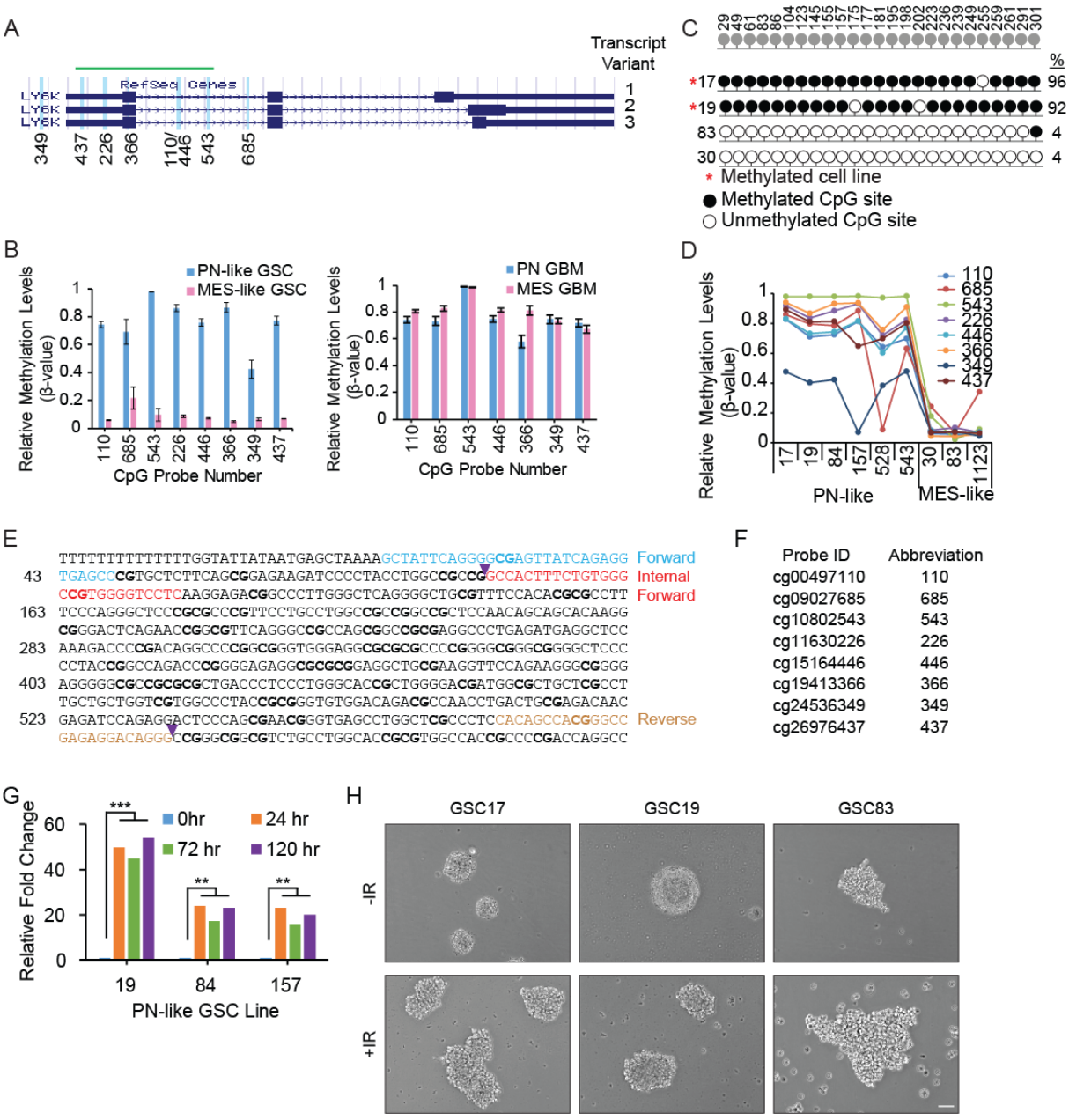

Figure 17.

DNA methylation of *LY6K* gene promoter regulates its expression and GSC response to irradiation. (**A**) Schematic showing the location of various CpG sites in the promoter region of *LY6K*. Light blue lines indicate CpG sites. Green bar indicates predicted CpG island. (**B**) Bisulfite sequencing analysis showing that PN-like GSC 17 and 19 have high methylation percentages, while MES-

Continued on next page

Figure 17 cont.

like GSC 83 and 30 have low methylation percentages. Base pair location is listed on top. (**C**) Relative methylation levels for CpG sites in the *LY6K* promoter in PN-like or MES-like GSCs (left) or PN or MES GBM (right). (**D**) β-values for the indicated individual CpG sites along the *LY6K* CpG island for indicated PN-like and MES-like GSCs. (**E**) Illustration of nested primers used for CoBRA PCR, showing forward (blue), internal forward (red), and reverse (brown) primers, with CpG sites bolded. Sequence between the purple arrowheads is the PCR-amplified sequence. The base pair location is indicated on the left. (**F**) Table showing the CpG probe IDs and abbreviations used in (**A**), (**C**), and (**D**). (**G**) Visual representation showing how PN-like GSC17 and GSC19 change from having tight spheres typical of PN-like GSCs to having loose spheres, similar to MES-like GSC83 in the presence of IR. Scale bar in G is 200 μm. (**H**) Relative fold change of *LY6K* expression in PN-like GSC 17, 19, and 157 at the indicated timepoints, before and after 2 Gy IR.

CHAPTER 4: DISCUSSION

Sustained cell proliferation resulting from aberrant signal transduction is a hallmark of cancer.[14] Previous studies have shown the prevalence of LY6K and the LY6 family members in other human cancers including breast[78], esophageal[67], and lung[65] cancers, as well as the role of *LY6K* as an oncogene that is correlated with poor patient survival.[66] In all cancers examined to date, *LY6K* expression is correlated with poor patient survival. However, the function of LY6K in GBM tumorigenicity is unknown. Here, we show for the first time that *LY6K* expression correlates with poor prognosis of GBM patients in multiple datasets, and multivariate analyses show that patients below 60 years of age with low levels of *LY6K* have a survival advantage. Our data indicate that *LY6K* expression is higher in MES GBM samples and is differentially expressed between PN-like and MES-like GSCs. Functionally, increased expression of *LY6K* promotes GBM tumorigenicity *in vitro* and *in vivo*. This is especially relevant, given recent evidence showing the utility of alternative splicing events of *LY6K* as a prognostic indication of GBM patient survival,[92] as well as the potential of using LY6K in immunotherapy.[54]shRNA-mediated knockdown of *LY6K* in MES-like GSCs significantly decreases cell proliferation, sphere forming frequencies, and *in vivo* tumor growth and tumor volume. These phenotypes can be rescued upon re-expression of *LY6K* in these cells. Complimentarily, overexpression of *LY6K* in PN-like GSCs or U87 glioma cells increases their tumorigenic behaviors.

Mechanistically, we report that LY6K promotes tumorigenicity of GSCs and GBM cells by enhancing MAPK signaling. Knockdown of *LY6K* in MES-like GSCs decreases basal levels of p-ERK1/2 but fails to alter other cancer signaling pathways. Commensurate to the tumorigenic

phenotypes seen *in vitro* and *in vivo*, p-ERK1/2 can be rescued with re-expression of *LY6K*. Similarly, overexpression of *LY6K* in PN-like GSCs and U87 cells, which normally have undetectable levels of LY6K, leads to a significant increase in p-ERK1/2, proportional to the increased cell growth observed *in vitro*.

Although MAPK signaling is often the result of RTK-mediated signal transduction, we found no evidence that RTKs including EGFR, PDGFRα, MET, or AXL are involved in LY6K-induced ERK1/2 signal enhancement. Despite this, we did find evidence to support the notion of EGF-mediated signaling. EGF stimulation significantly increases levels of p-ERK1/2 in PN-like GSCs which have undetectable expression of EGFR, as well as in U87 cells which have low levels of EGFR. Moreover in U87 cells, EGFR activation following EGF stimulation was similar regardless of LY6K expression. In PN-like GSC528 cells, EGF stimulations caused a profound increase in p-ERK1/2 but resulted in no detectable p-EGFR or total EGFR levels. We subsequently tested the effect of inhibiting RAF or MEK, the two kinases that are directly upstream of ERK1/2. In both GSC528 and U87 cells, RAF inhibition led to a decrease in p-ERK1/2, such that expression was nearly undetectable. RAF inhibition also decreased levels of p-AKT, indicating the involvement of RAF in multiple signaling pathways. MEK inhibition however was subtle. In response to MEK inhibition, PN-like GSC528 had decreases in p-ERK1/2 levels commensurate to RAF inhibition. However, U87 cells showed suppression of LY6K-induced p-ERK1/2 but retained basal levels of p-ERK1/2. This is likely due to the presence of difference classes of MEK enzymes in these two cell types.[134] Taken together, these results indicate that LY6K-induced ERK1/2 signaling is further enhanced by EGF, but occurs in an EGFR-independent mechanism. In addition,

LY6K affects ERK1/2 signaling specifically and does not alter other cancer-related signaling pathways, such as AKT signaling.

Given that RTK signaling is unlikely to be the cause of the enhancement seen in ERK1/2 activation, we searched for potential interactors of LY6K who may be responsible for this effect. Reverse phase protein array analysis showed that CAV-1 is the only protein that significantly correlates with *LY6K* levels. As CAV-1 is a membrane-bound protein that is found in lipid rafts, it seemed a likely candidate to study further. In addition, disrupting actin polymerization and subsequent membrane formation by treating with latrunculin A decreased the level of p-ERK1/2 and suppressed LY6K-induced p-ERK1/2. This indicates that proper membrane assembly is necessary for LY6K to function. Reverse co-immunoprecipitation analysis showed a direct interaction between LY6K and CAV-1, giving further evidence for CAV-1 being the mediator between LY6K and ERK1/2 signal enhancement. Moreover, *CAV-1* is associated with poor patient survival in glioma patients and multivariate analysis showed that high expression of *LY6K* and *CAV-1* gives the poorest overall GBM patient survival. Correspondingly, knockdown of CAV-1 decreased the levels of p-ERK1/2 and diminished p-ERK1/2 resulting from EGF stimulation in U87 cells expressing LY6K. Again, we tested the effect of inhibiting RAF or MEK in the presence or absence of *CAV-1* knockdown. As described previously, in the presence of LY6K, p-ERK1/2 levels decrease with MEK inhibition and are undetectable with RAF inhibition. However, if CAV-1 is also knocked down, then p-ERK1/2 levels are undetectable with both RAF and MEK inhibition.

Finally, we examined the importance of the GPI anchor on LY6K function. LY6K is predicted to have a GPI anchor, but is known to exist in soluble form in rodents.[60] We first confirmed the presence of the GPI anchor using a Kyte-Doolittle Hydropathy analysis, which showed the presence of highly hydrophobic amino acid residues at both the N- and C-termini. We also used a prediction software to determine that the most likely position for GPI anchor attachment (the ω-site)[163] was at amino acid position 137. We experimentally confirmed this by treating cells containing LY6K with phosphatidylinositol-phospholipase C (PI-PLC), which specifically cleaves GPI-anchored proteins from the membrane. Treatment with PI-PLC decreased overall levels of LY6K, indicating that the enzyme successfully cleaved LY6K at the membrane, and this was associated with a decrease in overall p-ERK1/2 levels. Additionally, we genetically ablated the GPI-anchor domain of LY6K and found that this inhibited proper membrane localization through immunofluorescent analysis. Immunoblotting (IB) analysis showed that removing the GPI anchor domain abolished the ability of LY6K to enhance p-ERK1/2 levels, even with EGF stimulation. Furthermore, xenograft experiments showed that LY6K lacking the GPI anchor domain is unable to increase tumor growth beyond controls, unlike wild-type LY6K. This indicates that LY6K must be membrane-bound in order to properly function and respond to EGF. Overall, our studies thus indicate that membrane-bound LY6K interacts with CAV-1, thereby enhancing ERK1/2 activity and subsequently promoting cell proliferation in GBM (Fig. 18).

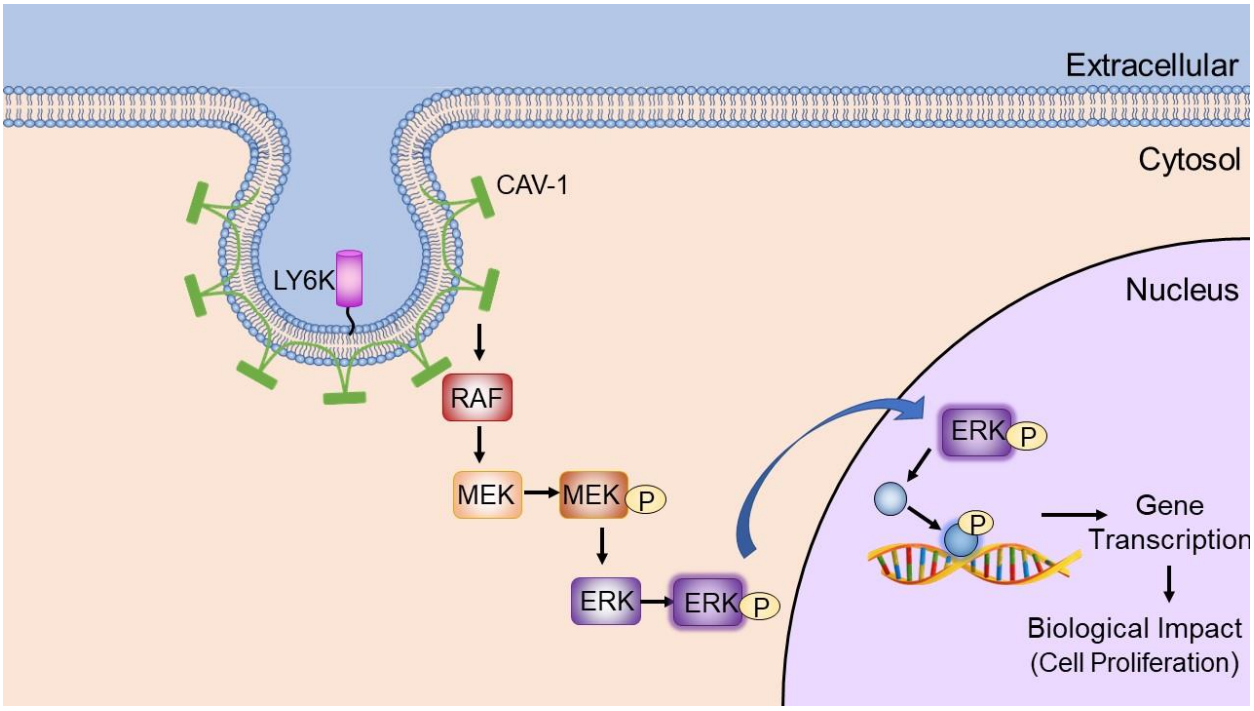

Figure 18: Summary

Schematic depiction of how membrane-bound LY6K associates with CAV-1 to enhance ERK1/2 signaling, thereby promoting GBM cell proliferation and tumorigenicity. Our model proposes that LY6K must be GPI-anchored in order to effectively interact with CAV-1 within caveolae. Following this interaction, the LY6K/CAV-1 complex can act on the MAPK signaling pathway and affect RAF and MEK to eventually increase the amount of activated p-ERK1/2. p-ERK1/2 can then translocate to the nucleus and activate transcription factors that are responsible for many different downstream effects. For the purposes of our model, p-ERK1/2 can help to promote gene that increase cell proliferation, thereby increasing GSC growth and tumorigenicity.

Previous studies have demonstrated *LY6K* and its family members as cancer-initiating genes in several types of human cancers.[65,67,78] In breast cancer, LY6K and LY6E are required for TGFβ signaling and promote drug resistance and cancer cell escape from immune surveillance.[78] However, the precise mechanisms responsible for these functions are unknown. In this study, we show that *LY6K* is markedly up-regulated in GBM, and LY6K promotes GBM tumorigenicity via ERK1/2-mediated signaling. Although ERK1/2 activation is often a result of RTK-stimulated signaling, we found no evidence that any RTK examined is responsible for LY6K-induced ERK1/2 activation. Rather, LY6K stimulates ERK1/2 activity through association with CAV-1. Our data are also consistent with previous studies that CAV-1 transport from the cell surface to early endocytic vesicles activates ERK1/2 signaling.[156]. Moreover, in the absence of EGF stimulation, inhibition of RAF or MEK, protein kinases directly upstream of ERK1/2, markedly attenuates LY6K-induced ERK1/2 activity.

Given that EGF is known to recruit CAV-1 to endocytic compartments and subsequently activate MAPK signaling,[156] it is possible that LY6K acts as a mediator in this exchange to ensure efficient activation of the MAPK pathway. Moreover, other members of the LY6 family are also known to utilize caveolin-mediated internalization to modulate cell signaling.[173] Indeed, pharmacologic inhibition of proper membrane formation or *CAV-1* KD dampens LY6K-induced ERK1/2 activity. Notably, genetic ablation of the GPI-anchor domain of LY6K caused improper localization of LY6K and abolished LY6K-enhancement of p-ERK1/2, even in the presence of EGF. Moreover, GPI anchor ablation also resulted in decreased cell proliferation *in vitro* and suppressed tumor growth in xenograft experiments. These data suggest that proper membrane

localization of LY6K is critical for its role in enhancing ERK1/2 signaling and promoting tumorigenicity in GBM. Although our results indicate that membrane-anchored LY6K and CAV-1 interact to promote ERK1/2 signaling, future studies designed to illuminate the precise mechanism by which LY6K and CAV-1 interact are warranted. As both proteins are localized to lipid rafts[173], it is also plausible that other proteins in the lipid bilayer or perhaps the lipids themselves are helping to facilitate this interaction.

A clinically relevant finding in this study is that *LY6K* promoter methylation maintains its silencing and contributes to GBM response to radiation therapy (RT). LY6K is a member of the cancer/testis antigen family of proteins, which can become aberrantly expressed in cancers originating from non-reproductive tissues through modulation of DNA methylation profiles. Our DNA methylation analysis of a cohort of PN-like or MES-like GSCs[102] revealed that the *LY6K* gene promoter is hypermethylated in PN-like GSCs, but hypomethylated in MES-like GSCs. This methylation profile results in *LY6K* silencing in PN-like GSCs and *LY6K* expression in MES-like GSCs. Moreover, RT is the first line of treatment in the standard care of GBM patients. Consistent with our recent reports,[158,180] IR exposure of PN-like GSCs markedly reduced DNA methylation and induced expression of *LY6K*, at both the gene and protein levels. Importantly, we found that in MES-like GSC83 cells with knockdown of endogenous *LY6K*, re-expression of exogenous LY6K-WT significantly increased cell proliferation, while expression of the LY6K-ΔGPI mutant failed to increase proliferation relative to knockdown alone. Significantly, when these cells were exposed to IR and subsequently analyzed for cell proliferation, only LY6K-WT maintained the high growth potential seen in non-IR conditions. GSCs expressing either a vector control or LY6K-

ΔGPI failed to maintain high cell proliferation. These data indicate that cells expressing LY6K-WT acquired resistance to IR and were thus able to survive the damaging effects of RT.[179] These data indicate that in GBM patients with *LY6K* upregulation, targeting LY6K-CAV-1-ERK1/2 signaling may be a feasible approach to enhance GBM tumor response to RT.

Future Directions and Conclusions

Taken together, our data reveal a novel function for LY6K and a previously unknown role in GBM biology. We show that LY6K interacts with CAV-1 to enhance ERK1/2 signal transduction in GBM using both GSCs and established GBM cell lines. While our results clearly indicate that LY6K modulates the ERK1/2 signaling pathway, future studies should examine the precise mechanism by which this occurs. We show that CAV-1 is crucial to this enhancement and that CAV-1 directly interacts with LY6K. However, it is important to understand exactly how CAV-1 interacts with LY6K at the membrane. Given that LY6K is bound to the extracellular side of the membrane, while CAV-1 is on the inner leaflet, future studies should determine how these two proteins interact and whether such association affects downstream signaling. Perhaps there are other integral membrane proteins or transmembrane proteins that are facilitating this interaction. It is even possible that the phospholipids of the membrane are enhancing signaling.[181,182]

In addition, we show that the interaction between LY6K and CAV-1 influences ERK1/2 signaling. However, the mechanism that allows these two proteins to interact with and enhance ERK1/2 remains elusive. We show that inhibiting either RAF or MEK suppresses LY6K-induces ERK1/2 signal enhancement, thereby indicating that the function of LY6K occurs upstream of these kinases. Future studies should examine which particular part of the MAPK pathway is being

influenced by LY6K. Elucidating this would allow for investigations into targeting that piece and potentially provide an avenue for stopping LY6K-mediated GBM tumorigenicity. Moreover, while our studies indicate that there are no RTKs (including EGFR) that are responsible for the effects seen in ERK1/2 signaling, we did find evidence that cells expressing LY6K respond to both EGF and erlotinib, an EGFR inhibitor. Even GSC528, which does not express any detectable levels of EGFR had some response to erlotinib. These data indicate that LY6K is responsive to agents targeting the membrane. Elucidating the exact role of LY6K at the membrane an prove to be very useful while targeting this protein for GBM or other cancers. Future studies should focus on whether erlotinib can target receptors other EGFR or any other kinases and whether those kinases are related to LY6K.

Another interesting avenue for future research is whether LY6K can act on ERK1/2 signaling in other systems. The normal function of LY6K is to promote sperm migration during reproduction.[57,58,60,62] Future studies should examine whether the involvement of LY6K in sperm migration is dependent on ERK1/2 signaling and whether LY6K can interact with CAV-1 in sperm. Moreover, LY6K is known to be oncogenic in various types of human cancers.[65-68,78] Few studies have examine the role of LY6K in cell signaling,[73,75,78] and no other study has examine LY6K as an effector in ERK1/2 signaling. Future experiments should focus on how LY6K functions in other cancers and whether it can act on ERK1/2 signaling through association with CAV-1 in cancers outside of GBM. In addition, the function of LY6K as an oncogene appears to be limited to GBM and not relevant in low grade-gliomas. In low grade-gliomas, *LY6K* is not significantly correlated with patient survival, indicating that it might function in a context-

dependent manner. Studies examining this further will provide valuable information about the precise oncogenic potential of *LY6K* and its utility in therapeutic intervention.

Moreover, our studies showed that membrane-associated LY6K associates with CAV-1, and this can induce tumorigenic behaviors. However, genetic ablation of the GPI-anchor domain of *LY6K* appears to halt these behaviors. It is interesting that in the GPI-mutant form of *LY6K*, there is no modification to the signal peptide of *LY6K*. Thus, it is possible that LY6K-ΔGPI is still being targeted to the membrane, but it unable to be anchored in the membrane. In mice, LY6K has been shown to have two isoforms, one of which is soluble.[57,60] It would be interesting to see whether the *LY6K-ΔGPI* mutant form is retained in the cell or whether it is secreted, as has been shown for other members of the LY6 family.[66] Moreover, future studies should also examine whether there are any isoforms of *LY6K* that are soluble in normal primate cells. Investigating their function may provide new insights regarding the mechanistic roles of LY6K.

Finally, future studies should also examine implications of targeting LY6K in immunotherapies, especially in combination with temozolomide treatment and IR. Various studies have examined the potential of LY6K in vaccine-based therapies. As LY6K may suppress the immune system, [79] targeting LY6K would be a useful tool to make "immune-cold" tumors such as GBM into "hot" tumors. Peptide vaccine therapies aimed at LY6K have shown immune responses and some improvement in patient survival in esophageal, lung, head and neck, and gastric cancers[80-87,90,91]

As previously mentioned, while the role of LY6K has been implicated in several types of cancers, the role and mechanism of LY6K action in GBM biology has yet to be elucidated. A

recent study that was aimed at identifying prognostic indicators for GBM with respect to alternative splicing mechanisms showed that a set of five genes were useful in predicting overall and disease-free survival.[92] *LY6K* is one of the five genes, and together with the other genes, was found to be a useful tool in predicting patient survival.[92] Furthermore, peptide-based vaccine cocktails containing an LY6K-based epitope induced CTL responses in glioma patients.[54] These studies indicate that LY6K is an important factor in GBM patients and immunotherapies derived from LY6K may be a useful mechanism for increase GBM patient survival.

We show here that *LY6K* expression is regulated by gene promoter methylation and modulating the methylation status corresponds to changes in expression. We also show that *LY6K* methylation and expression can change depending on the presence of IR. In cells that have high levels of methylation of the *LY6K* promoter and correspondingly low levels of *LY6K* expression, IR can induce promoter demethylation and gene expression. In addition, only cells expressing WT-LY6K are resistant to radiation. On the other hand, GSCs expressing a control vector or the GPI-mutant LY6K have decreased growth rates following IR. Given this resistance pattern, combining IR with vaccine-based immunotherapies may provide a useful method for eliciting immune responses to LY6K and promoting sensitivity to IR in GSCs expressing *LY6K*.

In conclusion, we demonstrate that LY6K has oncogenic roles in GBM and correlates with poor GBM patient prognosis. *LY6K* expression increases cell proliferation *in vitro* and promotes tumor growth in immunocompromised mice, while suppression of *LY6K* decreases cell proliferation and tumor growth in orthotopic xenografts. Mechanistically, LY6K promotes GBM tumorigenicity by activating the MAPK pathway via interactions with CAV-1. Interestingly, we

show that proper membrane localization is absolutely crucial for this effect. Mutant forms of *LY6K* that lack the membrane anchoring domain are unable to enhance ERK1/2 signaling or promote tumorigenic behaviors. Finally, we show that *LY6K* expression is governed by gene promoter methylation and that the *LY6K* promoter becomes demethylated with IR. Given that localization of LY6K to the membrane is required for LY6K oncogenic activity, LY6K could be considered as a potential target for antibody-guided therapy, which, in conjunction with temozolomide and IR therapies, may help to overcome GBM recurrence and resistance to RT.

REFERENCES:

1. Allen NJ, Lyons DA. Glia as architects of central nervous system formation and function. *Science.* 2018; 362(6411):181-185.

2. Molofsky AV, Deneen B. Astrocyte development: A Guide for the Perplexed. *Glia.* 2015; 63(8):1320-1329.

3. Ostrom QT, Bauchet L, Davis FG, et al. The epidemiology of glioma in adults: a "state of the science" review. *Neuro Oncol.* 2014; 16(7):896-913.

4. Louis DN, Perry A, Reifenberger G, et al. The 2016 World Health Organization Classification of Tumors of the Central Nervous System: a summary. *Acta Neuropathol.* 2016; 131(6):803-820.

5. Aldape K, Brindle KM, Chesler L, et al. Challenges to curing primary brain tumours. *Nat Rev Clin Oncol.* 2019; 16(8):509-520.

6. Miller JJ, Shih HA, Andronesi OC, Cahill DP. Isocitrate dehydrogenase-mutant glioma: Evolving clinical and therapeutic implications. *Cancer.* 2017; 123(23):4535-4546.

7. Turkalp Z, Karamchandani J, Das S. IDH mutation in glioma: new insights and promises for the future. *JAMA Neurol.* 2014; 71(10):1319-1325.

8. Wang Q, Hu B, Hu X, et al. Tumor Evolution of Glioma-Intrinsic Gene Expression Subtypes Associates with Immunological Changes in the Microenvironment. *Cancer Cell.* 2017; 32(1):42-56 e46.

9. Verhaak RG, Hoadley KA, Purdom E, et al. Integrated genomic analysis identifies clinically relevant subtypes of glioblastoma characterized by abnormalities in PDGFRA, IDH1, EGFR, and NF1. *Cancer Cell.* 2010; 17(1):98-110.

10. Neftel C, Laffy J, Filbin MG, et al. An Integrative Model of Cellular States, Plasticity, and Genetics for Glioblastoma. *Cell.* 2019; 178(4):835-849 e821.

11. Lathia JD, Mack SC, Mulkearns-Hubert EE, Valentim CL, Rich JN. Cancer stem cells in glioblastoma. *Genes Dev.* 2015; 29(12):1203-1217.

12. Morrison SJ, Kimble J. Asymmetric and symmetric stem-cell divisions in development and cancer. *Nature.* 2006; 441(7097):1068-1074.

13. Avgustinova A, Benitah SA. Epigenetic control of adult stem cell function. *Nat. Rev. Mol. Cell Biol.* 2016; 17(10):643-658.

14. Hanahan D, Weinberg RA. Hallmarks of cancer: the next generation. *Cell.* 2011; 144(5):646-674.

15. Batlle E, Clevers H. Cancer stem cells revisited. *Nat. Med.* 2017; 23(10):1124-1134.

16. Quintana E, Shackleton M, Sabel MS, Fullen DR, Johnson TM, Morrison SJ. Efficient tumour formation by single human melanoma cells. *Nature.* 2008; 456(7222):593-598.

17. Jiang YZ, Ma D, Suo C, et al. Genomic and Transcriptomic Landscape of Triple-Negative Breast Cancers: Subtypes and Treatment Strategies. *Cancer Cell.* 2019; 35(3):428-440 e425.

18. Zhou J, Chen Q, Zou Y, Chen H, Qi L, Chen Y. Stem Cells and Cellular Origins of Breast Cancer: Updates in the Rationale, Controversies, and Therapeutic Implications. *Front. Oncol.* 2019; 9:820.

19. Qin J, Liu X, Laffin B, et al. The PSA(-/lo) prostate cancer cell population harbors self-renewing long-term tumor-propagating cells that resist castration. *Cell Stem Cell.* 2012; 10(5):556-569.

20. Hwang WL, Jiang JK, Yang SH, et al. MicroRNA-146a directs the symmetric division of Snail-dominant colorectal cancer stem cells. *Nat. Cell Biol.* 2014; 16(3):268-280.

21. Mao P, Joshi K, Li J, et al. Mesenchymal glioma stem cells are maintained by activated glycolytic metabolism involving aldehyde dehydrogenase 1A3. *Proc. Natl. Acad. Sci. U. S. A.* 2013; 110(21):8644-8649.

22. Beck B, Blanpain C. Unravelling cancer stem cell potential. *Nat. Rev. Cancer.* 2013; 13(10):727-738.

23. Kim WT, Ryu CJ. Cancer stem cell surface markers on normal stem cells. *BMB Rep.* 2017; 50(6):285-298.

24. Behnan J, Stangeland B, Hosainey SA, et al. Differential propagation of stroma and cancer stem cells dictates tumorigenesis and multipotency. *Oncogene.* 2017; 36(4):570-584.

25. Yousefi M, Li L, Lengner CJ. Hierarchy and Plasticity in the Intestinal Stem Cell Compartment. *Trends Cell Biol.* 2017; 27(10):753-764.

26. Jadhav U, Saxena M, O'Neill NK, et al. Dynamic Reorganization of Chromatin Accessibility Signatures during Dedifferentiation of Secretory Precursors into Lgr5+ Intestinal Stem Cells. *Cell Stem Cell.* 2017; 21(1):65-77 e65.

27. Shimokawa M, Ohta Y, Nishikori S, et al. Visualization and targeting of LGR5(+) human colon cancer stem cells. *Nature.* 2017; 545(7653):187-192.

28. Liau BB, Sievers C, Donohue LK, et al. Adaptive Chromatin Remodeling Drives Glioblastoma Stem Cell Plasticity and Drug Tolerance. *Cell Stem Cell.* 2017; 20(2):233-246 e237.

29. Gupta PB, Fillmore CM, Jiang G, et al. Stochastic state transitions give rise to phenotypic equilibrium in populations of cancer cells. *Cell.* 2011; 146(4):633-644.

30. Najafi M, Mortezaee K, Majidpoor J. Cancer stem cell (CSC) resistance drivers. *Life Sci.* 2019; 234:116781.

31. Nassar D, Blanpain C. Cancer Stem Cells: Basic Concepts and Therapeutic Implications. *Annu. Rev. Pathol.* 2016; 11:47-76.

32. Al-Hajj M, Wicha MS, Benito-Hernandez A, Morrison SJ, Clarke MF. Prospective identification of tumorigenic breast cancer cells. *Proc. Natl. Acad. Sci. U. S. A.* 2003; 100(7):3983-3988.

33. Liu S, Wicha MS. Targeting breast cancer stem cells. *J. Clin. Oncol.* 2010; 28(25):4006-4012.

34. Murillo-Garzon V, Kypta R. WNT signalling in prostate cancer. *Nat Rev Urol.* 2017; 14(11):683-696.

35. Cojoc M, Peitzsch C, Kurth I, et al. Aldehyde Dehydrogenase Is Regulated by beta-Catenin/TCF and Promotes Radioresistance in Prostate Cancer Progenitor Cells. *Cancer Res.* 2015; 75(7):1482-1494.

36. Zeuner A, Todaro M, Stassi G, De Maria R. Colorectal cancer stem cells: from the crypt to the clinic. *Cell Stem Cell.* 2014; 15(6):692-705.

37. Chen DS, Mellman I. Oncology meets immunology: the cancer-immunity cycle. *Immunity.* 2013; 39(1):1-10.

38. Chen DS, Mellman I. Elements of cancer immunity and the cancer-immune set point. *Nature.* 2017; 541(7637):321-330.

39. Gimple RC, Bhargava S, Dixit D, Rich JN. Glioblastoma stem cells: lessons from the tumor hierarchy in a lethal cancer. *Genes Dev.* 2019; 33(11-12):591-609.

40. Alexander BM, Cloughesy TF. Adult Glioblastoma. *J. Clin. Oncol.* 2017; 35(21):2402-2409.

41. Topalian SL, Taube JM, Anders RA, Pardoll DM. Mechanism-driven biomarkers to guide immune checkpoint blockade in cancer therapy. *Nat. Rev. Cancer.* 2016; 16(5):275-287.

42. Jackson CM, Choi J, Lim M. Mechanisms of immunotherapy resistance: lessons from glioblastoma. *Nat. Immunol.* 2019; 20(9):1100-1109.

43. Ladomersky E, Zhai L, Lenzen A, et al. IDO1 Inhibition Synergizes with Radiation and PD-1 Blockade to Durably Increase Survival Against Advanced Glioblastoma. *Clin. Cancer Res.* 2018; 24(11):2559-2573.

44. Lim M, Xia Y, Bettegowda C, Weller M. Current state of immunotherapy for glioblastoma. *Nat. Rev. Clin. Oncol.* 2018; 15(7):422-442.

45. Desjardins A, Gromeier M, Herndon JE, 2nd, et al. Recurrent Glioblastoma Treated with Recombinant Poliovirus. *N. Engl. J. Med.* 2018; 379(2):150-161.

46. Iorgulescu JB, Reardon DA, Chiocca EA, Wu CJ. Immunotherapy for glioblastoma: going viral. *Nat. Med.* 2018; 24(8):1094-1096.

47. Zhang D, Tang DG, Rycaj K. Cancer stem cells: Regulation programs, immunological properties and immunotherapy. *Semin. Cancer Biol.* 2018; 52(Pt 2):94-106.

48. Tivnan A, Heilinger T, Lavelle EC, Prehn JH. Advances in immunotherapy for the treatment of glioblastoma. *J. Neurooncol.* 2017; 131(1):1-9.

49. Di Tomaso T, Mazzoleni S, Wang E, et al. Immunobiological characterization of cancer stem cells isolated from glioblastoma patients. *Clin. Cancer Res.* 2010; 16(3):800-813.

50. Ames E, Canter RJ, Grossenbacher SK, et al. NK Cells Preferentially Target Tumor Cells with a Cancer Stem Cell Phenotype. *J. Immunol.* 2015; 195(8):4010-4019.

51. Castriconi R, Daga A, Dondero A, et al. NK cells recognize and kill human glioblastoma cells with stem cell-like properties. *J. Immunol.* 2009; 182(6):3530-3539.

52. Xu Q, Liu G, Yuan X, et al. Antigen-specific T-cell response from dendritic cell vaccination using cancer stem-like cell-associated antigens. *Stem Cells.* 2009; 27(8):1734-1740.

53. Vik-Mo EO, Nyakas M, Mikkelsen BV, et al. Therapeutic vaccination against autologous cancer stem cells with mRNA-transfected dendritic cells in patients with glioblastoma. *Cancer Immunol. Immunother.* 2013; 62(9):1499-1509.

54. Kikuchi R, Ueda R, Saito K, et al. A Pilot Study of Vaccine Therapy with Multiple Glioma Oncoantigen/Glioma Angiogenesis-Associated Antigen Peptides for Patients with Recurrent/Progressive High-Grade Glioma. *J Clin Med.* 2019; 8(2).

55. Stupp R, Mason WP, van den Bent MJ, et al. Radiotherapy plus concomitant and adjuvant temozolomide for glioblastoma. *N. Engl. J. Med.* 2005; 352(10):987-996.

56. Loughner CL, Bruford EA, McAndrews MS, Delp EE, Swamynathan S, Swamynathan SK. Organization, evolution and functions of the human and mouse Ly6/uPAR family genes. *Hum Genomics.* 2016; 10:10.

57. Endo S, Yoshitake H, Tsukamoto H, et al. TEX101, a glycoprotein essential for sperm fertility, is required for stable expression of Ly6k on testicular germ cells. *Sci. Rep.* 2016; 6:23616.

58. Fujihara Y, Okabe M, Ikawa M. GPI-anchored protein complex, LY6K/TEX101, is required for sperm migration into the oviduct and male fertility in mice. *Biol. Reprod.* 2014; 90(3):60.

59. Pandey A, Yadav SK, Vishvkarma R, et al. The dynamics of gene expression during and post meiosis sets the sperm agenda. *Mol. Reprod. Dev.* 2019.

60. Maruyama M, Yoshitake H, Tsukamoto H, Takamori K, Araki Y. Molecular expression of Ly6k, a putative glycosylphosphatidyl-inositol-anchored membrane protein on the mouse testicular germ cells. *Biochem. Biophys. Res. Commun.* 2010; 402(1):75-81.

61. Tsukamoto H, Yoshitake H, Mori M, et al. Testicular proteins associated with the germ cell-marker, TEX101: involvement of cellubrevin in TEX101-trafficking to the cell surface during spermatogenesis. *Biochem. Biophys. Res. Commun.* 2006; 345(1):229-238.

62. Yoshitake H, Tsukamoto H, Maruyama-Fukushima M, Takamori K, Ogawa H, Araki Y. TEX101, a germ cell-marker glycoprotein, is associated with lymphocyte antigen 6 complex locus k within the mouse testis. *Biochem. Biophys. Res. Commun.* 2008; 372(2):277-282.

63. Schiza C, Korbakis D, Jarvi K, Diamandis EP, Drabovich AP. Identification of TEX101-associated Proteins Through Proteomic Measurement of Human Spermatozoa Homozygous for the Missense Variant rs35033974. *Mol. Cell. Proteomics.* 2019; 18(2):338-351.

64. Fagerberg L, Hallstrom BM, Oksvold P, et al. Analysis of the human tissue-specific expression by genome-wide integration of transcriptomics and antibody-based proteomics. *Mol. Cell. Proteomics.* 2014; 13(2):397-406.

65. Luo L, McGarvey P, Madhavan S, Kumar R, Gusev Y, Upadhyay G. Distinct lymphocyte antigens 6 (Ly6) family members Ly6D, Ly6E, Ly6K and Ly6H drive tumorigenesis and clinical outcome. *Oncotarget.* 2016; 7(10):11165-11193.

66. Upadhyay G. Emerging Role of Lymphocyte Antigen-6 Family of Genes in Cancer and Immune Cells. *Front. Immunol.* 2019; 10:819.

67. Ishikawa N, Takano A, Yasui W, et al. Cancer-testis antigen lymphocyte antigen 6 complex locus K is a serologic biomarker and a therapeutic target for lung and esophageal carcinomas. *Cancer Res.* 2007; 67(24):11601-11611.

68. Zhang B, Zhang Z, Zhang X, Gao X, Kernstine KH, Zhong L. Serological antibodies against LY6K as a diagnostic biomarker in esophageal squamous cell carcinoma. *Biomarkers.* 2012; 17(4):372-378.

69. Ambatipudi S, Gerstung M, Pandey M, et al. Genome-wide expression and copy number analysis identifies driver genes in gingivobuccal cancers. *Genes Chromosomes Cancer.* 2012; 51(2):161-173.

70. Xu J, Liu H, Yang Y, et al. Genome-Wide Profiling of Cervical RNA-Binding Proteins Identifies Human Papillomavirus Regulation of RNASEH2A Expression by Viral E7 and E2F1. *MBio.* 2019; 10(1).

71. Matsuda R, Enokida H, Chiyomaru T, et al. LY6K is a novel molecular target in bladder cancer on basis of integrate genome-wide profiling. *Br. J. Cancer.* 2011; 104(2):376-386.

72. Mendillo ML, Santagata S, Koeva M, et al. HSF1 drives a transcriptional program distinct from heat shock to support highly malignant human cancers. *Cell.* 2012; 150(3):549-562.

73. Kong HK, Yoon S, Park JH. The regulatory mechanism of the LY6K gene expression in human breast cancer cells. *J. Biol. Chem.* 2012; 287(46):38889-38900.

74. Kong HK, Park SJ, Kim YS, et al. Epigenetic activation of LY6K predicts the presence of metastasis and poor prognosis in breast carcinoma. *Oncotarget.* 2016; 7(34):55677-55689.

75. Kim YS, Park SJ, Lee YS, Kong HK, Park JH. miRNAs involved in LY6K and estrogen receptor alpha contribute to tamoxifen-susceptibility in breast cancer. *Oncotarget.* 2016; 7(27):42261-42273.

76. Liao XH, Xie Z, Guan CN. MiRNA-500a-3p inhibits cell proliferation and invasion by targeting lymphocyte antigen 6 complex locus K (LY6K) in human non-small cell lung cancer. *Neoplasma.* 2018; 65(5):673-682.

77. Kong HK, Park JH. Characterization and function of human Ly-6/uPAR molecules. *BMB Rep.* 2012; 45(11):595-603.

78. AlHossiny M, Luo L, Frazier WR, et al. Ly6E/K Signaling to TGFbeta Promotes Breast Cancer Progression, Immune Escape, and Drug Resistance. *Cancer Res.* 2016; 76(11):3376-3386.

79. Son D, Kong HK, Kim Y, et al. Transgenic overexpression of human LY6K in mice suppresses mature T cell development in the thymus. *Oncol. Lett.* 2019; 17(1):379-387.

80. Suda T, Tsunoda T, Daigo Y, Nakamura Y, Tahara H. Identification of human leukocyte antigen-A24-restricted epitope peptides derived from gene products upregulated in lung and esophageal cancers as novel targets for immunotherapy. *Cancer Sci.* 2007; 98(11):1803-1808.

81. Mizukami Y, Kono K, Daigo Y, et al. Detection of novel cancer-testis antigen-specific T-cell responses in TIL, regional lymph nodes, and PBL in patients with esophageal squamous cell carcinoma. *Cancer Sci.* 2008; 99(7):1448-1454.

82. Kono K, Mizukami Y, Daigo Y, et al. Vaccination with multiple peptides derived from novel cancer-testis antigens can induce specific T-cell responses and clinical responses in advanced esophageal cancer. *Cancer Sci.* 2009; 100(8):1502-1509.

83. Iwahashi M, Katsuda M, Nakamori M, et al. Vaccination with peptides derived from cancer-testis antigens in combination with CpG-7909 elicits strong specific CD8+ T cell response in patients with metastatic esophageal squamous cell carcinoma. *Cancer Sci.* 2010; 101(12):2510-2517.

84. Kono K, Iinuma H, Akutsu Y, et al. Multicenter, phase II clinical trial of cancer vaccination for advanced esophageal cancer with three peptides derived from novel cancer-testis antigens. *J. Transl. Med.* 2012; 10:141.

85. Suzuki H, Fukuhara M, Yamaura T, et al. Multiple therapeutic peptide vaccines consisting of combined novel cancer testis antigens and anti-angiogenic peptides for patients with non-small cell lung cancer. *J. Transl. Med.* 2013; 11:97.

86. Fang H, Yamaguchi R, Liu X, et al. Quantitative T cell repertoire analysis by deep cDNA sequencing of T cell receptor alpha and beta chains using next-generation sequencing (NGS). *Oncoimmunology.* 2014; 3(12):e968467.

87. Ishikawa H, Imano M, Shiraishi O, et al. Phase I clinical trial of vaccination with LY6K-derived peptide in patients with advanced gastric cancer. *Gastric Cancer.* 2014; 17(1):173-180.

88. de Nooij-van Dalen AG, van Dongen GA, Smeets SJ, et al. Characterization of the human Ly-6 antigens, the newly annotated member Ly-6K included, as molecular markers for head-and-neck squamous cell carcinoma. *Int. J. Cancer.* 2003; 103(6):768-774.

89. Carrero I, Liu HC, Sikora AG, Milosavljevic A. Histoepigenetic analysis of HPV- and tobacco-associated head and neck cancer identifies both subtype-specific and common therapeutic targets despite divergent microenvironments. *Oncogene.* 2019; 38(19):3551-3568.

90. Yoshitake Y, Fukuma D, Yuno A, et al. Phase II clinical trial of multiple peptide vaccination for advanced head and neck cancer patients revealed induction of immune responses and improved OS. *Clin. Cancer Res.* 2015; 21(2):312-321.

91. Tomita Y, Yuno A, Tsukamoto H, et al. Identification of immunogenic LY6K long peptide encompassing both CD4+ and CD8+ T-cell epitopes and eliciting CD4+ T-cell immunity in patients with malignant disease. *Oncoimmunology.* 2014; 3:e28100.

92. Chen X, Zhao C, Guo B, Zhao Z, Wang H, Fang Z. Systematic Profiling of Alternative mRNA Splicing Signature for Predicting Glioblastoma Prognosis. *Front. Oncol.* 2019; 9:928.

93. Pope SD, Medzhitov R. Emerging Principles of Gene Expression Programs and Their Regulation. *Mol. Cell.* 2018; 71(3):389-397.

94. Carpenter S, Ricci EP, Mercier BC, Moore MJ, Fitzgerald KA. Post-transcriptional regulation of gene expression in innate immunity. *Nat. Rev. Immunol.* 2014; 14(6):361-376.

95. Ha M, Kim VN. Regulation of microRNA biogenesis. *Nat. Rev. Mol. Cell Biol.* 2014; 15(8):509-524.

96. Gebert LFR, MacRae IJ. Regulation of microRNA function in animals. *Nat. Rev. Mol. Cell Biol.* 2019; 20(1):21-37.

97. Huang T, Alvarez AA, Pangeni RP, et al. A regulatory circuit of miR-125b/miR-20b and Wnt signalling controls glioblastoma phenotypes through FZD6-modulated pathways. *Nature communications.* 2016; 7:12885.

98. Skvortsova K, Iovino N, Bogdanovic O. Functions and mechanisms of epigenetic inheritance in animals. *Nat. Rev. Mol. Cell Biol.* 2018; 19(12):774-790.

99. Jones PA, Issa JP, Baylin S. Targeting the cancer epigenome for therapy. *Nat Rev Genet.* 2016; 17(10):630-641.

100. Toh TB, Lim JJ, Chow EK. Epigenetics in cancer stem cells. *Mol. Cancer.* 2017; 16(1):29.

101. De Carvalho DD, Sharma S, You JS, et al. DNA methylation screening identifies driver epigenetic events of cancer cell survival. *Cancer Cell.* 2012; 21(5):655-667.

102. Pangeni RP, Zhang Z, Alvarez AA, et al. Genome-wide methylomic and transcriptomic analyses identify subtype-specific epigenetic signatures commonly dysregulated in glioma stem cells and glioblastoma. *Epigenetics.* 2018; 13(4):432-448.

103. Simpson AJ, Caballero OL, Jungbluth A, Chen YT, Old LJ. Cancer/testis antigens, gametogenesis and cancer. *Nat. Rev. Cancer.* 2005; 5(8):615-625.

104. Miousse IR, Kutanzi KR, Koturbash I. Effects of ionizing radiation on DNA methylation: from experimental biology to clinical applications. *Int. J. Radiat. Biol.* 2017; 93(5):457-469.

105. Cancer Genome Atlas Research N. Comprehensive genomic characterization defines human glioblastoma genes and core pathways. *Nature.* 2008; 455(7216):1061-1068.

106. Eskilsson E, Rosland GV, Solecki G, et al. EGFR heterogeneity and implications for therapeutic intervention in glioblastoma. *Neuro Oncol.* 2018; 20(6):743-752.

107. Pearson JRD, Regad T. Targeting cellular pathways in glioblastoma multiforme. *Signal Transduct Target Ther.* 2017; 2:17040.

108. Sugawa N, Ekstrand AJ, James CD, Collins VP. Identical splicing of aberrant epidermal growth factor receptor transcripts from amplified rearranged genes in human glioblastomas. *Proc. Natl. Acad. Sci. U. S. A.* 1990; 87(21):8602-8606.

109. Brennan CW, Verhaak RG, McKenna A, et al. The somatic genomic landscape of glioblastoma. *Cell.* 2013; 155(2):462-477.

110. Binder ZA, Thorne AH, Bakas S, et al. Epidermal Growth Factor Receptor Extracellular Domain Mutations in Glioblastoma Present Opportunities for Clinical Imaging and Therapeutic Development. *Cancer Cell.* 2018; 34(1):163-177 e167.

111. Thorne AH, Zanca C, Furnari F. Epidermal growth factor receptor targeting and challenges in glioblastoma. *Neuro Oncol.* 2016; 18(7):914-918.

112. Westphal M, Maire CL, Lamszus K. EGFR as a Target for Glioblastoma Treatment: An Unfulfilled Promise. *CNS Drugs.* 2017; 31(9):723-735.

113. Chistiakov DA, Chekhonin IV, Chekhonin VP. The EGFR variant III mutant as a target for immunotherapy of glioblastoma multiforme. *Eur. J. Pharmacol.* 2017; 810:70-82.

114. An Z, Aksoy O, Zheng T, Fan QW, Weiss WA. Epidermal growth factor receptor and EGFRvIII in glioblastoma: signaling pathways and targeted therapies. *Oncogene.* 2018; 37(12):1561-1575.

115. Lynch TJ, Bell DW, Sordella R, et al. Activating mutations in the epidermal growth factor receptor underlying responsiveness of non-small-cell lung cancer to gefitinib. *N. Engl. J. Med.* 2004; 350(21):2129-2139.

116. Tsao MS, Sakurada A, Cutz JC, et al. Erlotinib in lung cancer - molecular and clinical predictors of outcome. *N. Engl. J. Med.* 2005; 353(2):133-144.

117. Guo G, Gong K, Ali S, et al. A TNF-JNK-Axl-ERK signaling axis mediates primary resistance to EGFR inhibition in glioblastoma. *Nat. Neurosci.* 2017; 20(8):1074-1084.

118. Guo G, Gong K, Puliyappadamba VT, et al. Efficacy of EGFR plus TNF inhibition in a preclinical model of temozolomide-resistant glioblastoma. *Neuro Oncol.* 2019; 21(12):1529-1539.

119. Vivanco I, Robins HI, Rohle D, et al. Differential sensitivity of glioma- versus lung cancer-specific EGFR mutations to EGFR kinase inhibitors. *Cancer Discov.* 2012; 2(5):458-471.

120. Ma Y, Tang N, Thompson RC, et al. InsR/IGF1R Pathway Mediates Resistance to EGFR Inhibitors in Glioblastoma. *Clin. Cancer Res.* 2016; 22(7):1767-1776.

121. Samatar AA, Poulikakos PI. Targeting RAS-ERK signalling in cancer: promises and challenges. *Nat Rev Drug Discov.* 2014; 13(12):928-942.

122. Downward J. Targeting RAS signalling pathways in cancer therapy. *Nat. Rev. Cancer.* 2003; 3(1):11-22.

123. Cox AD, Der CJ, Philips MR. Targeting RAS Membrane Association: Back to the Future for Anti-RAS Drug Discovery? *Clin. Cancer Res.* 2015; 21(8):1819-1827.

124. Simanshu DK, Nissley DV, McCormick F. RAS Proteins and Their Regulators in Human Disease. *Cell.* 2017; 170(1):17-33.

125. Asati V, Mahapatra DK, Bharti SK. PI3K/Akt/mTOR and Ras/Raf/MEK/ERK signaling pathways inhibitors as anticancer agents: Structural and pharmacological perspectives. *Eur. J. Med. Chem.* 2016; 109:314-341.

126. Yaeger R, Corcoran RB. Targeting Alterations in the RAF-MEK Pathway. *Cancer Discov.* 2019; 9(3):329-341.

127. Cox AD, Fesik SW, Kimmelman AC, Luo J, Der CJ. Drugging the undruggable RAS: Mission possible? *Nat Rev Drug Discov.* 2014; 13(11):828-851.

128. Lindsay CR, Blackhall FH. Direct Ras G12C inhibitors: crossing the rubicon. *Br. J. Cancer.* 2019; 121(3):197-198.

129. Bunda S, Heir P, Srikumar T, et al. Src promotes GTPase activity of Ras via tyrosine 32 phosphorylation. *Proc. Natl. Acad. Sci. U. S. A.* 2014; 111(36):E3785-3794.

130. Lavoie H, Therrien M. Regulation of RAF protein kinases in ERK signalling. *Nat. Rev. Mol. Cell Biol.* 2015; 16(5):281-298.

131. Freeman AK, Ritt DA, Morrison DK. Effects of Raf dimerization and its inhibition on normal and disease-associated Raf signaling. *Mol. Cell.* 2013; 49(4):751-758.

132. Pratilas CA, Taylor BS, Ye Q, et al. (V600E)BRAF is associated with disabled feedback inhibition of RAF-MEK signaling and elevated transcriptional output of the pathway. *Proc. Natl. Acad. Sci. U. S. A.* 2009; 106(11):4519-4524.

133. Yao Z, Gao Y, Su W, et al. RAF inhibitor PLX8394 selectively disrupts BRAF dimers and RAS-independent BRAF-mutant-driven signaling. *Nat. Med.* 2019; 25(2):284-291.

134. Gao Y, Chang MT, McKay D, et al. Allele-Specific Mechanisms of Activation of MEK1 Mutants Determine Their Properties. *Cancer Discov.* 2018; 8(5):648-661.

135. Martinelli E, Morgillo F, Troiani T, Ciardiello F. Cancer resistance to therapies against the EGFR-RAS-RAF pathway: The role of MEK. *Cancer Treat. Rev.* 2017; 53:61-69.

136. Janne PA, Shaw AT, Pereira JR, et al. Selumetinib plus docetaxel for KRAS-mutant advanced non-small-cell lung cancer: a randomised, multicentre, placebo-controlled, phase 2 study. *Lancet Oncol.* 2013; 14(1):38-47.

137. Flaherty KT, Infante JR, Daud A, et al. Combined BRAF and MEK inhibition in melanoma with BRAF V600 mutations. *N. Engl. J. Med.* 2012; 367(18):1694-1703.

138. Zhao YJ, Adjei AA. The clinical development of MEK inhibitors. *Nature Reviews Clinical Oncology.* 2014; 11(7):385-400.

139. Kolch W. Coordinating ERK/MAPK signalling through scaffolds and inhibitors. *Nat. Rev. Mol. Cell Biol.* 2005; 6(11):827-837.

140. Chang L, Karin M. Mammalian MAP kinase signalling cascades. *Nature.* 2001; 410(6824):37-40.

141. Jovanovic KK, Roche-Lestienne C, Ghobrial IM, Facon T, Quesnel B, Manier S. Targeting MYC in multiple myeloma. *Leukemia.* 2018; 32(6):1295-1306.

142. Daniel PM, Filiz G, Tymms MJ, et al. Intratumor MAPK and PI3K signaling pathway heterogeneity in glioblastoma tissue correlates with CREB signaling and distinct target gene signatures. *Exp. Mol. Pathol.* 2018; 105(1):23-31.

143. Jaiswal BS, Durinck S, Stawiski EW, et al. ERK Mutations and Amplification Confer Resistance to ERK-Inhibitor Therapy. *Clin. Cancer Res.* 2018; 24(16):4044-4055.

144. Lake D, Correa SA, Muller J. Negative feedback regulation of the ERK1/2 MAPK pathway. *Cell. Mol. Life Sci.* 2016; 73(23):4397-4413.

145. Morrison DK. KSR: a MAPK scaffold of the Ras pathway? *J. Cell Sci.* 2001; 114(Pt 9):1609-1612.

146. McKay MM, Ritt DA, Morrison DK. Signaling dynamics of the KSR1 scaffold complex. *Proc. Natl. Acad. Sci. U. S. A.* 2009; 106(27):11022-11027.

147. Nett IR, Mulas C, Gatto L, Lilley KS, Smith A. Negative feedback via RSK modulates Erk-dependent progression from naive pluripotency. *EMBO Rep.* 2018; 19(8).

148. Pratilas CA, Solit DB. Targeting the mitogen-activated protein kinase pathway: physiological feedback and drug response. *Clin. Cancer Res.* 2010; 16(13):3329-3334.

149. Martinez-Outschoorn UE, Sotgia F, Lisanti MP. Caveolae and signalling in cancer. *Nat. Rev. Cancer.* 2015; 15(4):225-237.

150. Parton RG, del Pozo MA. Caveolae as plasma membrane sensors, protectors and organizers. *Nat. Rev. Mol. Cell Biol.* 2013; 14(2):98-112.

151. Goetz JG, Lajoie P, Wiseman SM, Nabi IR. Caveolin-1 in tumor progression: the good, the bad and the ugly. *Cancer Metastasis Rev.* 2008; 27(4):715-735.

152. Parat MO, Riggins GJ. Caveolin-1, caveolae, and glioblastoma. *Neuro Oncol.* 2012; 14(6):679-688.

153. Ketteler J, Klein D. Caveolin-1, cancer and therapy resistance. *Int. J. Cancer.* 2018; 143(9):2092-2104.

154. Mineo C, James GL, Smart EJ, Anderson RG. Localization of epidermal growth factor-stimulated Ras/Raf-1 interaction to caveolae membrane. *J. Biol. Chem.* 1996; 271(20):11930-11935.

155. Kortum RL, Fernandez MR, Costanzo-Garvey DL, et al. Caveolin-1 is required for kinase suppressor of Ras 1 (KSR1)-mediated extracellular signal-regulated kinase 1/2 activation, H-RasV12-induced senescence, and transformation. *Mol. Cell. Biol.* 2014; 34(18):3461-3472.

156. Pol A, Lu A, Pons M, Peiro S, Enrich C. Epidermal growth factor-mediated caveolin recruitment to early endosomes and MAPK activation. Role of cholesterol and actin cytoskeleton. *J. Biol. Chem.* 2000; 275(39):30566-30572.

157. Yun JH, Park SJ, Jo A, et al. Caveolin-1 is involved in reactive oxygen species-induced SHP-2 activation in astrocytes. *Exp. Mol. Med.* 2011; 43(12):660-668.

158. Huang T, Kim CK, Alvarez AA, et al. MST4 Phosphorylation of ATG4B Regulates Autophagic Activity, Tumorigenicity, and Radioresistance in Glioblastoma. *Cancer Cell.* 2017; 32(6):840-855 e848.

159. Huang T, Wan X, Alvarez AA, et al. MIR93 (microRNA -93) regulates tumorigenicity and therapy response of glioblastoma by targeting autophagy. *Autophagy.* 2019:1-12.

160. Phillips HS, Kharbanda S, Chen R, et al. Molecular subclasses of high-grade glioma predict prognosis, delineate a pattern of disease progression, and resemble stages in neurogenesis. *Cancer Cell.* 2006; 9(3):157-173.

161. Cerami E, Gao J, Dogrusoz U, et al. The cBio cancer genomics portal: an open platform for exploring multidimensional cancer genomics data. *Cancer Discov.* 2012; 2(5):401-404.

162. Gao J, Aksoy BA, Dogrusoz U, et al. Integrative analysis of complex cancer genomics and clinical profiles using the cBioPortal. *Sci Signal.* 2013; 6(269):pl1.

163. Mayor S, Riezman H. Sorting GPI-anchored proteins. *Nat. Rev. Mol. Cell Biol.* 2004; 5(2):110-120.

164. Hu Y, Smyth GK. ELDA: extreme limiting dilution analysis for comparing depleted and enriched populations in stem cell and other assays. *J. Immunol. Methods.* 2009; 347(1-2):70-78.

165. Laird PW. Principles and challenges of genomewide DNA methylation analysis. *Nat Rev Genet.* 2010; 11(3):191-203.

166. Pidsley R, CC YW, Volta M, Lunnon K, Mill J, Schalkwyk LC. A data-driven approach to preprocessing Illumina 450K methylation array data. *BMC Genomics.* 2013; 14:293.

167. King AJ, Patrick DR, Batorsky RS, et al. Demonstration of a genetic therapeutic index for tumors expressing oncogenic BRAF by the kinase inhibitor SB-590885. *Cancer Res.* 2006; 66(23):11100-11105.

168. Shang J, Lu S, Jiang Y, Zhang J. Allosteric modulators of MEK1: drug design and discovery. *Chem. Biol. Drug Des.* 2016; 88(4):485-497.

169. Randall EC, Emdal KB, Laramy JK, et al. Integrated mapping of pharmacokinetics and pharmacodynamics in a patient-derived xenograft model of glioblastoma. *Nature communications.* 2018; 9(1):4904.

170. Li Z, Xu M, Xing S, et al. Erlotinib effectively inhibits JAK2V617F activity and polycythemia vera cell growth. *J. Biol. Chem.* 2007; 282(6):3428-3432.

171. Plosker GL. Ruxolitinib: a review of its use in patients with myelofibrosis. *Drugs.* 2015; 75(3):297-308.

172. Bowman RL, Wang Q, Carro A, Verhaak RG, Squatrito M. GlioVis data portal for visualization and analysis of brain tumor expression datasets. *Neuro Oncol.* 2017; 19(1):139-141.

173. Ozhan G, Sezgin E, Wehner D, et al. Lypd6 enhances Wnt/beta-catenin signaling by promoting Lrp6 phosphorylation in raft plasma membrane domains. *Dev. Cell.* 2013; 26(4):331-345.

174. Mundy DI, Machleidt T, Ying YS, Anderson RG, Bloom GS. Dual control of caveolar membrane traffic by microtubules and the actin cytoskeleton. *J. Cell Sci.* 2002; 115(Pt 22):4327-4339.

175. Fujiwara I, Zweifel ME, Courtemanche N, Pollard TD. Latrunculin A Accelerates Actin Filament Depolymerization in Addition to Sequestering Actin Monomers. *Curr. Biol.* 2018; 28(19):3183-3192 e3182.

176. Lee PY, Wang JX, Parisini E, Dascher CC, Nigrovic PA. Ly6 family proteins in neutrophil biology. *J. Leukoc. Biol.* 2013; 94(4):585-594.

177. Lisanti MP, Field MC, Caras IW, Menon AK, Rodriguez-Boulan E. Mannosamine, a novel inhibitor of glycosylphosphatidylinositol incorporation into proteins. *EMBO J.* 1991; 10(8):1969-1977.

178. Cirit M, Grant KG, Haugh JM. Systemic perturbation of the ERK signaling pathway by the proteasome inhibitor, MG132. *PLoS One.* 2012; 7(11):e50975.

179. Antwih DA, Gabbara KM, Lancaster WD, Ruden DM, Zielske SP. Radiation-induced epigenetic DNA methylation modification of radiation-response pathways. *Epigenetics.* 2013; 8(8):839-848.

180. Minata M, Audia A, Shi J, et al. Phenotypic Plasticity of Invasive Edge Glioma Stem-like Cells in Response to Ionizing Radiation. *Cell Rep.* 2019; 26(7):1893-1905 e1897.

181. Simons K, Toomre D. Lipid rafts and signal transduction. *Nat. Rev. Mol. Cell Biol.* 2000; 1(1):31-39.

182. Sunshine H, Iruela-Arispe ML. Membrane lipids and cell signaling. *Curr. Opin. Lipidol.* 2017; 28(5):408-413.